Distribution Agreement

In presenting this thesis or dissertation as a partial fulfillment of the requirements for an advanced degree from Emory University, I hereby grant to Emory University and its agents the non-exclusive license to archive, make accessible, and display my thesis or dissertation in whole or in part in all forms of media, now or hereafter known, including display on the world wide web. I understand that I may select some access restrictions as part of the online submission of this thesis or dissertation. I retain all ownership rights to the copyright of the thesis or dissertation. I also retain the right to use in future works (such as articles or books) all or part of this thesis or dissertation.

Signature:

_____ _____

Xin Jia Date

Understanding signal transduction systems in prokaryotes and eukaryotes

By

Xin Jia
Doctor of Philosophy

Chemistry

Dr. Emily Weinert

Advisor

Dr. Stefan Lutz

Committee Member

Dr. Lanny Liebeskind

Committee Member

Accepted:

Lisa A. Tedesco, Ph.D. Dean of the James T. Laney School of Graduate Studies

---

Date

Understanding signal transduction systems in prokaryotes and eukaryotes

By

Xin Jia
B.S., University of Richmond, 2011

Advisor: Emily Weinert, Ph.D.

An abstract of
A dissertation submitted to the Faculty of the
James T. Laney School of Graduate Studies of Emory University
in partial fulfillment of the requirements for the degree of
Doctor of Philosophy
in Chemistry

2015

Abstract

Understanding signal transduction systems in prokaryotes and eukaryotes

By Xin Jia

The ability of cells to adapt to dynamic and diverse environment by altering their cellular behavior is crucial for adaptation and survival. However, the biochemical mechanisms and signaling transductions pathways involved in adaptation and survival are still poorly understood. In this dissertation, various analytical and biochemical techniques were employed to understand novel signal transduction pathways in both prokaryotic and eukaryotic systems.

A novel putative stressosome complex from the Gram-negative marine bacterium *Vibrio brasiliensis* that contained a heme-bound sensor protein and had the ability to sense environmental O_2 was described. The novel stressosome altered its signaling pathway in response to various environmental O_2 levels. The described complex presents an opportunity to interrogate the effects of ligand-dependent stressosome signaling both *in vitro* and *in vivo*, as well as provides further insights into its potential role in regulating virulence gene expressions in limited O_2 condition in the *Vibrio* genus.

Secondly, I reported our recent progress toward development of an efficient protocol to identify enzyme members of the 3',5'-cCMP signaling pathways. Following previously published protocols, we partially purified a putative soluble cytidylate cyclase that synthesizes 3',5'-cCMP from CTP in rat livers. Additionally, we also isolated a potential 3',5'-cCMP-binding protein, THO complex subunit 5, using 3',5'-cCMP affinity chromatography. The THO complex subunit 5 is involved in cellular proliferation

by controlling transcription and mRNA export, suggesting 3',5'-cCMP may be involved in regulating transcription through THO subunit 5.

Lastly, we developed a sensitive and versatile method to extract and quantify cyclic nucleotide monophosphates (cNMPs) using LC-MS/MS, including both 3',5'-cNMPs and 2',3'-cNMPs, in mammalian tissues and cells. This protocol allows for comparison of multiple cNMPs in the same systems and was used to examine the relationship between tissues levels of cNMPs in various systems. Utilizing this analytical method, I reported the first identification and quantification of 2',3'-cIMP in mammals. The developed analytical method offers a tool for quantification of cNMPs levels in cells and tissues of varying disease states, which will provide insight into the roles of cNMPs *in vivo*.

Understanding signal transduction systems in prokaryotes and eukaryotes

By

Xin Jia
B.S., University of Richmond, 2011

Advisor: Emily Weinert, Ph.D.

A dissertation submitted to the Faculty of the
James T. Laney School of Graduate Studies of Emory University
in partial fulfillment of the requirements for the degree of
Doctor of Philosophy
in Chemistry

2015

Acknowledgments

I would like to express my deepest gratitude to my Advisor, Dr. Emily Weinert, for her help, encouragement and guidance throughout my graduate study at Emory and during the writing of this thesis. Her technical and editorial advice was essential to the completion of my graduate study, and she has taught me innumerable lessons and insights on academic research in general. She has truly made my experience at Emory unforgettable, and made me the chemist I am. I would like to give special thanks to my committee members, Dr. Stefan Lutz and Dr. Lanny Liebeskind. I thank them for supporting this project and giving such thoughtful feedback over the years. I would also like to thank Dr. Fred Strobel for introducing me to the world of analytical chemistry, and continuously encouraging and guiding me to pursue a career in the analytical chemistry field.

To all of the current and past Weinert lab members, I enjoyed every moment working with everybody and I couldn't have asked for better colleagues and friends during my graduate study. I thank Ben Fontaine for providing me with continuous support and advice on the cyclic nucleotide project and for taking the time to proofread my thesis, and Dr. Justin Burns for the biomolecular training and supporting me with many insightful conversations. Also, graduate school would not be the same without my great friends Shawnna Joynt and Dr. Pravin Muthu. They always have believed in me academically and professionally. They made the best supporting system through my graduate life, and I know we will continue to be great friends in the future.

Last but not least, I would like to thank my parents for their dedication and many years of love and support during my undergraduate and graduate studies. Their continuous support and encouragement was what made this dissertation possible.

List of Frequently Used Abbreviations

Abbreviation	Full name
B. subtilis	*Bacillus subtilis*
V. brasiliensis	*Vibrio brasiliensis*
3’,5’-cNMPs	3’,5’-cyclic nucleotide monophosphate
2’,3’-cNMPs	2’,3’-cyclic nucleotide monophosphate
3’,5’-cAMP	adenosine 3’,5’-cyclic monophosphate
3’,5’-cGMP	guanosine 3’,5’-cyclic monophosphate
3’,5’-cCMP	cytidine 3’,5’-cyclic monophosphate
2’,3’-cAMP	adenosine 2’,3’-cyclic monophosphate
2’,3’-cGMP	guanosine 2’,3’-cyclic monophosphate
2’,3’-cCMP	cytidine 2’,3’-cyclic monophosphate
PDE	phosphodiesterase
PKA	adenosine 3’,5’-cyclic monophosphate-dependent protein kinase
PKG	guanosine 3’,5’-cyclic monophosphate-dependent protein kinase
sGC	soluble guanylate cyclase
MS	mass spectrometry
LC-MS/MS	liquid chromatography-tandem mass spectrometry

Table of Contents

List of Figures

List of Tables

List of Synthetic Schemes

Chapter 1: General Introduction

1.1 General Introduction

The ability of cells to adapt to dynamic and diverse environment by changing their cellular behavior is crucial for survival.[1] Therefore, a form of communication is needed to effectively process stimuli received at one cellular location into an appropriate response at another location.[1] This process is known as cellular signal transduction. Signal transduction cascades mediate the sensing and processing of environmental signals.[2] These signaling networks sense, amplify and integrate diverse extracellular and intracellular signals, and generate intracellular responses such as alterations of gene expression and enzymatic activity levels (Figure 1.1).[2]

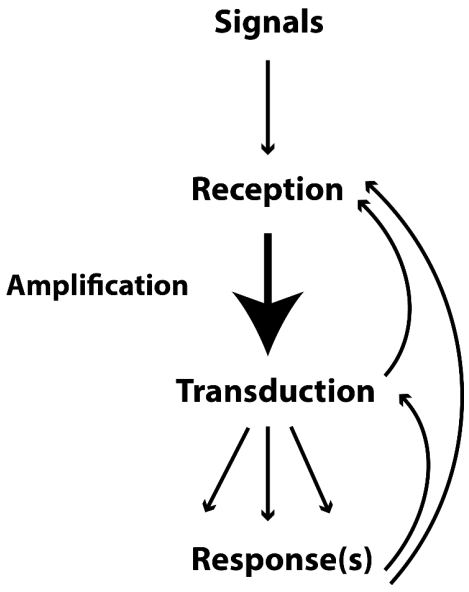

Figure 1.1. Principles of Signal Transduction.[2] An environmental or intracellular signal is first received by a cellular component. The signal is then amplified and transduced to

generate intracellular responses. Feedback regulation down-regulates the signaling pathway.

This chapter will provide background and historical information comparing and contrasting the types of signal transduction systems both in prokaryotes and eukaryotes. As presented in this chapter, many domain structures and signaling transduction mechanisms present in eukaryotes and prokaryotes are analogues to each other. Eukaryotes evolved from prokaryotes; proteins involved in both pathways are homologous, yet differentially regulated. Pedagogically, prokaryotes have much simpler systems, and studying signaling pathways provides insights into the expanding universe of signaling systems in eukaryotes.

1.2 Prokaryotic Signaling Transduction

1.2.1 Introduction

Adaptation to varying environmental conditions is crucial for growth and survival of bacteria. In terms of the number of modular domains involved in transducing signals, bacterial signaling systems can be characterized as one-component and two-component systems, and many involve transmembrane proteins that sense and transmit extracellular signals to intracellular components that in turn generate cellular responses.[3] In one component system, a single protein contains an input domain directly fuses to an output domain.[4] This single protein is usually referred to as a single-molecule transcriptional regulator, due to its role in regulating transcription level through single-molecules.[5] For example, the gas-, redox potential- and light-sensing PAS (Per-Arnt-Sim) and the DNA-

binding HTH are input and output domains in the single-molecule transcriptional regulator RocR in *Bacillus subtilis*.[5-6]

Two-component signaling transduction is ubiquitous in bacteria, and typically consists of a histidine protein kinase and a response regulator.[3a] The kinase domain receives environmental stimuli through a sensing domain, leading to autophosphorylation of a conserved histidine residue, before phosphorylating its response regulator, which in turn leads to numerous cellular responses including changes in enzymatic activity and gene expression.[7]

1.2.2 Heme-Based Sensor Proteins in Bacteria

1.2.2.1 Introduction

The protoporphyrin IX-iron complex, known as heme, is one of the most abundant co-factors in biological systems. The heme-O_2 complex serves as an O_2 carrier in hemoglobin, an O_2 storage site in myoglobin and a catalytic site for O-O bond scission in cytochrome P450 monooxygenase.[8] Additionally, various gaseous molecules including nitric oxide (NO), carbon monoxide (CO) and hydrogen sulfide (H_2S) also bind heme and regulate numerous cellular responses.[8b, 8d, 9] Importantly, molecular O_2 and CO only bind exclusively to Fe(II) but not Fe(III) in heme protein, whereas NO binds to Fe both in Fe(II) and Fe(III) states (Figure 1.2).[8b]

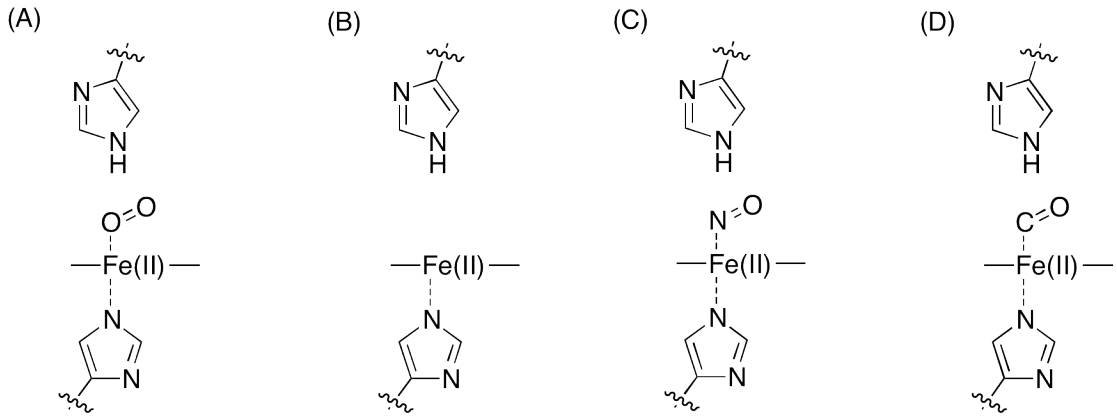

Figure 1.2. The heme/porphyrin iron complex in myoglobin.[8c] In myoglobin, a proximal histidine residue is bond to the Fe atom trans to the O_2 binding distal site and a distal histidine is involved in the distal hydrogen network to bound ligands. (A), O_2 free 5-coordinated Fe(II) complex; (B), for heme-based NO sensor; the Fe(II)-NO complex is formed (C), and for heme-based CO sensor, the Fe(II)-CO complex is formed (D).[8d, 10]

In general, heme-based gas sensors consist of an N-terminal heme iron-bound sensing domain and a C-terminal functional domain (Figure 1.3).[8c, 11] Binding gaseous molecules at the heme causes a conformational change at the sensing domain. This conformational change transmits the ligand-binding signal to its functional domain, which in turn regulates cellular functions in response to binding of the gaseous molecules (Figure 1.3).[8c, 11a, b]

The iron atom in the heme/porphyrin iron complex has two coordination sites, the fifth and sixth coordination sites, one on each side of the heme-porphyrin ring. In myoglobin, the fifth coordination site is bind by a highly conserved histidine residue on the proximal side of the heme pocket.[11b] The sixth coordinate is available to bind O_2

when the Fe atom is in Fe(II) state.[8c] The hydrogen bond network between coordinated gaseous molecules and polar distal residues stabilizes the bound O_2 (Figure 1.2).[8c]

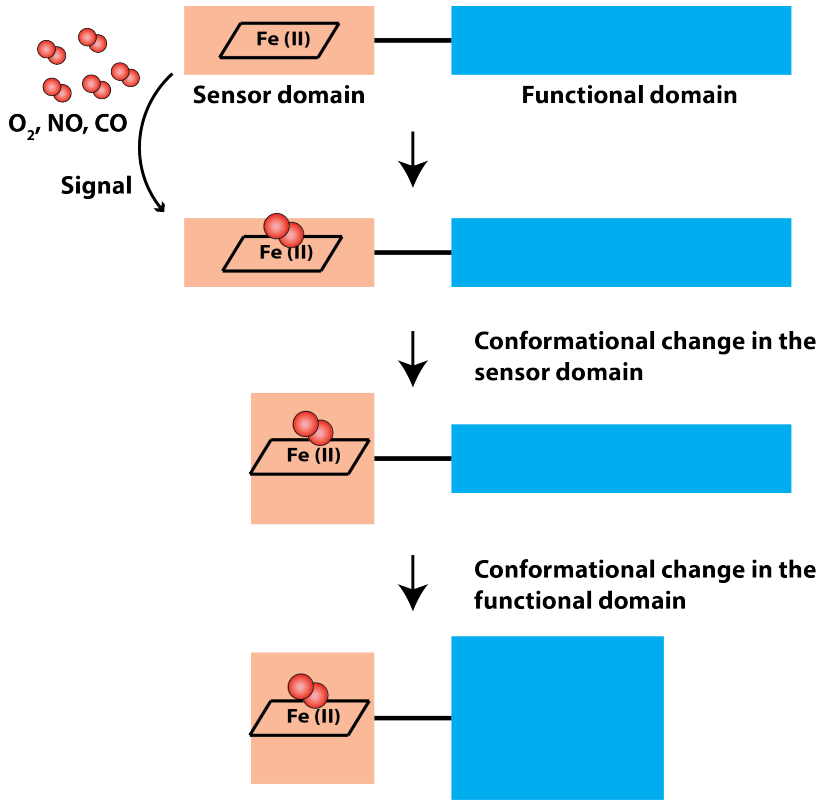

Figure 1.3. Illustration of the signaling transduction mechanism in heme-bond GCSs.[8c] The conformational changes induced by gaseous molecule binding are propagated to the functional output domain, promoting cellular responses such as changes in catalytic rates or gene expression levels.

1.2.2.2 Heme-Based Globin-Coupled Sensors (GCSs)

Heme-bound globin-coupled sensors (GCSs) are composed of an N-terminal oxygen sensing/binding globin domain and a C-terminal functional domain, such as a histidine kinase, phosphodiesterase (PDE), diguanylate cyclase (DGC), and methyl

accepting chemotaxis.[11c, 12] HemAT in Gram-positive bacterium *Bacillus subtilis* detects environmental O_2 levels and transmits the signal to downstream proteins that control the direction of the movement through O_2 gradient (Figure 1.4).[13] Structural studies suggest that the structural changes associated with O_2 binding are mainly due to changes in the spin state of heme iron as well as the formation of hydrogen bonds between O_2 and polar distal residues.[14] Other gaseous molecules, such as NO and CO also bind to the heme iron site, but leads to different structural changes, due to only the changes in the spin state of heme iron.[13-14] The molecular structure and ligand binding mechanism of the *B. subtilis* HemAT sensing domain have been well characterized.[15] The distal pocket hydrogen-bonding network is achieved through binding of O_2 to the Tyr70 and Thr95 amino acid residue (Figure 1.4).[15-16] The X-ray structure shows the key residue Tyr70 leads to distinct conformational changes associated with binding and removal of the gas ligand.[15] Additionally, resonance Raman (RR) spectral studies revealed multiple conformations of the heme pocket associated with ligand binding and removal. In HemAT, O_2 interacts with key resides in the distal side of the heme-pocket through three forms of proposed interactions: a closed form, with an interaction between Thr95 and O_2; an open α-form, with interactions between the distal residues and Thr95; and an open β form, with interactions between two distal residues (Figure 1.4).[17] The multiple hydrogen bonding patterns with bound O_2 in the heme pocket implies HemAT has multiple O_2 dissociation rates.

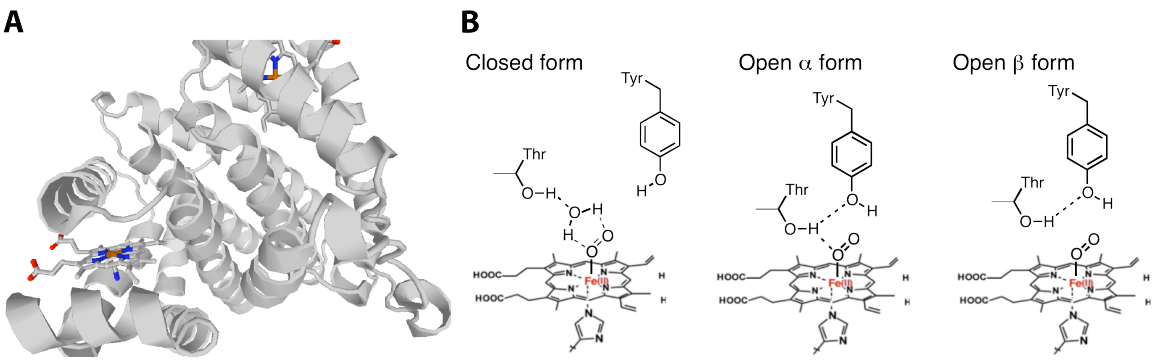

Figure 1.4. Crystal structure of the heme-bond sensing domain dimer of *B. subtilis* HemAT (PDBID 1OR4) (A) and key residues important for heme and ligand binding in the heme-pocket (B).[8c, 17] Both Tyr70 and Thr95 in the distal side of the heme-pocket are involved in the distal hydrogen-bonding network with gas ligand O_2 (B).

Additionally, *Bpe*GReg from whooping cough pathogen *Bordetella pertussis*, contains a N-terminal heme-bound globin domain and C-terminal DGC-containing domain that synthesizes a second messenger, bis- (3'-5')- cyclic diguanylate monophosphate (c-di-GMP), upon O_2 binding.[18] Dimeric or tetrameric form of *Bpe*GReg is the active form; an active site in each monomer binds to one GTP molecule, allowing two molecules of GTP to form c-di-GMP.[19] *Bpe*GReg in *B. pertussis* is known to be involved in biofilm formation, which is important for bacterial virulence, due to the role of c-di-GMP in stimulating expression of biofilm-associated exopolysaccharides (EPSs), a structural scaffold of biofilms.[20] O_2 binds to the heme of DGC-containing GCSs increases the catalytic activity of DGCs, which leads to up-regulation of biofilm formation in *B. pertussis*; this property distinguishes DGCs from other heme-based sensors containing PAS (Per-Arnt-Sim) and GAF (cGMP-specific and stimulated

phosphodiesterase, Adenylate cyclases and *E. coli* Formate hydrogen lyase transcriptional activator) domains, as their catalytic activities are enhanced through O_2 dissociation.[8c, 11c, 12, 21] In fact, O_2 sensing by globins to enhance biofilm production is a widespread phenomenon in various bacteria.[11c]

Other heme-containing GCSs include *E. coli Ec*DOS (*E. coli* Direct Oxygen Sensor), which contains a PDE catalytic domain that hydrolyzes c-di-GMP to linear di-GMP in response to O_2 availability, is involved in maintaining c-di-GMP homeostasis.[18-19, 22]

1.2.3 Prokaryotic Kinase Pathway

The ability for all organisms to adapt to changes in their environment is crucial for survival. Protein phosphorylation is one of the most common pathways to alter enzymatic activity and cellular responses required to change growth conditions in all life forms. Bacterial two-component signaling systems contain a kinase and a response regulator protein (Figure 1.5).[3c, 23] Kinases in prokaryotes usually phosphorylate histidine and aspartate amino acid residues, whereas eukaryotic kinases are evolved to phosphorylate serine, threonine and tyrosine residues.[1, 24] In *E. coli*, extracellular stimuli activate a histidine kinase EnvZ, which transfers the γ-phospohryl group in ATP to the histidine residue in kinase EnvZ, before transferring it to the Asp side chain in the regulatory protein OmpR (Figure 1.6).[25]

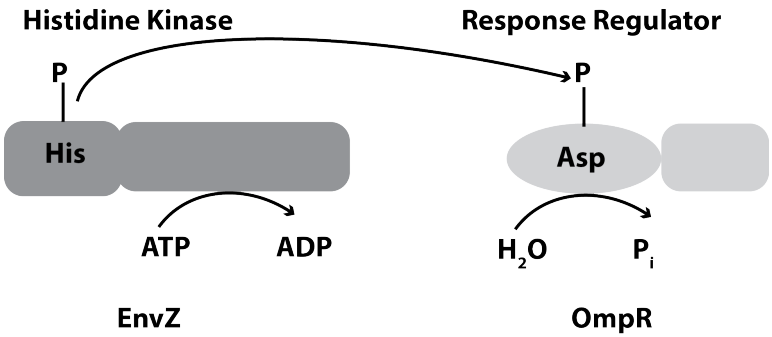

Figure 1.5. Schematic diagram of a bacterial two-component signaling system exemplified by the *E. coli* osmoregulatory system.[24] The phosphoryl transfer between kinase EnvZ and response regulator OmpR controls the expression of genes that are responsible for outer membrane porin production in *E. coli*.[26]

1. Autophosphorylation $ATP + HK\text{-}His \rightleftharpoons HK\text{-}His\text{-}P + ADP$

2. Phosphorylation $HK\text{-}His + RR\text{-}Asp \rightleftharpoons HK\text{-}His + RR\text{-}Asp\text{-}P$

3. Dephosphorylation $RR\text{-}Asp\text{-}P + H_2O \rightleftharpoons RR\text{-}Asp + P_i$

HK: histine kinase
RR: response regulator

Figure 1.6. Chemistry of the prokaryotic two-component phosphoryl transfer reaction involving a protein kinase and a response regulator.[24]

Histidine kinases contain an N-terminal sensing domain and a C-terminal catalytic region. For example, *E. coli* osmosensor EnvZ is composed of a periplasmic N-terminal sensing domain and a cytoplasmic C-terminal catalytic domain.[27] The N-terminal sensing domains in bacteria share little sequence identity, allowing them to sense various environmental signals.[24] The conserved C-terminal catalytic core of bacterial histidine

kinase include a dimerization domain and a catalytic domain responsible for ATP-binding and phosphotransfer.[28] In EnvZ, the nucleotide-binding region is highly flexible, which is required for the conformational changes after ATP binding.[27a, 29]

In most prokaryotic systems, the response regulator is the terminal component of the pathway, responsible for generating adaptive responses once activated.[24, 30] Common structures of response regulators include a conserved N-terminal regulator domain and a variable C-terminal output domain.[30] Most regulator domains are transcription factors with DNA-binding domains that function to alter gene expression levels, with a few exceptions, including *E. coli* CheB which regulates chemotaxis and RegA which controls cAMP hydrolysis in the *Dictyostelium* species.[30] The regulatory domains of response regulators exist in equilibrium between active and inactive forms.[24] Phosphorylation of the regulator domain pushes the equilibrium towards the active form. The conformational change induced by phosphorylation affects a large portion of the regulatory domain, activating the functional domain through protein-protein interactions.[24] The output domains are responsible for DNA-binding and controlling subsequent gene transcription. OmpR/PhoB subfamily is the largest and well-characterized response regulator subfamily. The OmpR/PhoB protein members contain a recognition helix that binds to the major groove of DNA and regulate expression levels of genes that encode outer membrane porin proteins.[31] However the active site structure, DNA-binding region, and the catalytic mechanism differ even in proteins within the same regulator family.[31]

The general stress response is also regulated by kinases in bacteria.[32] The response to stress provides cells with a protective mechanism against a wide range of

environmental stress, and many kinase pathways are involved in stress sensing.[33] The general stress-response pathway was first identified and characterized in the Gram-positive model bacterium *B. subtilis*. The *B. subtilis* stressosome, a 1.8 MDa signaling complex of a "general stress response" module, is involved in activation of the general stress response sigma factor, σ^B, in response to diverse environmental stresses.[34]

Although the ubiquitous two-component signal transduction system of prokaryotes has been found in a limited number of yeast strains, it is absent in mammals.[24, 35] Thus studying prokaryotic two-component systems have gained promise for facilitating the discovery of structurally unique broad-spectrum antibiotics.[24]

1.3 Mammalian Second Messenger Signal-Transduction Pathways

1.3.1 Introduction

Although the structures and activities of the modular domains are conserved, configurations of eukaryotic and prokaryotic two-component systems are different.[1, 24] In eukaryotes, the two-component system is also regulated by other signaling components, enabling signals to transmit from the cytoplasm to the nucleus, where transcription occurs.[1, 24] One mechanism by which eukaryotes regulate intracellular pathways is second messenger signaling. Second messengers, such as adenosine 3',5'-cyclic monophosphate (3',5'-cAMP) and guanosine 3',5'-cyclic monophosphate (3',5'-cGMP) are released by the cells in response to exposure to primary messengers, such as hormones and neurotransmitters.

3’,5’-cAMP and 3’,5’-cGMP consist of a purine base, a ribose ring and a cyclized phosphate group, where the cyclization occurs between the 3’- and 5’-positions, yielding a six-membered cyclized phosphate ring fused in trans-configuration with the five-membered furanose ring (Figure 1.7).

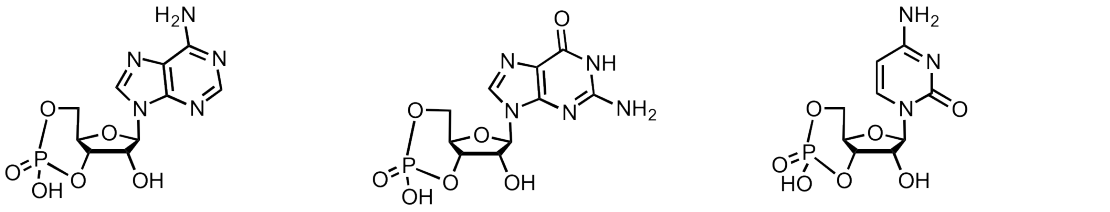

Figure 1.7. Structures of three cyclic 3’,5’-nucleotide monophosphates (3’,5’-cNMPs), 3’,5’-cAMP, 3’,5’-cGMP and 3’,5’-cCMP.

Second messengers, such as 3’,5’-cAMP and 3’,5-cGMP, perform crucial roles in regulating cellular metabolism and mediating numerous biochemical processes in mammals.[36] The second messenger signaling pathway, once considered simple and straightforward, is extremely complex. This is mainly due to the presence of multiple isoforms of cyclases (the enzyme synthesizes cyclic nucleotides) and phosphodiesterases (PDEs) (the enzyme hydrolyzes cyclic nucleotides), which inter-regulate the intracellular second messengers levels.[37] The complexity also comes from the fact that activation of these cyclases or PDEs is not linear, but is instead regulated by intracellular ion (Na^+ and Ca^{2+}) concentration, allosteric regulations, and protein-protein interaction between different isoforms.[37]

1.3.2 The Second Messenger Signaling Pathway

In 1956, Earl Sutherland isolated 3',5'-cAMP in various rat organs.[38] The discovery of 3',5'-cAMP led to our current paradigm of hormone signaling involving second messengers. Earl Sutherland recognized the importance of 3',5'-cAMP in regulating cellular signaling transduction and proposed the secondary messenger hypothesis to describe the physiological importance of 3',5'-cAMP in mammals (Figure 1.8).[39] Hormone adrenalin secreted from adrenal glands exterior to the cell acts as a primary messenger. The adrenalin circulating in the bloodstream binds to a G protein-coupled receptor outside of the cell membrane, causing a conformational change in the receptor protein.[39-40] This change transmits a signal to and activates adenylate cyclase, a cAMP-synthesizing enzyme on the interior of the cell membrane; and activation of this enzyme results in synthesis and release of 3',5'-cAMP into the cell as a secondary messenger.[39] Within the cell, cAMP acts as a secondary messenger that activates cAMP-dependent protein kinase (PKA). Activated PKA in turn phosphorylates the corresponding downstream substrate proteins, causing alterations in their activities.[40-41] The signal can also be regulated by phosphodiesterase, which hydrolyzes 3',5'-cAMP to 5'-AMP, and in turn reducing the intensity of the 3',5'-cAMP response.[42]

3',5'-cAMP mediates various intracellular processes in response to activation of G protein-coupled receptors by a primary messenger. Over the past few decades, the types of the metabolic responses generated by hormone-induced activation of PKAs were found to vary widely among different tissue cells in mammals (Table 1.1).[36a, 40] For instance, 3',5'-cAMP-dependent responses regulate glycogen metabolism in liver and

muscle cells through coordinated regulation of both stimulatory and inhibitory pathways.[36a] The dual regulation activates enzyme degrading glycogen to glucose-1-phosphate while inhibiting enzymes responsible for glycogen synthesis.[36a] Elevation of 3',5'-cAMP stimulated by catecholamine in the smooth muscle leads to muscle relaxation.[33, 43] The increase of 3',5'-cAMP level activates production of fatty acids by lipases.[44] These fatty acids are used as energy sources in kidney, heart and muscles.[44]

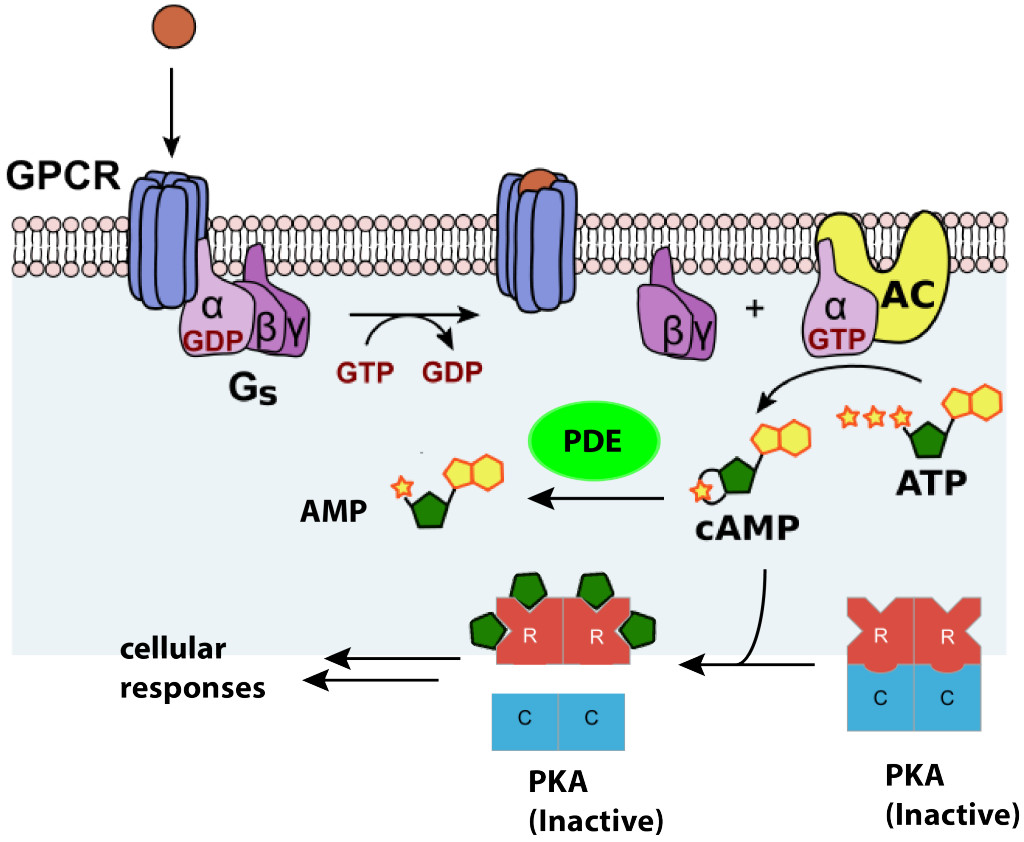

Figure 1.8. Secondary messenger signaling pathway.[36a, 45] A primary messenger, such as hormone, binds to a G-protein coupled receptor on the exterior of the cell membrane, causing a conformational change that activates adenylate cyclase. 3',5'-cAMP

synthesized by adenylate cyclase binds to and activates PKAs, which phosphorylate downstream proteins, promoting various cellular responses in mammalian cells.

Table 1.1. Examples of hormone-induced cellular responses in eukaryotes.[36a, 46]

Tissues	Induced hormones	Cellular responses
Adipose	Epinephrine and glucagon	Increased lipolysis, decreased amino acid uptake and decreased glycogen synthetase activity
Liver	Epinephrine and glucagon	Increased conversion of glycogen to glucose, decreased synthesis of glycogen and increased gluconeogenesis
Ovary	Follicle-stimulating hormone (FSH) and Luteinizing hormone (LH)	Increased production of estradiol and progesterone
Cardiac muscle cells	Epinephrine	Increased contractility
Skeletal muscle	Epinephrine	Increased glycogen to glucose conversion
Thyroid	(Thyroid-stimulating hormone) TSH	Increased thyroid hormone release
Bones	Parathyroid hormone	Increased calcium resorption from bones
Kidney	Vasopressin	Increased rennin production

1.3.3 Adenylate Cyclase

The enzyme responsible for converting ATP to 3',5'-cAMP is adenylate cyclase (Figure 1.9).[39] Adenylate cyclase is located within the plasma membrane; upon activation of adenylate cyclase by hormones located on the external surface of the target cells, 3',5'-cAMP is formed and released within the cells.[39] Communication between the external and internal environment allows the cells to adapt to extracellular environmental changes and is extremely crucial for stress adaptation and maintaining homeostasis. Extracellular

signals can be recognized and transmitted through a system involving three membrane components: G protein-coupled receptors, heterotrimeric G protein, and adenylate cyclase.[39]

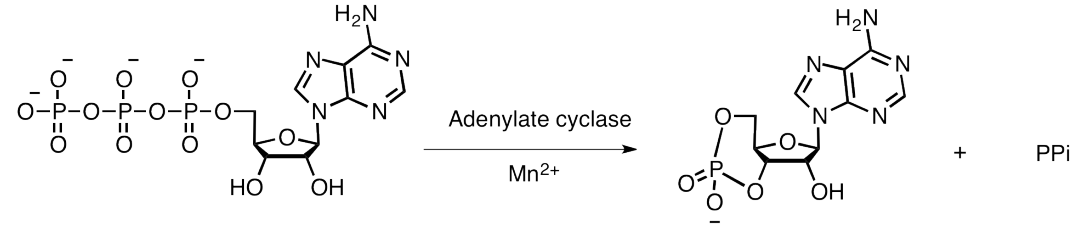

Figure 1.9. Synthesis of 3',5'-cAMP from ATP by adenylate cyclase.

In mammals, many different cell-surface receptors couple to a trimeric G protein to form a signal-transducing protein unit. Cell-surface receptors include numerous hormone and neurotransmitter receptors, light-activated receptors in the eyes, as well as odorant receptors in the nose. Although activating different receptors lead to various cellular responses, the signaling transduction mechanism proceeds in very similar ways. The most important energy sources glucose and fatty acids are generated by binding epinephrine to β-adrenergic receptors coupled to a G protein on the surface of the liver, heart muscles, and kidneys. β-adrenergic receptors are important drug targets for management of cardiac arrhythmias and treatment of hypertension. The activated heterotrimeric G protein exchanges GTP to GDP, and triggers the dissociation of $G_{s\alpha}$, a G protein subunit, from the G protein complex (Figure 1.8).[47] The dissociated $G_{s\alpha}$ binds and activates adenylate cyclase.[47] G proteins link cell-surface receptors and adenylate

cyclases through protein-protein interactions, providing a signaling cascade between hormone binding to an extracellular receptor and activation of intracellular adenylate cyclase.

To date, there are 10 homologs of adenylate cyclases characterized in mammals, including 9 transmembrane enzymes and one soluble adenylate cyclase.[48] All membrane-bound isoforms contain two transmembrane regions M_1 and M_2 and two catalytic domains C_1 and C_2.[49] The two catalytic domains C_1 and C_2 locate on the cytosolic side of the plasma membrane.[49a] Despite the fact that each isoform of adenylate cyclase is involved in unique and diverse signaling responses, their catalytic domains are highly-conserved, not only in bacterial and fungal adenylate cyclases, but also in other cyclases, such as guanylate cyclase, the enzyme responsible for 3',5'-cGMP synthesis.[49c] The cyclization reaction proceeds by attacking the α-phosphate group by the 3'-OH, resulting in inversion of configuration at the α-phosphate.[50] Therefore, in the catalytic site, the 3'-OH must be activated to be able to attack the α-phosphate position, and ATP must be stabilized in such a conformation where 3'-OH can easily approach the α-phosphate group.[51]

Adenylate cyclase activity requires Mg^{2+} or Mn^{2+} as metal cofactors.[52] Mg^{2+} binds to ATP to form magnesium-ATP complex, and it may bind to the regulatory site on the enzyme.[53] It has been confirmed that two Mg^{2+} ions are required in the magnesium-ATP complex.[49b, 54] Moreover, the regulatory effects of Ca^{2+} vary in different adenylate cyclase isoforms.[55] Ca^{2+} activates type I and VIII enzymes through activation of calmodulin, while inhibits type III and IX enzymes via calmodulin-dependent kinase.[55-56]

1.3.4 Discovery of Guanosine 3',5'-Cyclic Monophosphate (3',5'-cGMP) and Guanylate Cyclase

While 3',5'-cAMP has widespread effects on mammalian metabolic pathways, a second naturally occurring cyclic nucleotide, guanosine 3', 5'-cyclic monophosphate (3',5'-cGMP) is analogous but has a more restricted role and plays a crucial role in, for instance, visual excitation by regulating ion channel conductance.[36b] Enzymes responsible for 3',5'-cGMP metabolism are analogous to those of 3',5'-cAMP, such as guanylate cyclase, 3',5'-cGMP-dependent protein kinase, and 3',5'-cGMP phosphodiesterase (PDE).

Guanylate cyclase catalyzes the conversion of GTP to 3',5'-cGMP. The enzyme family consists of both soluble and membrane-bound isozymes that are expressed in nearly all cell types.[36b] To date, there are seven membrane-bound guanylate cyclases (pGCs) identified in mammals. They contain highly conserved structures, which include an N-terminal extracellular binding domain, a transmembrane domain, a middle domain, and a C-terminal catalytic domain (Figure 1.10).[36b] The structure of the transmembrane domain varies among different pGCs. The hydrophilic region of the transmembrane domain enables membrane localization of the pGCs. The kinase domain is absent in soluble guanylate cyclase (sGC). The pGCs family consist of 11 subdomains and 33 conserved amino acids that are important for catalytic activitiy.[57] Similar to adenylate cyclase, dimerization of two catalytic subunits to form one active site results in binding of one substrate per dimer in pGCs.[51a] The structure of the catalytic domain of guanylate cyclase is closely related to adenylate cyclase, and it is highly conserved in both pGCs

and sGCs.[48b] The invariant amino acid residues interacting with the purine ring in the catalytic domains of adenylate cyclase is also conserved in pGCs to control substrate specificity.[48b]

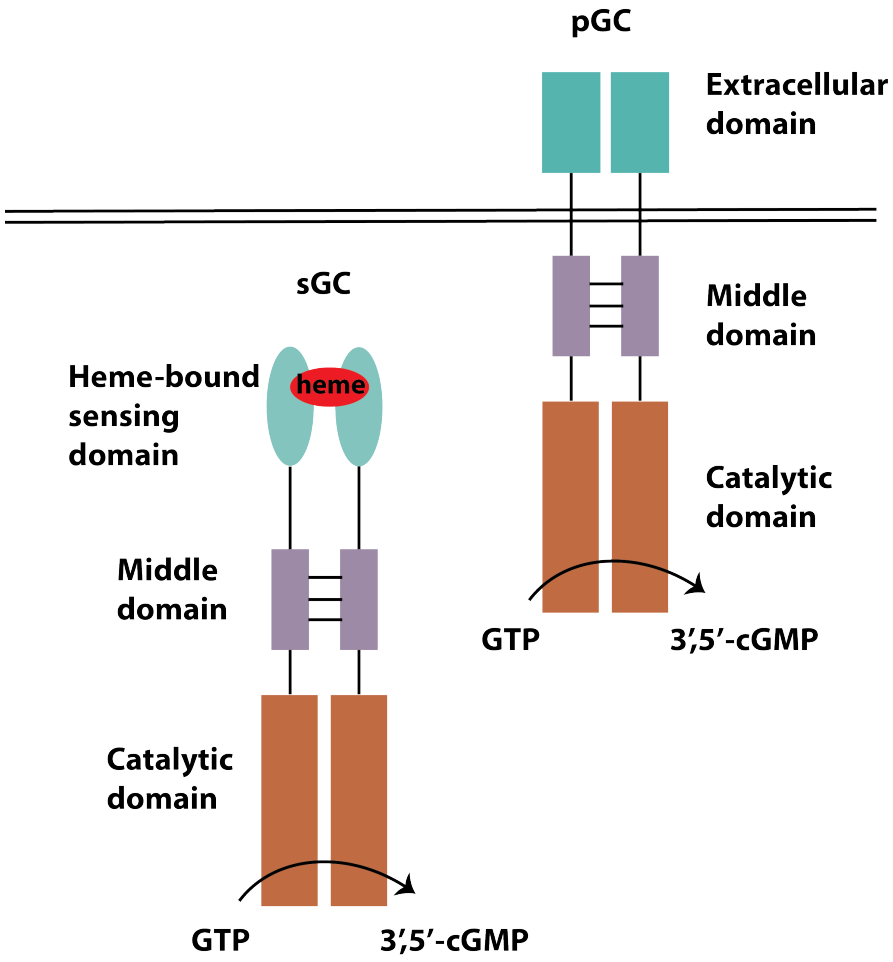

Figure 1.10. Illustration of mammalian membrane-bound and soluble guanylyl cyclase (sGC).[36b]

sGCs regulate a wide range of biological functions, including visual signal transduction, smooth muscle relaxation, vasodilatation and platelet aggregation.[58] Each subunit of sGCs contain an N-terminal heme-bound H-NOX (Heme-Nitric Oxide/

Oxygen) domain and C-terminal catalytic domain.[36b] As mentioned in section 1.2.2, the heme-bound sensing domain senses environmental signals such as gaseous O_2, NO and CO, and alters the activity of the catalytic domain.

1.3.5 3',5'-Cyclic Nucleotide Phosphodiesterase (PDE)

PDE regulates cellular responses via breakdown of 3',5'-cNMP at the 3'-cyclic phosphate bond (Figure 1.11).[59] Recent studies using enzymatic fractionation and sequencing techniques have revealed the genomic complexity of the PDE family and the molecular identity of each enzyme member. Similar to adenylate cyclase, activities of PDE are not only regulated at the transcriptional level, but also at the protein level via phosphorylation state, allosteric regulation and various protein-protein interactions.[60]

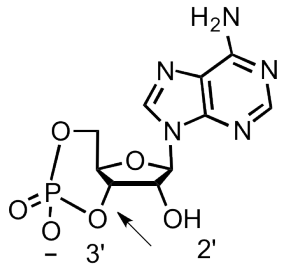

Figure 1.11. PDE hydrolyzes 3'-cyclic phosphate bond of 3',5'-cAMP.

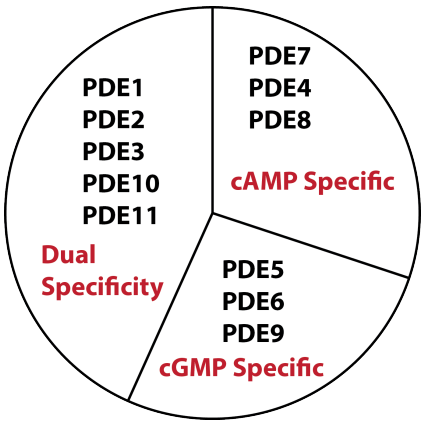

Figure 1.12. Classification of the mammalian PDE family.[60] The 11 previously identified PDE family members can be categorized based on substrate specificity.

To date, there are 11 different PDE family members reported, and each family member contains several different isoforms that differ in their structure, kinetic properties, substrate specificity and intracellular localization. Some hydrolyze 3',5'-cAMP specifically, others hydrolyze 3',5'-cGMP selectively, while the rest are multifunctional PDEs, recognizing and hydrolyzing more than one substrate (Figure 1.12).[60b] Enzymes in the PDE4 sub-family are known to have low K_m and high substrate specificity for 3',5'-cAMP.[60b] Enzymes in PDE 7 and 8 also are 3',5'-cAMP specific.[60b] Enzymes in PDE 9 family are activated by binding of 3',5'-cGMP at the allosteric binding site on the N-terminal half of the PDE.[60b] Additionally, PDE families 1, 2, 3, 10 and 11 that show broad substrate specificity can be used for studying activity for atypical cyclic nucleotides such as 3',5'-cCMP. The different families of PDEs are not uniformly distributed within the cell, providing another important tool for controlling compartmentalized concentrations of 3',5'-cNMPs.[61]

As signaling networks of 3',5'-cAMP and 3',5'-cGMP are involved in regulation of numerous physiological responses, the role of the PDE family as therapeutic targets has been investigated for decades and shown great promise. PDE5 inhibitors sildenafil (Viagra), tadalafil (Cialis) and vardenafil (Levitra) are commercial drugs for treating erectile dysfunction and PDE3 inhibitors such as cilostazol (Pletal) are used for treatment of acute heart failure.[60b]

1.3.6 3',5'-cAMP-Dependent Protein Kinase (PKA)

The most common downstream effector of 3',5'-cAMP is PKA (Figure 1.8). The inactive PKAs contain two regulatory domains and two catalytic sites.[62] Regulation of

PKAs involves 3',5'-cAMP binding to one of the regulatory subunits and activates kinase activity.[62b] Each regulatory domain binds two 3',5'-cAMP molecules; after binding, the inactive enzyme dissociates into a regulatory subunit dimer with four molecules of 3',5'-cAMP bound, as well as two active catalytic domains.[62]

Amplification of a signal cascade is achieved though activation of PKAs, as active PKAs can phosphorylate numerous substrates.[62] If the substrate protein is also a kinase, it can further amplify the signal. This series of signal cascade amplifications can occur on a millisecond scale, allowing cells to quickly respond to environmental changes. Activation of PKAs also leads to stimulation of phosphorylase, which catalyzes hydrolysis of glycogen to glucose-1-phosphate. Protein phosphorylation is the one of most abundant protein post-translational modifications, and is a common way to regulate enzymatic activities and cellular responses. In fact, protein kinases have become important group of drug targets, as kinase inhibitors have been developed to treat cancer and chronic inflammatory diseases.[62a]

1.3.7 Cytidine 3',5'-Cyclic Monophosphate (3',5'-cCMP)

While 3',5'-cAMP and 3',5'-cGMP are well-established second messengers, a potential third naturally occurring pyrimidine cyclic nucleotide, 3',5'-cCMP, was initially reported in Leukemia L-1210 cells.[63] Elevation of 3',5'-cCMP concentration was later detected in urine samples of acute leukemia patients and in rapidly dividing tissues.[64] Subsequently, putative proteins capable of synthesizing and hydrolyzing 3',5'-cCMP, cytidylate cyclase and 3',5'-cCMP-specific phosphodiesterase (cCMP-specific PDE), as well as 3',5'-cCMP-dependnt protein kinases were reported, but have yet to be

conclusively identified and characterized.[59b, c, 65] 3',5'-cCMP has shown to stimulate phosphorylation of Rab23, a negative regulator of the tumorigenic sonic hedgehog (shh) signaling pathway.[66] The shh signaling pathway controls neural tube development, and is one of the key regulators during animal development.[67] One explanation is that phosphorylation of Rab23 inactivate its inhibitory effect on shh, thereby allowing the upregulation of shh pathway which ultimately leads to tumor formation.[66] The identification of Rab23 as a response target for 3',5'-cCMP confirms the role of 3',5'-cCMP in signaling pathways in the brain. While the potential role of 3',5'-cCMP in tumorigenesis and cellular proliferation has been suggested over the past few decades, its biological functions still remain unknown.[66] Studying 3',5'-cCMP and its role as a signaling molecule could lead to discoveries of novel signaling pathways and offer a platform to study the interplay of the signaling networks.

1.3.8 Early Characterization of Cytidylate Cyclase

Bloch and Ignarro reported the first isolation of a partically purified cCMP-specific cytidylate cyclase from mouse liver by monitoring the formation of [α-^{32}P] cCMP from tissue homogenates incubated with [α-^{32}P] CTP and Mn^{2+} in 1977.[65a] Although the putative cytidylate cyclase has different characteristics than known cyclases, such as different pI, temperature optima and different response to inhibitors of known cyclases, the identity of this putative cytidylate cyclase was still vigorously challenged over the next few decades.[65a] Several groups have repeated the assay procedure of Ignarro's group and the obtained ^{32}P-labelled product yielded three major peaks after being purified on an ion-exchange chromatography, and only one of the

purified products co-eluted with authentic 3',5'-cCMP.[68] It was also found that several tissue-extracted compounds that were chromatographically separated from authentic cCMP show cross-reactivity with anti-cCMP antibody.[40, 69] Using fast atom bombardment (FAB)-based mass spectrometry, Newton isolated 3',5'-cCMP as well as four other novel cytidine compounds.[70] The other novel cytidine compounds include, cytidine 3', 5' cyclic pyrophosphate, cytidine 2'-monophosphate 3', 5' cyclic monophosphate, cytidine 2'-O-aspartyl-3', 5'-cyclic monophosphate and cytidine 2'-O-glutamyl-3'5'-cyclic monophosphate, all of which were found to be cCMP-immunoreactive.[71] Recent research also has revealed the promiscuity of purified soluble guanylyl cyclase (sGC) and its ability to synthesize cGMP, cAMP and cCMP at various rates, casting doubt on the authenticity of the previous isolated cytidylate cyclase.[72] Therefore, the identity of the previously purified multifunctional cytidylate cyclase, as well as isolation and characterization of an authentic cytidylate cyclase in rat tissues still remains unclear.

1.3.9 Discovery of 3',5'-cCMP Phosphodiesterase (PDE) and Potential 3',5'-cCMP-Dependent Protein Kinase

The first isolated PDE in rat liver that preferentially hydrolyzed 3',5'-cCMP over 3',5'-cAMP and 3',5'-cGMP was reported by Cheng and Bloch.[65c] It was later discovered that this multifunctional PDE was not only capable of hydrolyzing 3',5'-cNMPs, but also 2',3'-cNMPs.[59b, 69c] A second putative cCMP-specific PDE which showed specificity for 3',5'-cCMP was isolated from rat liver using ammonium sulfate precipitation.[73] The putative cCMP-specific PDE has a molecular weight of 28 kDa, a pH optimum around

7.2-7.4, and a K_m for 3',5'-cCMP around 9 mM, which is an order of magnitude greater than that of the promiscuous enzyme mentioned previously.[73] The cCMP-specific phosphodiesterase contains significantly more cysteine, aspartate, and arginine amino acid residues per mole, indicating this putative PDE is not merely a fragmentation of the previously identified PDEs.[73] However, revealing the true identity of previously identified PDEs has been unfruitful, as further characterization and determination of the molecular identity of these enzymes remain inconclusive.[74]

A 3',5'-cCMP-binding protein was partially purified from the soluble fraction of rat organs. This 3',5'-cCMP-binding protein has a molecular weight of 50 kDa, and exhibits a binding specificity toward 3',5'-cCMP. However, further purification and characterization of this protein was unsuccessful. Recent studies have found that 3',5'-cCMP interacts and stimulates purified PKA and PKG in lung and intestine tissues, suggesting its role in regulating physiological process of lung and intestine.[75]

1.4 Eukaryotic 2',3'-cAMP-Adenosine Pathway

1.4.1 Introduction

In addition to 3',5'-cyclic nucleotides (3',5'-cNMPs), presence of the 2',3'-regioisomers, 2',3'-cyclic nucleotides (2',3'-cNMPs) have been reported in mammalian and other cell types.[76] The five-membered cyclic phosphate ring bears considerable ring strain, therefore 2',3'-cyclic nucleotides are more prone to hydrolysis than the corresponding 3',5'-cyclic nucleotide regioisomers (Figure 1.13).[76d]

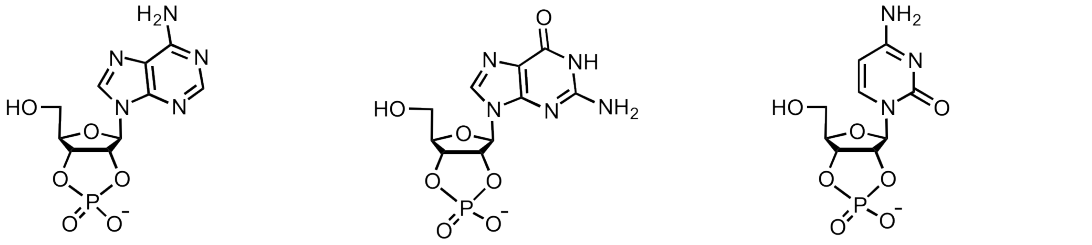

Adenosine 2', 3'-cyclic monophosphate (2',3'-cAMP)

Guanosine 2', 3'-cyclic monophosphate (2',3'-cGMP)

Cytidine 2', 3'-cyclic monophosphate (2',3'-cCMP)

Figure 1.13. Structures of 2’,3’-cyclic nucleotides monophosphates (2’,3’-cNMPs).

Using liquid chromatography-tandem mass spectrometry (LC-MS/MS), Jackson reported the first detection and identification of 2’,3’-cAMP in rat kidney.[77] In addition to 2’,3’-cAMP, various atypical cyclic nucleotides, such as 2’,3’-cGMP and 2’,3’-cAMP, were found in multiple mammalian organs as well as in Tobacco plants.[76a-c] 2’,3’-cAMP is known to participate in a post-injury mechanism in mammals, and 2’,3’-cAMP and GMP have been shown to correlate with leaf wounding stress in Arabidopsis.[78] Despite the mounting evidence suggesting that these nucleotides may be important signaling molecules in post-injury mechanisms, the role of the atypical cyclic nucleotides *in vivo* is unknown.

1.4.2 2’,3’-cAMP-Adenosine Pathway

In 2001, Jackson proposed the 2’,3’-cAMP-adenosine pathway, postulating a role for 2’,3’-cAMP in response to acute organ damage.[76b, c] Previous NMR studies have suggested that 2’,3’-cAMP is a degradation product of mRNA.[79] Tissue injury triggers mRNA degradation, therefore it is highly likely to also activates 2’,3’-cAMP-adenosine pathway.[76d, 79]

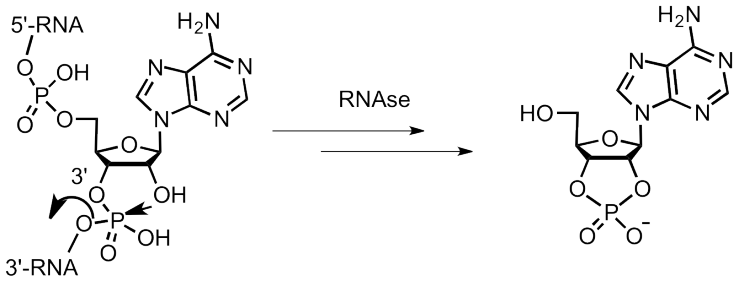

Figure 1.14. Proposed mechanism for RNase-mediated mRNA degradation.[80]

Stimulation of mRNA turnover leads to ribonuclease (RNase)-mediated mRNA degradation, in which RNase cleaves the phosphodiester bonds in the poly-A tail to form 2',3'-cAMP (Figure 1.14).[76d, 79] Membrane-bound active transporter such as MRP4 and MRP5 that are used to transport various nucleotides and nucleosides are likely to also transport 2',3'-cNMPs from cells (Figure 1.15).[81] Multiple isoforms of intracellular and extracellular PDEs, such as 2',3'-cAMP-3'-phosphodiesterase (CNPase) and 2',3;-cAMP-2'-phosphodiesterase (RNase) can hydrolyze 2',3'-cAMP to its corresponding 3'-AMP or 2'-AMP product respectively (Figure 1.15).[79, 82] In addition to 5'-AMP, both 2'- and 3'-AMP were found to be precursors to adenosine in kidneys, as increasing level of 2'- and 3'-AMP induces production of adenosine as efficiently as 5'-AMP.[83] Adenosine is an important metabolite involved in post-injury mechanisms, as extracellular adenosine binds to adenosine receptors and protects organs from injuries.[83] Therefore, it is possible that the 2',3'-cAMP-adenosine pathway is one of the redundant pathways nature created to maintain the adenosine concentration. Additionally, 2'3'-cAMP is known to facilitate activation of the mitochondrial permeability transition pores, which leads to apoptosis and necrosis.[76d]

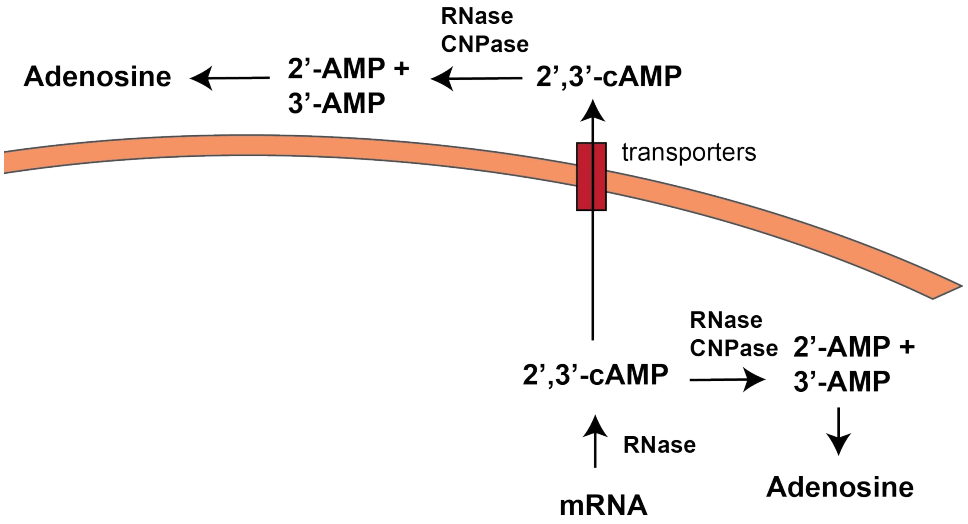

Figure 1.15. Proposed extracellular and intracellular 2',3'-cAMP-adenosine signaling pathway.[76d] mRNA degradation using RNase produces 2',3'-cAMP, which can be transported outside the cell through MRP4 and MRP5. Increasing concentration of 2'- and 3'-AMP elevates the production of adenosine.

To date, there are multiple isoforms of CNPase reported in renal cells; all of them hydrolyze 2',3'-cAMP to its corresponding 2'-AMP.[84] In the deletion strain deficient in CNPases, 2',3'-cAMP accumulation and adenosine reduction have been observed.[84] CNPase is the third most abundant protein in myelin sheath in the brain, therefore 2',3'-cAMP-adenosine pathway may be involved in the recovery mechanism after brain injury.[82] Despite the progress that has been made to establish the physiological roles of the atypical 2',3'-cyclic nucleotides, the enzymes involved in the signaling pathway, as well as the their physiological roles still remain inconclusive.

1.5 Aim and Scope of the Dissertation

This dissertation focuses on understanding various signal transduction pathways in prokaryotic and eukaryotic systems. Although kinases are known to be involved in essential signal transduction pathways in stress adaptation in bacteria, the bacterial mechanisms used to sense stress remains unclear.[32] We discovered a novel sensing mechanism used by Gram-negative bacteria to adapt to limited O_2 condition by altering their stress-response pathways. Additionally, studying signaling pathways of cNMPs, the naturally occurring potential secondary messengers, provide understandings of their role in survival and tumorigenesis, and allow for the study of the interplay between different secondary messenger systems in eukaryotes.

In chapter 2, a novel stressosome-based signal transducer that is hypothesized to regulate the environmental stress response in Gram-negative marine bacterium *Vibrio brasiliensis* is described. The stressosome contains a heme-bound GCS that senses environmental O_2, and alters phosphorylation activity in response to gaseous ligands. The described complex presents an opportunity to interrogate the effects of ligand-dependent stressosome signaling both *in vitro* and *in vivo*, as well as provides further insights into how this stress response pathway could potentially be involved in regulating virulence gene transcriptions in the *Vibrio* genus.

In chapter 3, I report our recent progress toward development of an efficient protocol to identify enzyme members of the 3',5'-cCMP signaling pathways. Following previously published protocols, we have partially purified a putative soluble cytidylate cyclase that synthesizes 3',5'-cCMP from CTP in rat livers. Additionally, we also have

isolated a potential 3',5'-cCMP-binding protein, THO complex subunit 5, using 3',5'-cCMP affinity chromatography. THO complex subunit 5 is involved in cellular proliferation by controlling transcription and mRNA export, suggesting 3',5'-cCMP may be involved in regulating transcription through THO subunit 5.

In chapter 4, we developed a sensitive and versatile method to extract and quantify cyclic nucleotide monophosphates (cNMPs) using LC-MS/MS, including both 3',5'-cNMPs and 2',3'-cNMPs, in mammalian tissues and cells.[85] This protocol allows for comparison of multiple cNMPs in the same systems and was used to examine the relationship between tissues levels of cNMPs in various systems. Utilizing this analytical method, I report the first identification and quantification of 2',3'-cIMP in mammals.[85] The developed analytical method offers a tool for quantification of cNMPs levels in cells and tissues of varying disease states, which will provide insight into the roles of cNMPs *in vivo*.

1.6 References

1. Cashin, P.; Goldsack, L.; Hall, D.; O'Toole, R., Contrasting signal transduction mechanisms in bacterial and eukaryotic gene transcription. *FEMS Microbiol Lett* **2006,** *261* (2), 155-64.

2. Berg JM, T. J. a. S. L., *Biochemistry. 5th edition*. W H Freeman: New York, 2002.

3. (a) Goudreau, P. N.; Stock, A. M., Signal transduction in bacteria: molecular mechanisms of stimulus-response coupling. *Curr Opin Microbiol* **1998,** *1* (2), 160-9; (b) Ottemann, K. M.; Koshland, D. E., Jr., Converting a transmembrane receptor to a soluble receptor: recognition domain to effector domain signaling after excision of the transmembrane domain. *Proc Natl Acad Sci USA* **1997,** *94* (21), 11201-4; (c) Parkinson, J. S.; Kofoid, E. C., Communication modules in bacterial signaling proteins. *Annu Rev Genet* **1992,** *26*, 71-112.

4. Ulrich, L. E.; Koonin, E. V.; Zhulin, I. B., One-component systems dominate signal transduction in prokaryotes. *Trends Microbiol* **2005,** *13* (2), 52-6.

5. Calogero, S.; Gardan, R.; Glaser, P.; Schweizer, J.; Rapoport, G.; Debarbouille, M., RocR, a novel regulatory protein controlling arginine utilization in Bacillus subtilis, belongs to the NtrC/NifA family of transcriptional activators. *J Bacteriol* **1994,** *176* (5), 1234-41.

6. Li, M.; Khursigara, C. M.; Subramaniam, S.; Hazelbauer, G. L., Chemotaxis kinase CheA is activated by three neighbouring chemoreceptor dimers as effectively as by receptor clusters. *Mol Microbiol* **2011,** *79* (3), 677-85.

7. Yeh, K. C.; Wu, S. H.; Murphy, J. T.; Lagarias, J. C., A cyanobacterial phytochrome two-component light sensory system. *Science* **1997,** *277* (5331), 1505-8. 8. (a) Guengerich, F. P., New trends in cytochrome p450 research at the half-century mark. *J Biol Chem* **2013,** *288* (24), 17063-4; (b) Poulos, T. L., Heme enzyme structure and function. *Chem Rev* **2014,** *114* (7), 3919-62; (c)

Shimizu, T.; Huang, D.; Yan, F.; Stranava, M.; Bartosova, M.; Fojtikova, V.;

Martinkova, M., Gaseous O2, NO, and CO in signal transduction: structure and function relationships of heme-based gas sensors and heme-redox sensors. *Chem Rev* **2015,** *115* (13), 6491-533; (d) Jain, R.; Chan, M. K., Mechanisms of ligand discrimination by heme proteins. *J Bio Inorg Chem* **2003,** *8* (1-2), 1-11.

9. (a) Fukuto, J. M.; Carrington, S. J.; Tantillo, D. J.; Harrison, J. G.; Ignarro, L. J.; Freeman, B. A.; Chen, A.; Wink, D. A., Small molecule signaling agents: the integrated chemistry and biochemistry of nitrogen oxides, oxides of carbon, dioxygen, hydrogen sulfide, and their derived species. *Chem Res Toxicol* **2012,** *25* (4), 769-93. 10. (b) Uchida, T.; Kitagawa, T., Mechanism for transduction of the ligand-binding signal in heme-based gas sensory proteins revealed by resonance Raman spectroscopy. *Accounts Chem Res* **2005,** *38* (8), 662-70.

11. (a) Farhana, A.; Saini, V.; Kumar, A.; Lancaster, J. R., Jr.; Steyn, A. J., Environmental heme-based sensor proteins: implications for understanding bacterial pathogenesis. *Antioxid Redox Sig* **2012,** *17* (9), 1232-45; (b) Gilles-Gonzalez, M. A.; Gonzalez, G., Heme-based sensors: defining characteristics, recent developments, and regulatory hypotheses. *J Inorg Biochem* **2005,** *99* (1), 1-22; (c) Martinkova, M.; Kitanishi, K.; Shimizu, T., Heme-based globin-coupled oxygen sensors: linking oxygen binding to functional regulation of diguanylate cyclase, histidine kinase, and methyl-accepting chemotaxis. *J Bio Chem* **2013,** *288* (39), 27702-11.

12. Freitas, T. A.; Hou, S.; Alam, M., The diversity of globin-coupled sensors. *FEBS letters* **2003,** *552* (2-3), 99-104.

13. Hou, S.; Larsen, R. W.; Boudko, D.; Riley, C. W.; Karatan, E.; Zimmer, M.; Ordal, G. W.; Alam, M., Myoglobin-like aerotaxis transducers in Archaea and Bacteria. *Nature* **2000,** *403* (6769), 540-4.

14. El-Mashtoly, S. F.; Gu, Y.; Yoshimura, H.; Yoshioka, S.; Aono, S.; Kitagawa, T., Protein conformation changes of HemAT-Bs upon ligand binding probed by ultraviolet resonance Raman spectroscopy. *J Bio Chem* **2008,** *283* (11), 6942-9.

15. Aono, S.; Nakajima, H.; Ohta, T.; Kitagawa, T., Resonance Raman and ligand-binding analysis of the oxygen-sensing signal transducer protein HemAT from Bacillus subtilis. *Method Enzymol* **2004,** *381*, 618-28.

16. Kitanishi, K.; Kobayashi, K.; Kawamura, Y.; Ishigami, I.; Ogura, T.; Nakajima, K.; Igarashi, J.; Tanaka, A.; Shimizu, T., Important roles of Tyr43 at the putative heme distal side in the oxygen recognition and stability of the Fe(II)-O2 complex of YddV, a globin-coupled heme-based oxygen sensor diguanylate cyclase. *Biochem* **2010,** *49* (49), 10381-93.

17. Ohta, T.; Yoshimura, H.; Yoshioka, S.; Aono, S.; Kitagawa, T., Oxygen-sensing mechanism of HemAT from Bacillus subtilis: a resonance Raman spectroscopic study. *J Am Chem Soc* **2004,** *126* (46), 15000-1.

18. Tuckerman, J. R.; Gonzalez, G.; Sousa, E. H.; Wan, X.; Saito, J. A.; Alam, M.; Gilles-Gonzalez, M. A., An oxygen-sensing diguanylate cyclase and phosphodiesterase couple for c-di-GMP control. *Biochem* **2009,** *48* (41), 9764-74.

19. Wan, X.; Tuckerman, J. R.; Saito, J. A.; Freitas, T. A.; Newhouse, J. S.; Denery, J. R.; Galperin, M. Y.; Gonzalez, G.; Gilles-Gonzalez, M. A.; Alam, M., Globins

synthesize the second messenger bis-(3'-5')-cyclic diguanosine monophosphate in bacteria. *J Mol Biol* **2009,** *388* (2), 262-70.

20. Hengge, R., Principles of c-di-GMP signalling in bacteria. *Nature Rev. Microbiol* **2009,** *7* (4), 263-73.

21. Gilles-Gonzalez, M. A.; Gonzalez, G., Signal transduction by heme-containing PAS-domain proteins. *J Appl Physiol (1985)* **2004,** *96* (2), 774-83.

22. Kitanishi, K.; Kobayashi, K.; Uchida, T.; Ishimori, K.; Igarashi, J.; Shimizu, T., Identification and functional and spectral characterization of a globin-coupled histidine kinase from Anaeromyxobacter sp. Fw109-5. *J Bio Chem* **2011,** *286* (41), 35522-34.

23. (a) Nixon, B. T.; Ronson, C. W.; Ausubel, F. M., Two-component regulatory systems responsive to environmental stimuli share strongly conserved domains with the nitrogen assimilation regulatory genes ntrB and ntrC. *Proc Natl Acad Sci USA* **1986,** *83* (20), 7850-4; (b) Hess, J. F.; Oosawa, K.; Kaplan, N.; Simon, M. I., Phosphorylation of three proteins in the signaling pathway of bacterial chemotaxis. *Cell* **1988,** *53* (1), 79-87.

24. Stock, A. M.; Robinson, V. L.; Goudreau, P. N., Two-component signal transduction. *Annu Rev Biochem* **2000,** *69*, 183-215.

25. Yang, Y.; Park, H.; Inouye, M., Ligand binding induces an asymmetrical transmembrane signal through a receptor dimer. *J Mol Bio* **1993,** *232* (2), 493-8.

26. Falke, J. J.; Bass, R. B.; Butler, S. L.; Chervitz, S. A.; Danielson, M. A., The two-component signaling pathway of bacterial chemotaxis: a molecular view of signal

transduction by receptors, kinases, and adaptation enzymes. *Annu Rev cell Dev Bi* **1997,** *13*, 457-512.

27. (a) Tanaka, T.; Saha, S. K.; Tomomori, C.; Ishima, R.; Liu, D.; Tong, K. I.; Park, H.; Dutta, R.; Qin, L.; Swindells, M. B.; Yamazaki, T.; Ono, A. M.; Kainosho, M.; Inouye, M.; Ikura, M., NMR structure of the histidine kinase domain of the E. coli osmosensor EnvZ. *Nature* **1998,** *396* (6706), 88-92; (b) Tomomori, C.; Tanaka, T.; Dutta, R.; Park, H.; Saha, S. K.; Zhu, Y.; Ishima, R.; Liu, D.; Tong, K. I.; Kurokawa, H.; Qian, H.; Inouye, M.; Ikura, M., Solution structure of the homodimeric core domain of Escherichia coli histidine kinase EnvZ. *Nat Struct Biol* **1999,** *6* (8), 729-34. 28. Swanson, R. V.; Bourret, R. B.; Simon, M. I., Intermolecular complementation of the kinase activity of CheA. *Mol Microbiol* **1993,** *8* (3), 435-41.

29. Stock, J. B.; Ninfa, A. J.; Stock, A. M., Protein phosphorylation and regulation of adaptive responses in bacteria. *Microbiol Rev* **1989,** *53* (4), 450-90.

30. Lukat, G. S.; McCleary, W. R.; Stock, A. M.; Stock, J. B., Phosphorylation of bacterial response regulator proteins by low molecular weight phospho-donors. *Proc Nat Acad Sci USA* **1992,** *89* (2), 718-22.

31. Aiba, H.; Nakasai, F.; Mizushima, S.; Mizuno, T., Phosphorylation of a bacterial activator protein, OmpR, by a protein kinase, EnvZ, results in stimulation of its DNA-binding ability. *J Biochem* **1989,** *106* (1), 5-7.

32. Marles-Wright, J.; Lewis, R. J., The stressosome: molecular architecture of a signalling hub. *Biochem Soc Trans* **2010,** *38* (4), 928-33.

33. Lundholm, L.; Mohme-Lundholm, E.; Svedmyr, N., Second symposium on catecholamines. Physiological interrelationships. Introductory remarks. *Pharmacol Rev* **1966,** *18* (1), 255-72.

34. (a) Dufour, A.; Voelker, U.; Voelker, A.; Haldenwang, W. G., Relative levels and fractionation properties of Bacillus subtilis sigma(B) and its regulators during balanced growth and stress. *J Bacteriol* **1996,** *178* (13), 3701-9 sigma; (b) Chen, C. C.; Lewis, R. J.; Harris, R.; Yudkin, M. D.; Delumeau, O., A supramolecular complex in the environmental stress signalling pathway of Bacillus subtilis. *Mol Microbiol* **2003,** *49* (6), 1657-69; (c) Marles-Wright, J.; Grant, T.; Delumeau, O.; van Duinen, G.; Firbank, S. J.; Lewis, P. J.; Murray, J. W.; Newman, J. A.; Quin, M. B.; Race, P. R.; Rohou, A.; Tichelaar, W.; van Heel, M.; Lewis, R. J., Molecular architecture of the "stressosome," a signal integration and transduction hub. *Science* **2008,** *322* (5898), 92-6.

35. Brown, J. L.; North, S.; Bussey, H., SKN7, a yeast multicopy suppressor of a mutation affecting cell wall beta-glucan assembly, encodes a product with domains homologous to prokaryotic two-component regulators and to heat shock transcription factors. *J Bacteriol* **1993,** *175* (21), 6908-15.

36. (a) Sutherland, E. W., Studies on the mechanism of hormone action. *Science* **1972,** *177* (4047), 401-8; (b) Lucas, K. A.; Pitari, G. M.; Kazerounian, S.; Ruiz-Stewart, I.; Park, J.; Schulz, S.; Chepenik, K. P.; Waldman, S. A., Guanylyl cyclases and signaling by cyclic GMP. *Pharmacol Rev* **2000,** *52* (3), 375-414.

37. Meyer, T., Cell signaling by second messenger waves. *Cell* **1991,** *64* (4), 675-8.

38. Sutherland, E. W.; Rall, T. W., Fractionation and characterization of a cyclic adenine ribonucleotide formed by tissue particles. *J Biol Chem* **1958,** *232* (2), 1077-91.

39. Sutherland, E. W.; Rall, T. W.; Menon, T., Adenyl cylase. I. Distribution, preparation, and properties. *J Bio Chem* **1962,** *237*, 1220-7.

40. Anderson, T. R., Cyclic cytidine 3',5'-monophosphate (cCMP) in cell regulation. *Mol Cell Endocrinol* **1982,** *28* (3), 373-85.

41. (a) Beebe S. J., C. J. D., Cyclic nucleotide-dependent protein kinases. *Enzymes* **1986,** *17*, 43-111; (b) Shabb, J. B., Physiological substrates of cAMP-dependent protein kinase. *Chem Rev* **2001,** *101* (8), 2381-411; (c) Johnson, D. A.; Akamine, P.; Radzio-Andzelm, E.; Madhusudan, M.; Taylor, S. S., Dynamics of cAMP-dependent protein kinase. *Chem Rev* **2001,** *101* (8), 2243-70.

42. Conti, M.; Beavo, J., Biochemistry and physiology of cyclic nucleotide phosphodiesterases: essential components in cyclic nucleotide signaling. *Annu Rev Biochem* **2007,** *76*, 481-511.

43. (a) Northrop, G.; Parks, R. E., Jr., The Effects of Adrenergic Blocking Agents and Theophylline on 3',5'-Amp-Induced Hyperglycemia. *J Pharmacol Exp Ther* **1964,** *145*, 87-91; (b) Hess, M. E.; Haugaard, N., The effect of epinephrine and aminophylline on the phosphorylase activity of perfused contracting heart muscle. *J Pharmacol Exp Ther* **1958,** *122* (2), 169-75.

44. Vaughan, M.; Steinberg, D., Effect of Hormones on Lipolysis and Esterification of Free Fatty Acids during Incubation of Adipose Tissue in Vitro. *J Lipid Res* **1963,** *4*, 193-9.

45. (a) Nakane, T., Activation of adenylate cyclase by GPCR and Gs. Wikimedia Commons, 2011; (b) Cummings, P. B., Pearson Benjamin Cummings. *Pearson Education. Inc.* **2008**.

46. Gerhart-Hines, Z.; Dominy, J. E., Jr.; Blattler, S. M.; Jedrychowski, M. P.; Banks, A. S.; Lim, J. H.; Chim, H.; Gygi, S. P.; Puigserver, P., The cAMP/PKA pathway rapidly activates SIRT1 to promote fatty acid oxidation independently of changes in NAD(+). *Mol Cell* **2011,** *44* (6), 851-63.

47. (a) Kozasa, T.; Gilman, A. G., Purification of recombinant G proteins from Sf9 cells by hexahistidine tagging of associated subunits. Characterization of alpha 12 and inhibition of adenylyl cyclase by alpha z. *J Biol Chem* **1995,** *270* (4), 1734-41; (b) Lambright, D. G.; Noel, J. P.; Hamm, H. E.; Sigler, P. B., Structural determinants for activation of the alpha-subunit of a heterotrimeric G protein. *Nature* **1994,** *369* (6482), 621-8.

48. (a) Hanoune, J.; Defer, N., Regulation and role of adenylyl cyclase isoforms. *Ann Rev Pharmacol* **2001,** *41*, 145-74; (b) Krupinski, J.; Coussen, F.; Bakalyar, H. A.; Tang, W. J.; Feinstein, P. G.; Orth, K.; Slaughter, C.; Reed, R. R.; Gilman, A. G., Adenylyl cyclase amino acid sequence: possible channel- or transporter-like structure. *Science* **1989,** *244* (4912), 1558-64; (c) Sunahara, R. K.; Dessauer, C. W.; Gilman, A. G., Complexity and diversity of mammalian adenylyl cyclases. *Annu Rev Pharmacol* **1996,** *36*, 461-80.

49. (a) Zhang, G.; Liu, Y.; Ruoho, A. E.; Hurley, J. H., Structure of the adenylyl cyclase catalytic core. *Nature* **1997,** *386* (6622), 247-53; (b) Hurley, J. H., Structure, mechanism, and regulation of mammalian adenylyl cyclase. *J Bio* 39

Chem **1999,** *274* (12), 7599-602; (c) Rauch, A.; Leipelt, M.; Russwurm, M.; Steegborn, C., Crystal structure of the guanylyl cyclase Cya2. *Proc Natl Acad Sci U S A* **2008,** *105* (41), 15720-5.

50. Eckstein, F.; Romaniuk, P. J.; Heideman, W.; Storm, D. R., Stereochemistry of the mammalian adenylate cyclase reaction. *J Biol Chem* **1981,** *256* (17), 9118-20.

51. (a) Liu, Y.; Ruoho, A. E.; Rao, V. D.; Hurley, J. H., Catalytic mechanism of the adenylyl and guanylyl cyclases: modeling and mutational analysis. *Proc Natl Acad Sci U S A* **1997,** *94* (25), 13414-9; (b) Tesmer, J. J.; Sunahara, R. K.; Gilman, A. G.; Sprang, S. R., Crystal structure of the catalytic domains of adenylyl cyclase in a complex with Gsalpha.GTPgammaS. *Science* **1997,** *278* (5345), 1907-16.

52. (a) Murad, F.; Chi, Y. M.; Rall, T. W.; Sutherland, E. W., Adenyl cyclase. III. The effect of catecholamines and choline esters on the formation of adenosine 3',5'-phosphate by preparations from cardiac muscle and liver. *J Biol Chem* **1962,** *237*, 1233-8; (b) Klainer, L. M.; Chi, Y. M.; Freidberg, S. L.; Rall, T. W.; Sutherland, E. W., Adenyl cyclase. IV. The effects of neurohormones on the formation of adenosine 3',5'-phosphate by preparations from brain and other tissues. *J Biol Chem* **1962,** *237*, 1239-43; (c) Hirata, M.; Hayaishi, O., Adenyl cyclase of Brevibacterium liquefaciens. *Biochimica biophysica acta* **1967,** *149* (1), 1-11.

53. Rodbell, M.; Lin, M. C.; Salomon, Y.; Londos, C.; Harwood, J. P.; Martin, B. R.; Rendell, M.; Berman, M., Role of adenine and guanine nucleotides in the activity and response of adenylate cyclase systems to hormones: evidence for multisite transition states. *Adv Cyclic Nucl Res* **1975,** *5*, 3-29.

54. Somkuti, S. G.; Hildebrandt, J. D.; Herberg, J. T.; Iyengar, R., Divalent cation regulation of adenylyl cyclase. An allosteric site on the catalytic component. *J Biol Chem* **1982,** *257* (11), 6387-93.

55. Yeager, R. E.; Heideman, W.; Rosenberg, G. B.; Storm, D. R., Purification of the calmodulin-sensitive adenylate cyclase from bovine cerebral cortex. *Biochem* **1985,** *24* (14), 3776-83.

56. (a) Berridge, M. J., The interaction of cyclic nucleotides and calcium in the control of cellular activity. *Adv Cyclic Nucl Res* **1975,** *6*, 1-98; (b) Brostrom, M. A.; Brostrom, C. O.; Breckenridge, B. M.; Wolff, D. J., Regulation of adenylate cyclase from glial tumor cells by calcium and a calcium-binding protein. *J Bio Chem* **1976,** *251* (15), 4744-50; (c) Wei, J.; Wayman, G.; Storm, D. R., Phosphorylation and inhibition of type III adenylyl cyclase by calmodulin-dependent protein kinase II in vivo. *J Biol Chem* **1996,** *271* (39), 24231-5.

57. Hanks, S. K.; Quinn, A. M.; Hunter, T., The protein kinase family: conserved features and deduced phylogeny of the catalytic domains. *Science* **1988,** *241* (4861), 42-52.

58. Collier, J.; Vallance, P., Second messenger role for NO widens to nervous and immune systems. *Trends Pharmacol Sci* **1989,** *10* (11), 427-31.

59. (a) Helfman, D. M.; Brackett, N. L.; Kuo, J. F., Depression of cytidine 3':5'-cyclic monophosphate phosphodiesterase activity in developing tissues of guinea pigs. *Proc Natl Acad Sci U S A* **1978,** *75* (9), 4422-5; (b) Kuo, J. F.; Brackett, N. L.; Shoji, M.; Tse, J., Cytidine 3':5'-monophosphate phosphodiesterase in mammalian tissues. Occurrence and biological involvement. *J Biol Chem* **1978,** *253* (8), 2518-21; (c) Helfman, D. M.;

Shoji, M.; Kuo, J. F., Purification to homogeneity and general properties of a novel phosphodiesterase hydrolyzing cyclic CMP and cyclic AMP. *J Biol Chem* **1981,** *256* (12), 6327-34; (d) Butcher, R. W.; Sutherland, E. W., Adenosine 3',5'-phosphate in biological materials. I. Purification and properties of cyclic 3',5'-nucleotide phosphodiesterase and use of this enzyme to characterize adenosine 3',5'-phosphate in human urine. *J Biol Chem* **1962,** *237*, 1244-50.

60. (a) Bender, A. T.; Beavo, J. A., Cyclic nucleotide phosphodiesterases: molecular regulation to clinical use. *Pharmacol Rev* **2006,** *58* (3), 488-520; (b) Rujescu, D.; Bender, A.; Keck, M.; Hartmann, A. M.; Ohl, F.; Raeder, H.; Giegling, I.; Genius, J.; McCarley, R. W.; Moller, H. J.; Grunze, H., A pharmacological model for psychosis based on N-methyl-D-aspartate receptor hypofunction: molecular, cellular, functional and behavioral abnormalities. *Biol Psychiat* **2006,** *59* (8), 721-9.

61. (a) Lim, J.; Pahlke, G.; Conti, M., Activation of the cAMP-specific phosphodiesterase PDE4D3 by phosphorylation. Identification and function of an inhibitory domain. *J Biol Chem* **1999,** *274* (28), 19677-85; (b) Conti, M.; Mika, D.; Richter, W., Cyclic AMP compartments and signaling specificity: role of cyclic nucleotide phosphodiesterases. *J Gen Physiol* **2014,** *143* (1), 29-38; (c) Houslay, M. D., Underpinning compartmentalised cAMP signalling through targeted cAMP breakdown. *Trends Biochem Sci* **2010,** *35* (2), 91-100.

62. (a) Kirschner, L. S.; Yin, Z.; Jones, G. N.; Mahoney, E., Mouse models of altered protein kinase A signaling. *Endocr Relat Cancer* **2009,** *16* (3), 773-93; (b) Corbin, J. D.; Sugden, P. H.; West, L.; Flockhart, D. A.; Lincoln, T. M.; McCarthy, D., Studies on the properties and mode of action of the purified regulatory subunit of bovine heart

adenosine 3':5'-monophosphate-dependent protein kinase. *J Biol Chem* **1978,** *253* (11), 3997-4003.

63. Bloch, A., Cytidine 3',5'-monophosphate (cyclic CMP). I. Isolation from extracts of leukemia L-1210 Cells. *Biochem Biophys Res Commun* **1974,** *58* (3), 652-9.

64. Bloch, A., Isolation of cytidine 3',5'-monophosphate from mammalian tissues and body fluids and its effects on leukemia L-1210 cell growth in culture. *Adv Cyclic Nucleotide Res* **1975,** *5*, 331-8.

65. (a) Cech, S. Y.; Ignarro, L. J., Cytidine 3',5'-monophosphate (cyclic CMP) formation in mammalian tissues. *Science* **1977,** *198* (4321), 1063-5; (b) Cech, S. Y.; Ignarro, L. J., Cytidine 3',5'-monophosphate (cyclic CMP) formation by homogenates of mouse liver. *Biochem Biophys Res Commun* **1978,** *80* (1), 119-25; (c) Cheng, Y. C.; Bloch, A., Demonstration, in leukemia L-1210 cells, of a phosphodiesterase acting on 3':5'-cyclic CMP but not on 3':5'-cyclic AMP or 3':5'-cyclic GMP. *J Biol Chem* **1978,** *253* (8), 2522-4.

66. Bond, A. E.; Dudley, E.; Tuytten, R.; Lemiere, F.; Smith, C. J.; Esmans, E. L.; Newton, R. P., Mass spectrometric identification of Rab23 phosphorylation as a response to challenge by cytidine 3',5'-cyclic monophosphate in mouse brain. *Rapid Commun Mass Spectrom* **2007,** *21* (16), 2685-92.

67. Briscoe, J.; Therond, P. P., The mechanisms of Hedgehog signalling and its roles in development and disease. *Nat Rev Mol Cell Biol* **2013,** *14* (7), 416-29.

68. Gaion, R. M.; Krishna, G., Cytidylate cyclase: the product isolated by the method of Cech and Ignarro is not cytidine 3',5'-monophosphate. *Biochem Biophys Res Commun* **1979,** *86* (1), 105-11.

69. (a) Wikberg, J. E.; Wingren, G. B., Investigations on the occurrence of cytidine 3',5' monophosphate (cCMP) in tissues. *Acta Pharmacol Toxicol (Copenh)* **1981,** *49* (1), 52-8; (b) Wikberg, J. E.; Wingren, G. B.; Anderson, R. G., Cytidine 3',5' Monophosphate (cCMP) is not an Endogenous nucleotide in normal or regenerating rat livers. *Acta Pharmacol Toxicol (Copenh)* **1981,** *49* (5), 452-4; (c) Helfman, D. M.; Kuo, J. F., A homogeneous cyclic CMP phosphodiesterase hydrolyzes both pyrimidine and purine cyclic 2':3'- and 3':5'-nucleotides. *J Biol Chem* **1982,** *257* (2), 1044-7.

70. Newton, R. P.; Bayliss, M. A.; van Geyschem, J.; Harris, F. M.; Games, D. E.; Brenton, G.; Wilkins, A. C.; Diffley, P.; Walton, T. J., Kinetic analysis and multiple component monitoring of effectors of adenylyl cyclase activity by quantitative fast-atom bombardment mass spectrometry. *Rapid Commun Mass Spectrom* **1997,** *11* (9), 1060-6.

71. (a) Newton, R. P.; Hakeem, N. A.; Salvage, B. J.; Wassenaar, G.; Kingston, E. E., Cytidylate cyclase activity: identification of cytidine 3',5'-cyclic monophosphate and four novel cytidine cyclic phosphates as biosynthetic products from cytidine triphosphate. *Rapid Commun Mass Spectrom* **1988,** *2* (6), 118-26; (b) Newton, R. P.; Salvage, B. J.; Hakeem, N. A., Cytidylate cyclase: development of assay and determination of kinetic properties of a cytidine 3',5'-cyclic monophosphate-synthesizing enzyme. *Biochem J* **1990,** *265* (2), 581-6.

72. Beste, K. Y.; Burhenne, H.; Kaever, V.; Stasch, J. P.; Seifert, R., Nucleotidyl cyclase activity of soluble guanylyl cyclase alpha1beta1. *Biochem* **2012,** *51* (1), 194-204.

73. Newton, R. P.; Salih, S. G., Cyclic CMP phosphodiesterase: isolation, specificity and kinetic properties. *Int J Biochem* **1986,** *18* (8), 743-52.

74. Erich Schneider, M. K., Daniel Reinecke, Sabine Wolter, Heike Burhenne, Volkhard Kaever and Roland Seifert, Fishing for elusive cCMP-degrading phosphodiesterases. *BMC Pharmacol Toxicol* **2013,** *14*, 62.

75. Wolfertstetter, S.; Reinders, J.; Schwede, F.; Ruth, P.; Schinner, E.; Schlossmann, J., Interaction of cCMP with the cGK, cAK and MAPK Kinases in Murine Tissues. *PLoS One* **2015,** *10* (5), e0126057.

76. (a) Bahre, H.; Kaever, V., Measurement of 2',3'-cyclic nucleotides by liquid chromatography-tandem mass spectrometry in cells. *J Chromatogr B* **2014,** *964*, 208-11; (b) Pabst, M.; Grass, J.; Fischl, R.; Leonard, R.; Jin, C.; Hinterkorner, G.; Borth, N.; Altmann, F., Nucleotide and nucleotide sugar analysis by liquid chromatography-electrospray ionization-mass spectrometry on surface-conditioned porous graphitic carbon. *Anal Chem* **2010,** *82* (23), 9782-8; (c) Jackson, E. K.; Dubey, R. K., Role of the extracellular cAMP-adenosine pathway in renal physiology. *Am J Physiol Renal Physiol* **2001,** *281* (4), F597-612; (d) Jackson, E. K., The 2',3'-cAMP-adenosine pathway. *Am J Physiol: Renal Physiol* **2011,** *301* (6), F1160-7.

77. Ren, J.; Mi, Z.; Stewart, N. A.; Jackson, E. K., Identification and quantification of 2',3'-cAMP release by the kidney. *J Pharmacol Exp Ther* **2009,** *328* (3), 855-65.

78. (a) Jackson, E. K.; Gillespie, D. G., Extracellular 2',3'-cAMP and 3',5'-cAMP stimulate proliferation of preglomerular vascular endothelial cells and renal epithelial cells. *Am J Physiol Renal Physiol.* **2012,** *303* (7), F954-62; (b) Jackson, E. K.; Ren, J.; Gillespie, D. G.; Dubey, R. K., Extracellular 2 ',3 '-Cyclic Adenosine 5 '-Monophosphate Is a Potent Inhibitor of Preglomerular Vascular Smooth Muscle Cell and Mesangial Cell Growth. *Hypertension* **2010,** *56* (1), 151-U246; (c) Jackson, E. K., The 2',3'-cAMP-

adenosine pathway. *Am J Physiol Renal Physiol.* **2011,** *301* (6), F1160-7; (d) Jackson, E. K.; Ren, J.; Mi, Z., Extracellular 2',3'-cAMP is a source of adenosine. *J Biol Chem.* **2009,** *284* (48), 33097-106; (e) Verrier, J. D.; Jackson, T. C.; Gillespie, D. G.; Janesko-Feldman, K.; Bansal, R.; Goebbels, S.; Nave, K. A.; Kochanek, P. M.; Jackson, E. K., Role of CNPase in the oligodendrocytic extracellular 2',3'-cAMP-adenosine pathway. *Glia* **2013,** *61* (10), 1595-606; (f) Jackson, E. K.; Gillespie, D. G.; Mi, Z.; Cheng, D.; Bansal, R.; Janesko-Feldman, K.; Kochanek, P. M., Role of 2',3'-cyclic nucleotide 3'-phosphodiesterase in the renal 2',3'-cAMP-adenosine pathway. *Am J Physiol Renal Physiol.* **2014,** *307* (1), F14-24; (g) Jackson, E. K.; Mi, Z., In vivo cardiovascular pharmacology of 2',3'-cAMP, 2'-AMP, and 3'-AMP in the rat. *J Pharmacol Exp Ther.* **2013,** *346* (2), 190-200; (h) Verrier, J. D.; Jackson, T. C.; Bansal, R.; Kochanek, P. M.; Puccio, A. M.; Okonkwo, D. O.; Jackson, E. K., The brain in vivo expresses the 2',3'-cAMP-adenosine pathway. *J Neurochem.* **2012,** *122* (1), 115-25; (i) Van Damme, T.; Blancquaert, D.; Couturon, P.; Van Der Straeten, D.; Sandra, P.; Lynen, F., Wounding stress causes rapid increase in concentration of the naturally occurring 2',3'-isomers of cyclic guanosine- and cyclic adenosine monophosphate (cGMP and cAMP) in plant tissues. *Phytochem* **2014,** *103*, 59-66.

79. Thompson, J. E.; Venegas, F. D.; Raines, R. T., Energetics of catalysis by ribonucleases: fate of the 2',3'-cyclic phosphodiester intermediate. *Biochem* **1994,** *33* (23), 7408-14.

80. Wilusz, C. J.; Wormington, M.; Peltz, S. W., The cap-to-tail guide to mRNA turnover. *Nat Rev Mol Cell Biol* **2001,** *2* (4), 237-46.

81. van Aubel, R. A.; Smeets, P. H.; Peters, J. G.; Bindels, R. J.; Russel, F. G., The MRP4/ABCC4 gene encodes a novel apical organic anion transporter in human kidney proximal tubules: putative efflux pump for urinary cAMP and cGMP. *J Am Soc Nephrol* **2002,** *13* (3), 595-603.

82. Sprinkle, T. J., 2',3'-cyclic nucleotide 3'-phosphodiesterase, an oligodendrocyte-Schwann cell and myelin-associated enzyme of the nervous system. *Crit Rev Neurobiol* **1989,** *4* (3), 235-301.

83. Jackson, E. K.; Ren, J.; Mi, Z., Extracellular 2',3'-cAMP is a source of adenosine. *J Biol Chem* **2009,** *284* (48), 33097-106.

84. Jackson, E. K.; Gillespie, D. G.; Mi, Z.; Cheng, D.; Bansal, R.; Janesko-Feldman, K.; Kochanek, P. M., Role of 2',3'-cyclic nucleotide 3'-phosphodiesterase in the renal 2',3'-cAMP-adenosine pathway. *Am J Physiol Renal Physiol* **2014,** *307* (1), F14-24.

85. Jia, X.; Fontaine, B. M.; Strobel, F.; Weinert, E. E., A facile and sensitive method for quantification of cyclic nucleotide monophosphates in mammalian organs: basal levels of eight cNMPs and identification of 2',3'-cIMP. *Biomol* **2014,** *4* (4), 1070-

Chapter 2: A Novel O_2-Sensing Stressosome from a Gram-Negative Bacterium

Adapted from (Jia, X., Wang, J., and Weinert, E. E., A Novel O_2-Sensing Stressosome from A Gram-Negative Bacterium, Manuscript submitted for publication)

2.1 Introduction

Bacteria of the *Vibrio* genus are rod-shaped, Gram-negative gamma-proteobacteria that are highly abundant in marine waters and include a number of pathogenic species, such as *Vibrio cholerae*, which causes acute diarrhea, and *Vibrio vulnificus*, which causes life-threatening skin and soft tissue infections and has a ~50% mortality rate.[1] A number of gene clusters that control expression of genes directly or indirectly linked to bacterial virulence have been characterized; however additional pathways that regulate gene expression levels in response to stress adaptation and bacterial pathogenesis of the *Vibrio* phyla have yet to be identified.[2] Within Gram-positive bacteria, such as *Bacillus subtilis*, the stressosome, a ~1.8 MDa signaling complex, alters virulence gene expression levels through activation of the alternative sigma factor, σ^B, in response to diverse environmental stresses (Figure 2.1).[3] The core structure of the stressosome is composed of multiple copies of proteins RsbR and RsbS.[4] The upstream component of the stressosome-regulated stress signal transduction cascade is activated by RsbT kinase.[4] In the presence of stress, phosphorylation of the stressosome core by RsbT reduces its binding affinity, thus promoting release of RsbT, which binds and activates the downstream component RsbU phosphatase (Figure 2.1).[5] The activated RsbU triggers the release and activation of the general stress sigma factor, σ^B, which controls the expression of stress-responsive genes (Figure 2.1).[5] Stressosome-regulated signaling pathway is dynamic and mechanistically complex in bacteria, therefore, in this chapter, I will only focus on studying the signaling pathways involving the stressosome upstream components, RsbR, RsbS and RsbT.

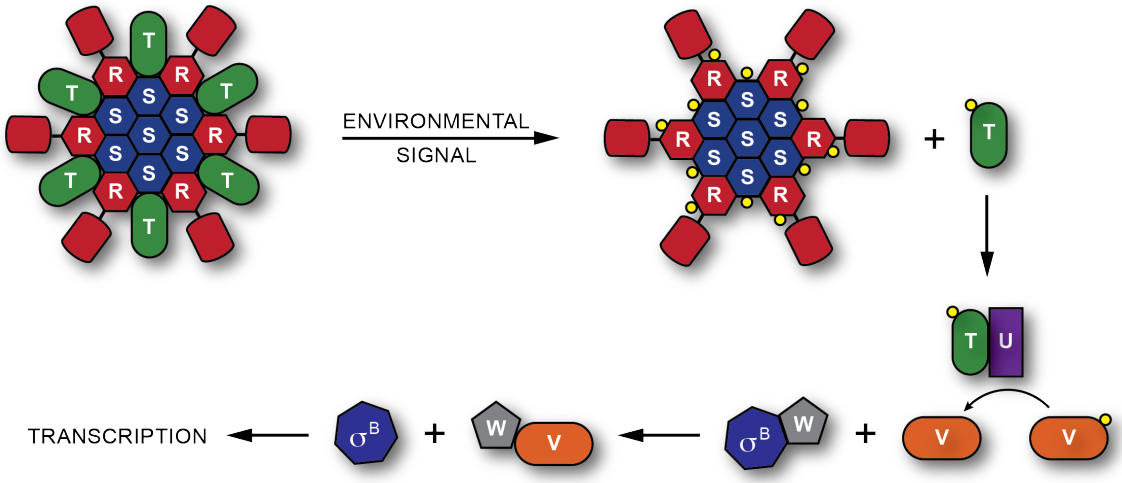

Figure 2.1. Proposed stressosome-regulated signaling pathway in response to environmental stress in *Bacillus subtilis*.

The *rsbR* homologs in *B. subtilis* encode a variable N-terminal sensing domain, and a C-terminal STAS (Sulfate Transport and Anti-anti-Sigma factor) domain.[6] RsbS consists of a STAS domain and RbsT is a kinase that transmits the stress signal via phosphorylation of downstream proteins, ultimately resulting in transcriptional changes of over 150 genes that are involved in stress response.[3, 6a, 7] The stressosome-regulated pathway is modulated by reversible protein phosphrorylation reactions by protein kinase RsbT.[3a, 7] The core of the stressosome complex consists of multiple copies of RsbR and RsbS interacting through STAS domain interactions, to which RsbT kinase binds in the absence of stress.[4] Genetic analysis has identified two RsbT-phosphorylable threonine residues in RsbR, T171 and T205.[5, 8] Phosphorylation of RsbR on T171 by RsbT is stress-independent, as low level of phosphorylated RsbR on T171 is present even in the absence of stress, which is required for subsequent signaling transductions.[6a, 7b] As part of

the stress-induced response, RsbT kinase first phosphorylates RsbR on the threonine residues and then RsbS on S59; increasing levels of phosphorylated RsbS triggers the stress-induced release of RsbT to activate downstream effectors.[8] Previous studies suggest that T171 in RsbR is the primary site of stress-induced phosphorylation by RsbT, whereas phosphorylation of RsbR T205 following strong stress activates a second feedback mechanism, which limits σ^B activation.[5, 9] Previously identified *B. subtilis* RsbR contains an N-terminal nonheme blobin domain with no bound cofactor.[6b] Therefore, the activating signals within Gram-positive bacteria remain elusive due to the lack of a ligand in the sensing domain, which makes elucidate the mechanism of stress sensing and signal transduction within stressosomes challenging. Although the structure of the *B subtilis* stressosome has been studied extensively, putative stressosome complexes within Gram-negative bacteria remain uncharacterized. Here, we report the first example, to our knowledge, of a functional stressosome from a Gram-negative bacterium that senses O_2 through a heme-bound RsbR (Figure 2.2).

Recently, putative homologs encoding core stressosome components (*rsbR*, *rsbS*, and *rsbT*) were identified in the genomes of various *Vibrio* species.[10] RsbR protein from *Vibrio* species comprises a unique class of stressosome sensor proteins in which the N-terminal domain consists of a heme-bound sensor globin domain. The protoporphyrin IX -iron complex, known as heme, is one of the most abundant co-factors in biological systems. On of the primary functions of the heme-based sensors function as O_2 carriers in hemoglobin, an O_2 storage site in myoglobin, and a catalytic site for O-O bond scission in cytochrome P450 monooxygenases (Refer to chapter 1, section 1.2.2 for more details on

heme-based sensor proteins).[11] As shown in the sequence alignment of the N-terminal domain of RsbR in *V. brasiliensis* with other heme-bound globin-coupled sensors (GCSs), the distal tyrosine and proximal histidine residues required for heme and ligand binding are conserved (Figure 2.3).[11c] In contrast, those key residues are not conserved in previously characterized RsbR proteins from *B. subtilis* and other Gram-positive bacteria.[11c] As previous studies have demonstrated, members of the *Vibrio* genus respond to anaerobiosis by promoting virulence gene induction or triggering biofilm dispersal.[12] Therefore, O_2-dependent stressosome signaling may play key roles in controlling virulence of *Vibrio* pathogens.[12] Furthermore, characterization of an O_2-sensitive RsbR protein and stressosome complex will allow for detailed analysis of the mechanism of ligand-dependent signal transduction within the stressosome, as well as identification of stressosome-responsive genes that are controlled in response to changes in environmental O_2 levels.

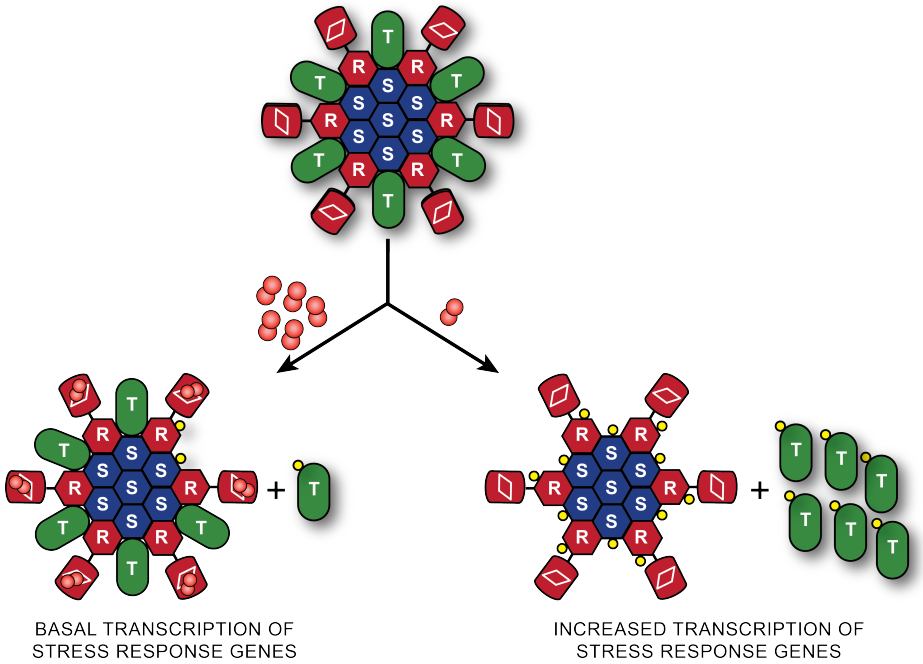

Figure 2.2. Stressosome-regulated signaling network in Gram-negative bacteria. O_2 binding to *V. brasiliensis* RsbR (red) results in basal phosphorylation of stressosome components by kinase RsbT (green). In contrast, dissociation of O_2 to yield Fe^{II}-unligated RsbR results in RsbT activation and increased phosphorylation of RsbR, RsbS (blue), and RsbT. *In vivo*, increased RsbT activity should result in transcription of stress response genes.

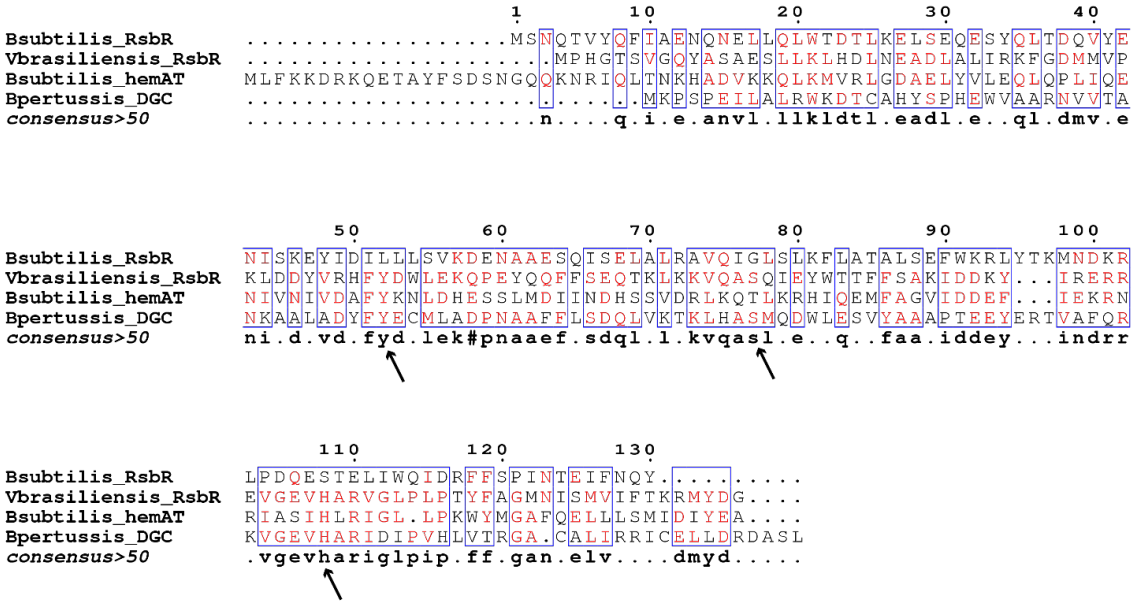

Figure 2.3. Sequence alignment of N-terminal globin domain of *V. brasiliensis* RsbR (WP_006879723), non-heme globin domain of *B. subtilis* RsbR (WP_009966610), and sensor globin domains from globin coupled sensors in *B. subtilis* (HemAT, WP_015252424) and *Bordetella pertussis* (*Bpe*GReg, WP_050861487). Arrows point to the proximal histidine and distal tyrosine and serine residues required for heme and ligand binding, and are conserved in sensor globin domains (Bsubtilis_hemAT,

Bpertussis_DGC, *V. brasiliensis*_RsbR) but not in *B. subtilis* non-heme globin domain (Bsubtilis_RsbR).

2.2 Results and Discussion

2.2.1 Expression and Purification of the Stressosome Components

To characterize the putative *V. brasiliensis* stressosome, candidate *rsb* genes encoding homologs of the stressosome components RsbR, RsbT and RsbS in *V. brasiliensis* were cloned into expression vectors and heterologously expressed (Figure 2.4). Upon purification, RsbR was found to bind heme, as predicted, and exhibited spectra characteristic of a histidyl-ligated sensor globin (Figure 2.5).[13] The putative kinase, RsbT, was found to be active and exhibited time-dependent autophosphorylation (Figure 2.6 and Table 2.1). Previous studies on RsbT proteins from *B. subtilis* identified an aspartate residue that is crucial for kinase activity.[14] Mutation of the homologous aspartate in *V. brasiliensis* RsbT (D87N) resulted in complete loss of kinase activity, suggesting that key residues responsible for kinase activity are conserved across species (Figure 2.7a).

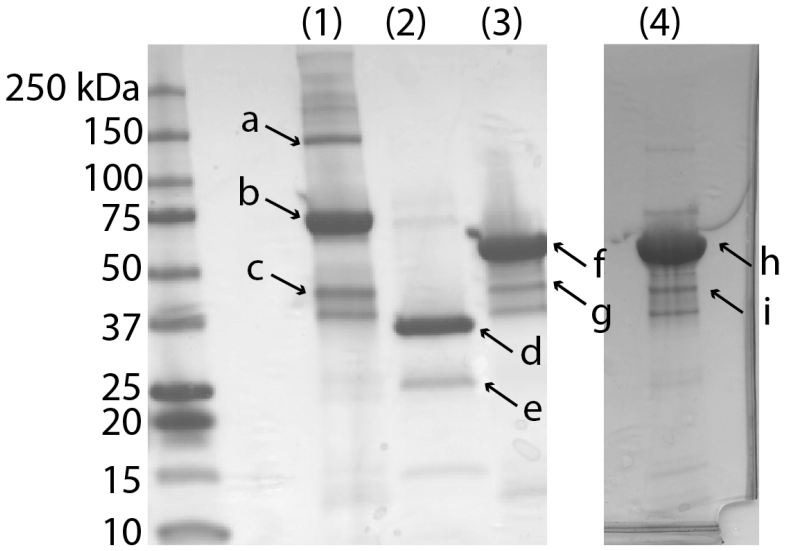

Figure 2.4. SDS-PAGE analysis of purified stressosome components RsbR, RsbS and RsbT from *V. brasiliensis*, and mutant RsbT D78N, stained with Coomasie. His_6-MBP-RsbR (Lane 1, b, 75 kDa, 5 μM), GST-RsbS (Lane 2, d, 39 kDa, 5 μM), His_6-MBP-RsbT (Lane 3, f, 58 kDa, 5 μM) and mutant RsbT (Lane 4, h, D87N, 10 μM) were separated on 4-20% acrylamide gels. N-terminal His_6-MBP or GST tagged constructs of RsbR, RsbS, and RsbT were used to improve stability of the proteins during purification and analysis. Bands at 42.5 (Lane 1, c; lane 3, g and lane 4 i) and 26 kDa (Lane 2, e) are small amount of detached MBP or GST tags. Higher molecular band at 150 kDa (Lane 1, a) corresponds to RsbR dimer that was not fully denatured.

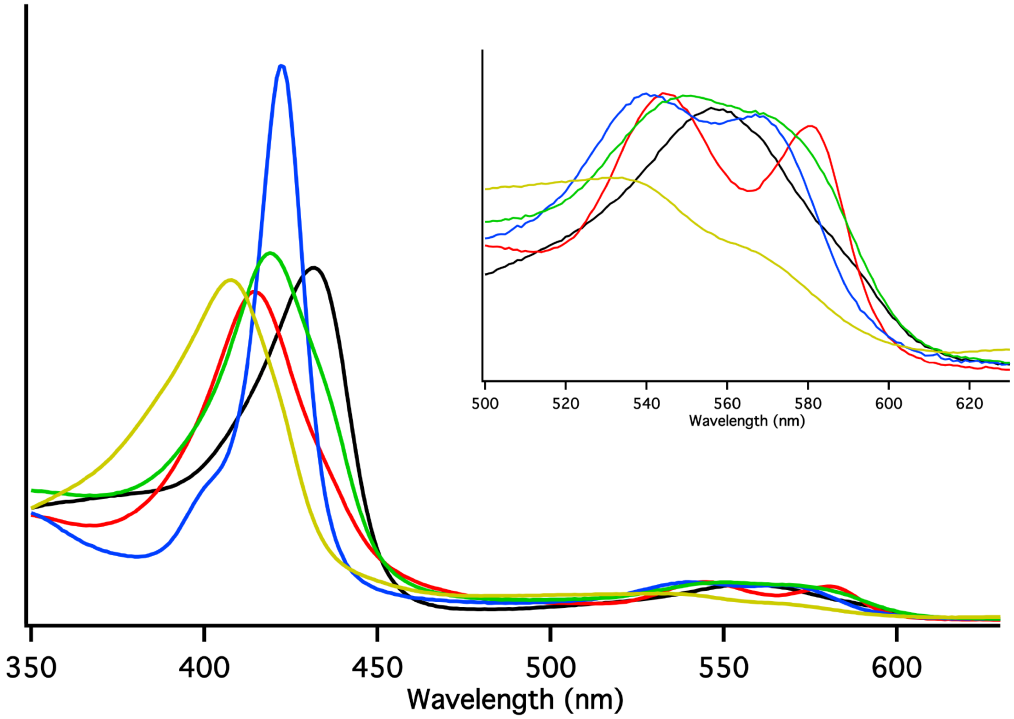

Figure 2.5. UV-Vis spectra of RsbR in *V. brasiliensis*. Expanded α/β band region is shown in the inset. Black, Fe^{II} (432, 556 nm); red, Fe^{II}-O_2 (417, 544, 581 nm); blue, Fe^{II}-CO (422, 540, 569 nm); green, Fe^{II}-NO (419, 549, 569 nm) and yellow, Fe^{III} (408, 534, 566 nm). *V. brasiliensis* Fe^{III} RsbR consists of a mixture of five- and six-coordinate heme species.

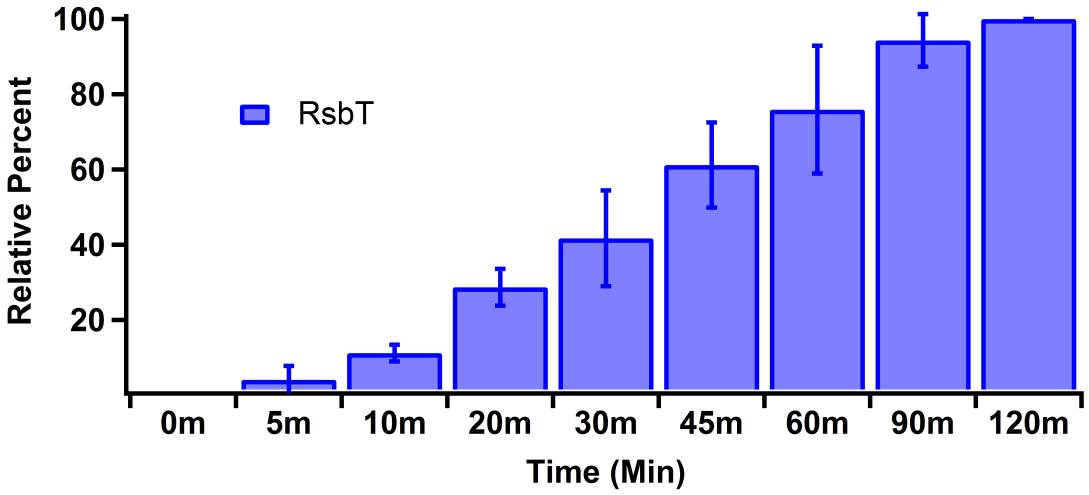

Figure 2.6. Average autophosphorylation kinetics of kinase RsbT. Kinetic experiments were run in triplicate, and mean and standard deviation values were calculated for each time point.

Table 2.1. RsbT autophosphorylation kinetics. Kinetic experiments were run at least in triplicate, mean and standard deviation of relative intensities are expressed as percentages (%).

Time (min) / Protein	0	5	10	20	30	45	60	90	120
RsbT	0 ± 0	4.1 ± 3.7	11.2 ± 2.2	28.7 ± 4.9	41.7 ± 12.7	61.2 ± 11.3	75.9 ± 17.0	94.3 ± 7.0	100.0 ± 0

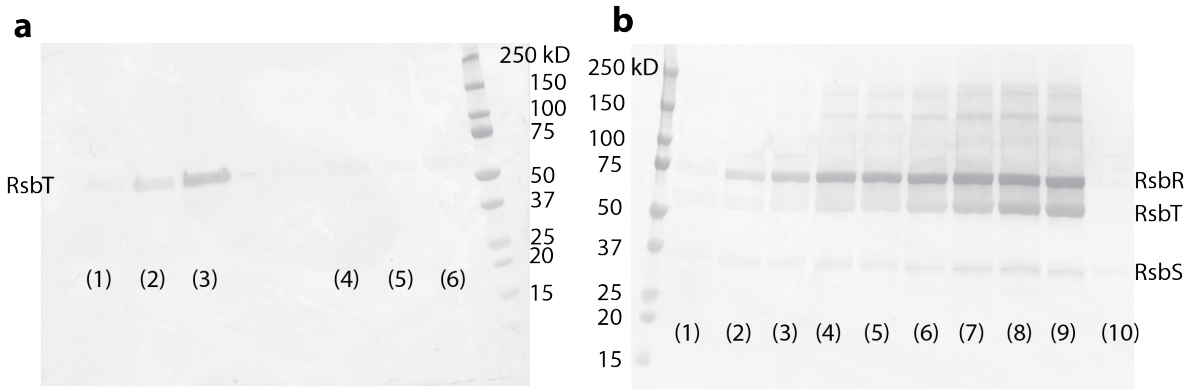

Figure 2.7. Representative western blots probing kinase activities. **a**. Comparison of RsbT (Lane (1)-(3)) and mutant RsbT D87N (Lane (4)-(6)) autophosphorylation activity. RsbT autophosphorylation reactions were quenched at 0 min (**1**), 20 min (**2**) and 90 min (**3**). RsbTD87N autophosphorylation reactions were quenched at 0 min (**4**), 20 min (**5**) and 90 min (**6**). **b**. RsbT kinase activity in the presence of RsbS and RsbR Fe^{II} state. Reactions were quenched at 0 min (**1**), 5 min (**2**), 10 min (**3**), 20 min (**4**), 30 min (**5**), 45 min (**6**), 60 min (**7**), 90 min (**8**), 120 min (**9**). Negative control reaction (**10**) was performed without addition of ATPγS to ensure there was no cross-activity with alkylated cysteine.

2.2.2 Kinase Activity of RsbT in Controlling Stressosome-Regulated Pathways

Within the stressosome complex, binding and controlled release of kinase RsbT are proposed to be controlled through sensing of the stress signal by RsbR (Figure 2.1).[7b, 8] In the absence of stress, basal RsbT phosphorylation activity results in low levels of phosphorylated RsbR, which is a prerequisite for subsequent signaling transductions in response to stress.[6a, 7b] Stress perception increases phosphorylation of the stressosome

sensor RsbR, which facilitates phosphorylation of RsbS by RsbT within the stressosome, decreasing affinity of RsbT for the RsbR/S stressosome core.[3a, 7a, b] To test the role of RsbR ligand sensing in controlling the phosphorylation cascade, effects of ligand binding to the sensor globin domain of RsbR on RsbT kinase activity were measured. The rates of phosphorylation of RsbR and RsbT occured in a time-dependent manner and varied depending on the ligation state of RsbR, with Fe^{II} RsbR leading to significantly faster phosphorylation rates than Fe^{II}-O_2 RsbR (Figure 2.8 and Table 2.2). These results suggest that dissociation of molecular O_2 to the heme of RsbR results in a conformational change that increases RsbT activity, likely through direct interactions with the kinase. Furthermore, RsbT is unable to phosphorylate RsbS in the absence of RsbR in *V. brasiliensis*. This is likely because phosphorylation of RsbR is required for the subsequent phosphorylation of RsbS and further signal transduction, highlighting the importance of the sensor protein RsbR in signal transmission within the stressosome core.[3a, 6a, 7b]

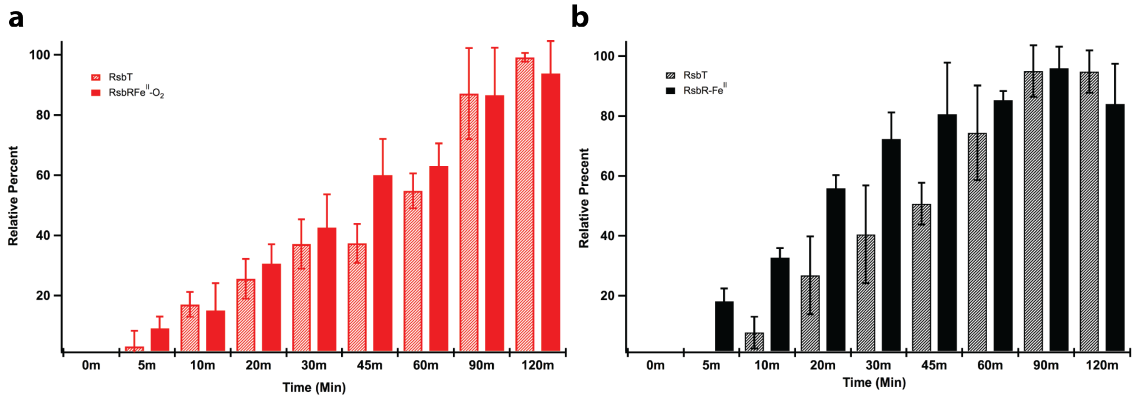

Figure 2.8. Average phosphorylation kinetics of kinase RsbT in a RsbR/T mixture. Average phosphorylation kinetics of RsbT in the presence of Fe^{II}-O_2 RsbR (**a**) and Fe^{II}

unligated RsbR (**b**). Kinetic experiments were run in at least triplicate, and mean and standard deviation values were calculated for each time point.

Table 2.2. RsbR/T phosphorylation kinetics. Phosphoryl transfer by RsbT was measured in the presence of RsbR in various ligation and oxidation states. Kinetic experiments were run at least in triplicate, mean and standard deviation of relative intensities are expressed as percentages (%). Ligation and oxidation states refer to that of RsbR in the reaction mixture.

	Time (min) / **Oxida-tion state**	**0**	**5**	**10**	**20**	**30**	**45**	**60**	**90**	**120**
RsbR	**Fe^{II}**	0 ± 0	18.1 ± 4.3	32.7 ± 3.2	55.9 ± 4.4	72.3 ± 8.9	80.6 ± 17.2	85.3 ± 3.0	95.9 ± 7.2	84.0 ± 13.4
	Fe^{II}-O_2	0 ± 0	9.0 ± 4.0	15.0 ± 9.0	30.6 ± 6.4	42.6 ± 11.0	60.1 ± 12.0	63.1 ± 7.5	86.5 ± 15.8	93.8 ± 10.8
RsbT	**Fe^{II}**	0 ± 0	0.5 ± 0.9	7.6 ± 5.3	26.8 ± 13.0	40.5 ± 16.3	50.7 ± 7.0	74.4 ± 15.8	95.0 ± 8.6	94.8 ± 7.1
	Fe^{II}-O_2	0 ± 0	3.0 ± 5.2	17.0 ± 4.2	25.6 ± 6.6	37.1 ± 8.2	37.3 ± 6.5	54.8 ± 5.8	87.1 ± 15.2	99.2 ± 1.4

2.2.3 Sensing in Fully Reconstituted Stressosome Complexes

To determine if RsbR can serve as a heme-based gas sensor within fully reconstituted stressosome complex, kinase activity of RsbT in RsbR/S/T mixtures was investigated with RsbR in various ligation and oxidation states (Figures 2.9 and 2.10 and

Table 2.3). Kinase RsbT was found to be most active when RsbR is in the Fe^{II} unligated state, with Fe^{II}-NO and Fe^{II}-CO yielding intermediate activity, and Fe^{II}-O_2 and Fe^{III} resulting in basal activity rates similar to RsbT alone (Figures 2.9 and 2.10 and Table 2.3). Similar effects of ligation/oxidation state have been observed for other members of the GCS family with different output domains, likely due to strong interactions between bound O_2 with distal pocket tyrosine and serine residues (Figure 2.12b).[11c, 15] Addition of Fe^{II}-O_2 RsbR did not decrease the rate of RsbT phosphoryl transfer, as compared to autophosphorylation of RsbT alone, while addition of Fe^{II} RsbR increased the rate of phosphoryl transfer, suggesting Fe^{II} RsbR functions as an activator of RsbT. In contrast, phosphorylation of RsbS in the RsbR/S/T mixture was undetectable when RsbR was included in the Fe^{II}-O_2 or Fe^{III} states, suggesting that RsbR/RsbS interactions can inhibit RsbS phosphorylation by RsbT, possibly by limiting RsbT access to the RsbS phosphorylation site. In addition, RsbT kinase activity is controlled by dual-mechanisms in *V. brasiliensis*, with phosphorylation of both RsbR and RsbS required for maximal rates of phosphoryl-transfer. While these data also suggest that RsbR could function as either an O_2 or redox sensor, in the RsbR/S/T mixture, Fe^{II}-O_2 RsbR is stable over the course of the reactions and autooxidizes at a rate similar to myoglobin (Figure 2.11).[15] Therefore, it is unlikely that RsbR is serving as a redox sensor *in vivo*, although reactive oxygen species that pathogenic *Vibrio* species are likely to encounter during infection will likely oxidize RsbR and lead to decreased stressosome signaling.

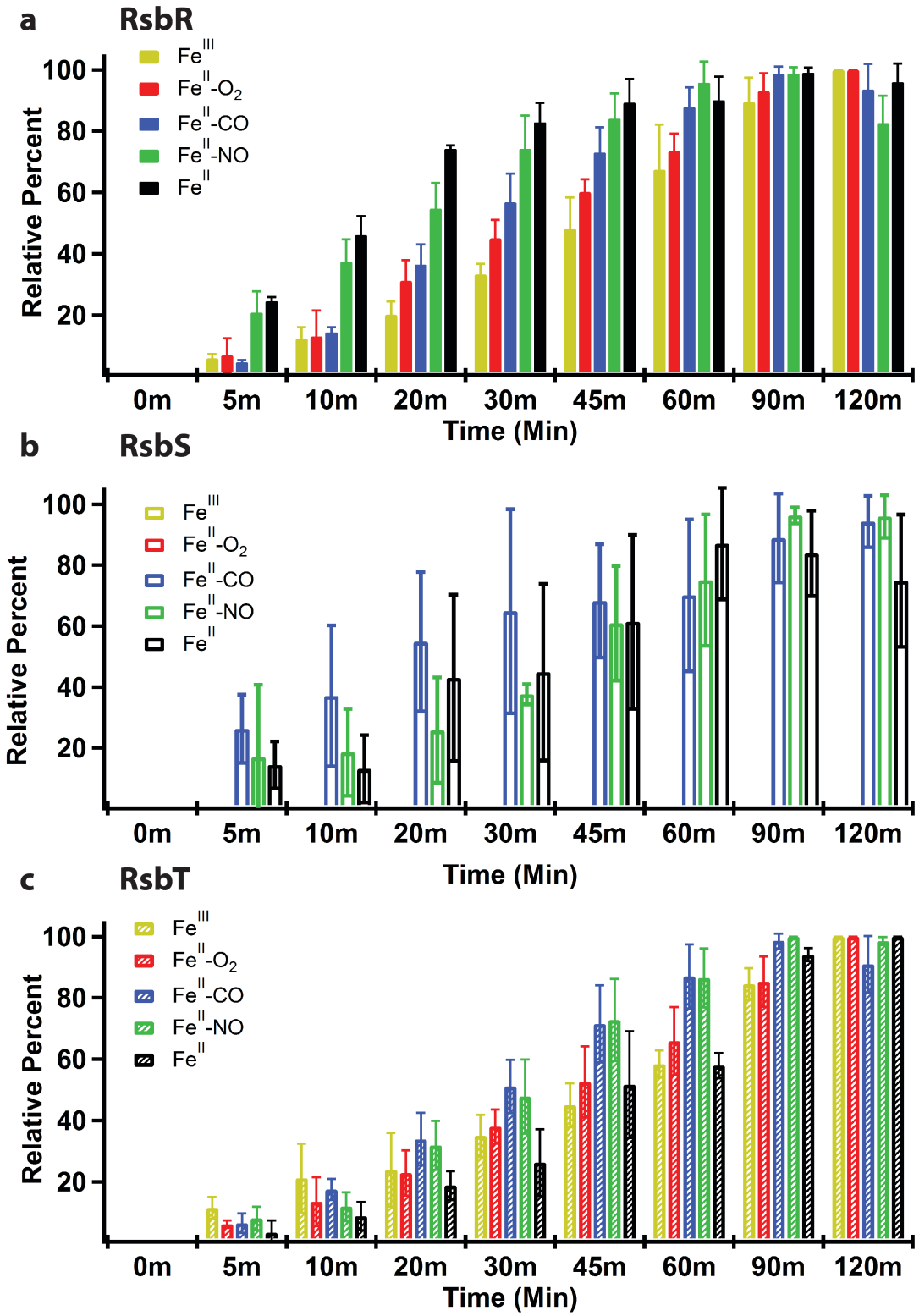
a
RsbR
Fe^III
Fe^II-O2
Fe^II-CO
Fe^II-NO
Fe^II
Relative Percent
100
80
60
40
20
0m
5m
10m
20m
30m
45m
60m
90m
120m
Time (Min)
b
RsbS
Fe^III
Fe^II-O2
Fe^II-CO
Fe^II-NO
Fe^II
Relative Percent
100
80
60
40
20
0m
5m
10m
20m
30m
45m
60m
90m
120m
Time (Min)
c
RsbT
Fe^III
Fe^II-O2
Fe^II-CO
Fe^II-NO
Fe^II
Relative Percent
100
80
60
40
20
0m
5m
10m
20m
30m
45m
60m
90m
120m
Time (Min)

Figure 2.9. Phosphorylation kinetics of kinase RsbT in the presence of RsbR in various ligation states and RsbS. Average rate of phosphorylation of RsbR (**a**), RsbS (**b**) and RsbT (**c**) in a RsbR/S/T mixture (ligation/oxidation states of RsbR: Fe^{III}, yellow; Fe^{II}-O_2, red; Fe^{II}-CO, blue; Fe^{II}-NO, green; Fe^{II} unligated, black). All experiments were performed at least in triplicate, and mean and standard deviation values are plotted for each time point. Phosphorylation of RsbS was undetectable when Fe^{III} or Fe^{II}-O_2 RsbR was included in the reaction mixture.

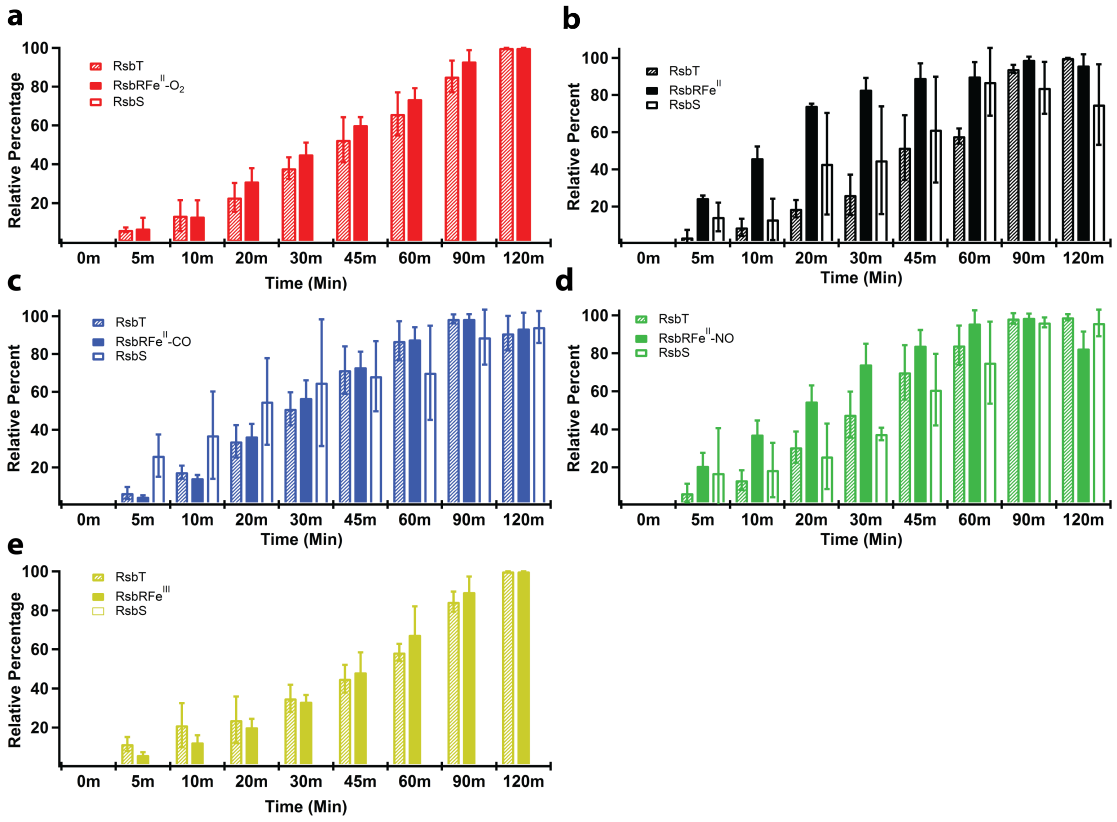

Figure 2.10. Autophosphorylation and phosphoryl transfer from RsbT to RsbR and RsbS in a RsbR/S/T mixture. Average phosphorylation kinetics in the presence of RsbR Fe^{II}-O_2 (**a**), Fe^{II} unligated (**b**), Fe^{II}-CO (**c**), Fe^{II}-NO (**d**), Fe^{III} (**e**). Kinetic experiments were run in

triplicate, and mean and standard deviation values were calculated for each time point. Phosphorylation of RsbS was undetectable when RsbR was in Fe^{II}-O_2 (**a**) and Fe^{III} (**e**) states.

Table 2.3. RsbR/S/T phosphorylation kinetics. Phosphoryl transfer by RsbT was measured in the presence of RsbR (in various ligation and oxidation states) and RsbS. Kinetic experiments were run at least in triplicate, mean and standard deviation of relative intensities are expressed as percentages (%). Ligation and oxidation states refer to that of RsbR in the reaction mixture. Phosphorylation of RsbS was undetectable when RsbR was in Fe^{III} and Fe^{II}-O_2 states in the reaction mixture.

	Time (min) / **Oxidation state**	**0**	**5**	**10**	**20**	**30**	**45**	**60**	**90**	**120**
RsbR	**Fe^{III}**	0 ± 0	5.9 ± 1.4	12.4 ± 3.6	20.2 ± 4.3	33.3 ± 3.4	48.3 ± 10.1	67.5 ± 14.6	89.5 ± 7.9	100.0 ± 0
	Fe^{II}-O_2	0 ± 0	6.9 ± 5.5	13.1 ± 8.4	31.2 ± 6.8	45.1 ± 6.0	60.2 ± 4.1	73.6 ± 5.6	93.1 ± 5.8	100.0 ± 0
	Fe^{II}-CO	0 ± 0	4.6 ± 0.7	14.4 ± 1.6	36.5 ± 6.6	56.8 ± 9.3	73.0 ± 8.2	87.8 ± 6.4	98.6 ± 2.5	93.6 ± 8.3
	Fe^{II}-NO	0 ± 0	20.8 ± 6.9	37.3 ± 7.4	54.7 ± 8.4	74.2 ± 10.9	84.1 ± 8.2	95.8 ± 6.9	98.7 ± 2.2	82.6 ± 8.9
	Fe^{II}	0 ± 0	24.6 ± 1.3	46.1 ± 6.2	74.2 ± 1.1	82.9 ± 6.3	89.3 ± 7.8	90.1 ± 7.7	99.1 ± 1.6	96.0 ± 6.0
RsbT	**Fe^{III}**	0 ± 0	11.5 ± 3.6	21.2 ± 11.3	23.9 ± 12.0	35.0 ± 6.9	45.0 ± 7.1	58.4 ± 4.4	84.5 ± 5.2	100.0 ± 0
	Fe^{II}-O_2	0 ± 0	6.2 ± 1.2	13.5 ± 8.0	22.9 ± 7.4	38.0 ± 5.6	52.6 ± 11.6	65.9 ± 11.1	85.3 ± 8.2	100.0 ± 0

	Fe^{II}-CO	0 ± 0	6.5 ± 3.2	17.5 ± 3.5	33.9 ± 8.6	51.1 ± 8.7	71.5 ± 12.6	87.0 ± 10.4	98.6 ± 2.4	91.0 ± 9.2
	Fe^{II}-NO	0 ± 0	8.1 ± 3.8	11.9 ± 4.7	31.9 ± 8.0	47.8 ± 12.1	72.8 ± 13.4	86.5 ± 9.6	100.0 ± 0	98.5 ± 1.3
	Fe^{II}	0 ± 0	3.4 ± 4.0	8.8 ± 4.6	18.8 ± 4.7	26.3 ± 10.9	51.7 ± 17.4	57.9 ± 4.1	94.1 ± 2.2	100.0 ± 0
RsbS	**Fe^{III}**	-	-	-	-	-	-	-	-	-
	Fe^{II}-O_2	-	-	-	-	-	-	-	-	-
	Fe^{II}-CO	0 ± 0	26.3 ± 11.2	37.1 ± 23.1	54.9 ± 22.9	64.9 ± 33.5	68.3 ± 18.6	70.1 ± 24.9	88.9 ± 14.6	94.3 ± 8.4
	Fe^{II}-NO	0 ± 0	17.0 ± 23.7	18.6 ± 14.3	25.8 ± 17.3	37.6 ± 3.3	60.9 ± 18.8	75.1 ± 21.6	96.3 ± 2.6	96.0 ± 7.0
	Fe^{II}	0 ± 0	14.4 ± 7.7	13.1 ± 11.1	43.0 ± 27.3	44.9 ± 29.0	61.4 ± 28.5	87.1 ± 18.3	83.9 ± 14.0	74.9 ± 21.7

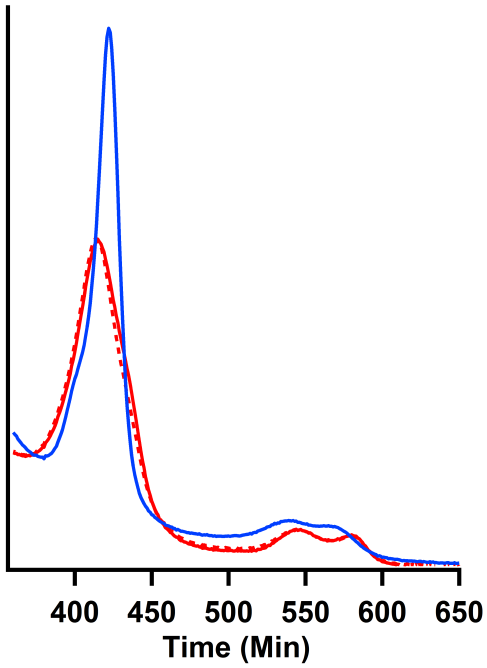

Figure 2.11. Autooxidation UV-Vis spectra of *V. brasiliensis* RsbR in RsbR/S/T complex. Spectra of RsbR Fe^{II}-O_2 in RsbR/S/T were taken at the beginning (solid red line) and after two hours (dashed red line). Heme ligand CO for Fe^{II} RsbR was added after two hours to produce diagnostic RsbR Fe^{II}-CO spectra (blue).

The response of the *V. brasiliensis* stressosome to gaseous ligand binding at the heme of RsbR provides a unique opportunity to interrogate the effects of RsbR/S/T protein interactions on signal sensing by RsbR. RsbR O_2 dissociation kinetics were determined to quantify changes in the RsbR sensing domain (Figure 2.12c). The O_2 dissociation rate of RsbR in *V. brasiliensis* exhibits bi-exponential kinetics, suggesting that RsbR exists in two conformations of the heme pocket (Figure 2.13).[16] Based on sequence alignments, distal pocket tyrosine and serine residues are predicted to provide key hydrogen bonding residues in the heme distal pocket and interact with bound ligands (Figure 2.3 and 2.12b). The biphasic O_2 dissociation kinetics suggest that these residues form multiple hydrogen bonding patterns with bound O_2, yielding multiple dissociation rates.[16-17] Formation of the RsbR/S/T complex alters O_2 dissociation from RsbR; both the slow (k_1) and fast (k_2) rates of individual protein RsbR and RsbR within RsbR/S/T complexes remain unchanged, but percentages of each rate are altered. These results suggest that RsbR/S/T interactions result in a greater percentage of RsbR heme-pockets being in the high affinity conformation (7.5% vs. 19.6%, respectively; Figure 2.12c). Thus, formation of RsbR/S/T complexes not only alters phosphoryl transfer rates from RsbT and allows for transfer to RsbS, but also changes the conformation of sensor protein RsbR, altering the effective O_2 affinity. These changes in O_2 dissociation kinetics

further suggest that conformational changes caused by O_2 binding in the heme-pocket of RsbR are not only important in regulation of the stressosome signaling pathway, but also control ligand binding affinity.

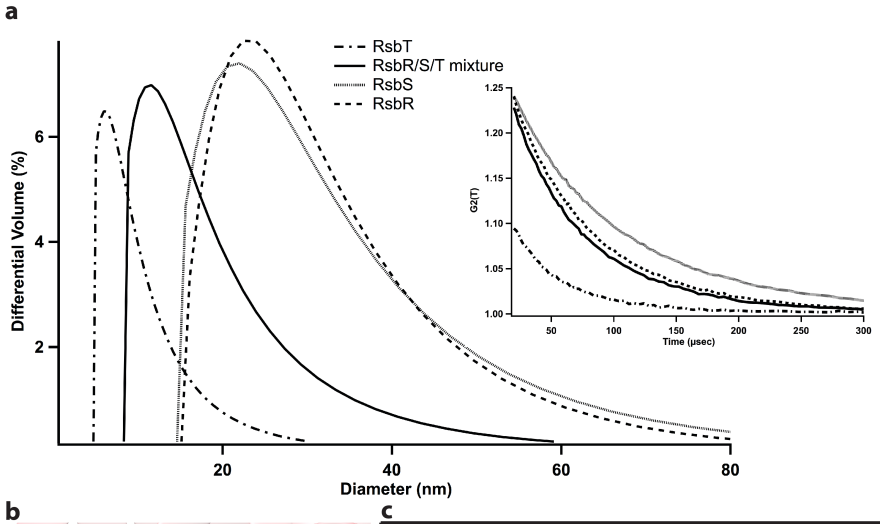

O_2 dissociation kinetics				
Protein	**k_1 (s^{-1})**	**k_2 (s^{-1})**	**% k_1**	**% k_2**
RsbR	**7.0 ± 0.3**	**67.4 ± 0.8**	**7.5 ± 1.7**	**92.5 ± 1.7**
RsbR/S/T	**7.9 ± 0.1**	**65.0 ± 0.7**	**19.6 ± 1.4**	**80.5 ± 1.4**

Figure 2.12. O_2 dissociation kinetics and structural analysis of the RsbR/S/T complex. (**a**) Dynamic light scattering (DLS) of RsbT, RsbS, RsbR and the RsbR/S/T mixture when RsbR is in Fe^{II}-O_2 ligation state; inset shows autocorrelation functions. **(b)** Homology model of the heme pocket of *V. brasiliensis* RsbR generated using Phyre2.[18] The heme, proximal histidine, and distal pocket hydrogen bond donors (tyrosine and

serine) are shown. (**c**) O_2 dissociation kinetics of RsbR alone and in the RsbR/S/T complex.

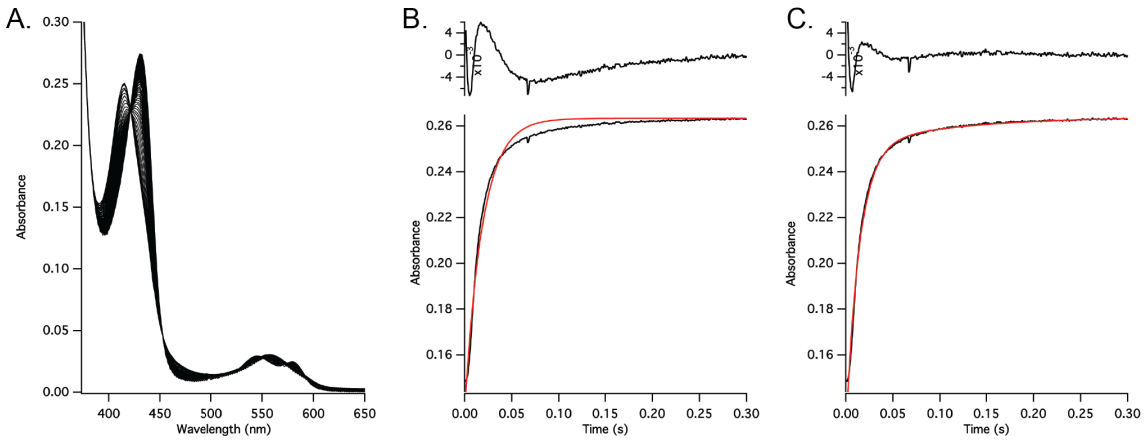

Figure 2.13. Stopped flow kinetics. (**a**) Representative overlayed stopped flow spectra of purified RsbR from *V. Brasilienesis.* Comparison of mono-exponential and bi-exponential fits (**b** and **c**, respectively) for representative O_2 dissociation experiments for RsbR. Raw data at 434 nm is shown in black and the calculated fit curve is in red. The fit residuals (difference between raw and fitted data) are shown in a black curve above each plot.

2.2.4 Stressosome Complex Structural Analysis

Dynamic light scattering (DLS) experiments of individual proteins and RsbR/S/T mixture were performed to provide independent validation of the protein-protein interactions and to determine the approximate size of the *V. brasiliensis* stressosome complex (Figure 2.12a). A previously reported cryo-EM structure of the *B. subtilus* stressosome core reported a diameter of approximately 30 nm.[3a] DLS of *V. brasiliensis* proteins show that the sizes of oligomers formed by individual proteins RsbR or RsbS are

poly-disperse (15-60 nm diameter range), likely oligomerizing through STAS domain interactions; the majority of oligomers have a diameter of approximately 20 nm. The majority of the kinase RsbT population forms considerably smaller oligomers (diameter ≈ 6 nm) with lower dispersity. In contrast, the RsbR/S/T mixture forms a complex with diameter of approximately 12 nm, which is smaller than the oligomers formed by individual RsbR and RsbS proteins, demonstrating that hetero-oligomeric protein-protein interactions between three proteins, likely mediated by RsbR and RsbS STAS domains, are different than interactions between homo-oligomers. Furthermore, DLS measurements mirror the trend in RsbT phosphorylation kinetics, highlighting that the three-protein complex RsbR/S/T forms key interactions involved in *V. brasiliensis* stressosome signaling transduction.

2.2.5 Conclusion

In summary, we report the first example of heme-bound RsbR as the sensing protein in a stressosome signaling complex, as well as the first characterization of a stressosome from a Gram-negative marine bacterium. These studies demonstrate a novel O_2-dependent stressosome signaling that is activated in O_2-depleted environments, and inhibited once the organism enters O_2-rich environments, or potentially upon interaction with reactive oxygen species. Our work provides a platform to study conformational changes within the stressosome complex upon ligand binding, which will aid in dissecting key protein-protein and domain-domain interactions involved in activation of stress-responsive genes. Studying the stressosome-regulated pathway also may provide insights into how free-living bacteria, such as members of the *Vibrio* genus become

human pathogens. One of the signals sensed by the *Vibrio* genus is O_2-limiting condition in the gut, therefore this O_2-sensing stressosome pathway could play a key role to sense low O_2 conditions and induce transcription of virulence genes.[1, 12b] Future *in vivo* work will allow for identification of ligand-dependent gene transcription and downstream effectors of the stressosome signaling pathway. Furthermore, understanding stressosome-regulated pathways in *V. brasiliensis* will help gain insights into stressosome-controlled signaling events in Gram-negative bacteria and the roles of O_2-dependent in the pathogenicity of the *Vibrio* genus.

2.3 Experimental

2.3.1 Cloning and Site-directed Mutagenesis

The wild-type *rsbR*, *rsbS* and *rsbT* genes used in this study were amplified from genomic DNA of *Vibrio brasiliensis* (DSMZ 17184). The primer sequences used in the overlap PCR reactions are listed in the table below. All oligonucleotides were synthesized by Integrated DNA Technology (IDT). Target genes *rsbR* and *rsbT* were cloned into the pMAL-c2X vector (Novagen), while *rsbS* was cloned into pGEX-4T1 vector (Novagen) for improved protein expression and stability. For construction of the *rsbS* expression plasmid, the PCR product was digested with endonucleases *Eco*RI and *Xho*I and inserted into pGEX-4T1 vector via *Eco*RI and *Xho*I restriction sites. To construct His-tags at the N-terminal of the MBP tags on RsbR and RsbT, the PCR products were digested with *Nde*I and *Eco*RI, and the purified *NdeI*-MBP-*EcoRI*

fragment was inserted into the pMAL-c2X vector via *Nde*I and *Eco*RI restriction sites. The resulting plasmid was named pHis-MBP. The *rsbR* or *rsbT* target gene was subsequently ligated into the *Hin*dIII and *Eco*RI sites on pHis-MBP. A Tev protease site also was introduced between MPB/GST tag and the target genes. The ligation mixture was transformed using *E. coli* DH5α cells. Positive transformants of all constructs were selected on LB plates containing 100 μg/mL ampicillin and DNA sequences were confirmed by sequencing (Eurofins).

The wild-type pHis-MBP-RsbT plasmid served as a template for site-directed mutagenesis (mutagenic primers are listed in the table). Positive transformants of all constructs were screened on LB plates containing 100 μg/mL ampicillin and the DNA sequences were confirmed by sequencing.

PCR primers

Name	Sequence 5'→ 3'
rsb-for	TTTGAATTCCATATGCCACATGGAACTTCGGTTG
rsb-rev	TAGCATTGACGCGATTTTGCGC
His-for	CATATGCACCACCACCACCACCACATGAAAATCGAAGAAGGTA AAC
His-rev	GAATTCTGACTGGAAGTACAGGTTCTCTGAA ATCCTTCCCTCG
rsbRpMAL-for	TTTCAGAATTCGGATCCTCTAGAATGCCACATGGAACTTCGGTTG
rsbRpMAL-rev	AAACGACGGCCAGTGCCAAGCTTTCACTCAGACAGCTGTTTTAAAG
rsbTpMAL-for	CGAGGGAAGGATTTTCAGAATTCATGCCCGACAGTGACTAC
rsbTpMAL-rev	AAACGACGGCCAGTGCCAAGCTTTTAGGATTTCCATTTAA
rsbSpGEX-for	TTCCGCGTGGATCCCCGGAATTCATGTCAAAGTCTATTTCA
rsbSpGEX-rev	CAGTCACGATGCGGCCGC TCGAGTCACTGTCGGGCACAAGC
rsbRTev-for	GATCGAGGGAAGGATTTCAGAGAACCTGTACTTCCAGGGCGAATTCG GATCCTCTAG

rsbRTev-rev	CTAGAGGATCCGAATTCGCCCTGGAAGTACAGGTTCTCTGAAATCCTTCCCTCGATC
rsbTTev-for	GATCGAGGGAAGGATTTCAGAGAACCTGTACTTCCAGGGCGAATTCATGCCCGACAG
rsbTTev-rev	CTGTCGGGCATGAATTCGCCCTGGAAGTACAGGTTCTCTGAAATCCTTCCCTCGATC
rsbSTev-for	GATCGAGGGAAGGATTTCAGAGAACCTGTACTTCCAGGGCGAATTCATGTCAAAGTC
rsbSTev-rev	GACTTTGACATGAATTCGCCCTGGAAGTACAGGTTCTCTGAAATCCTTCCCTCGATC

2.3.2 Protein Expression and Purification

Expression plasmids for wild-type RsbR, RsbS, RsbT, and mutant RsbT were transformed into chemically competent *E. coli* Tuner cells (Novagen). Cultures were grown in LB media at 37 °C until an optical density of 0.6-0.8 at 600 nm was reached. Cultures were then cooled to 18 °C and protein overexpression was induced by addition of 1 mM IPTG and incubation with shaking 16-18 hr. For RsbR expression, 500 μM 5-aminolevulinic acid (ALA) was added prior to addition of 1 mM IPTG to improve heme incorporation. All cells were harvested by centrifugation and lysed by homogenization (Avestin) after resuspension in buffer containing 50 mM Tris-HCl, pH 7.0, 250 mM NaCl and 5% (v/v) glycerol. Soluble proteins were separated from cell debris by ultracentrifugation at 186,000 *g* for 1hr. The supernatant with His_6-MBP-fused RsbR, RsbT and mutant RsbT were purified by nickel-NTA affinity chromatography. GST-tagged RsbS was purified by use of glutathione affinity chromatography. Representative SDS-PAGE of purified samples is shown in Figure 2.4.

2.3.3 Serine kinase autothiophosphorylation and thiophosphorylation assay using ATPγS.

Autophosphorylation and phosphoryl transfer kinetic experiments using ATP-γ-S were performed as previously described.[19] Briefly, serine kinase RsbT (5 μM) auto-thiophosphorylation reactions were initiated by addition of 500 μM ATPγS in reaction buffer containing 50 mM TEA, pH 7.5, 50 mM NaCl, 10 mM $MgCl_2$ and 5% glycerol (Buffer A). Thiophosphorylation reactions of RsbT (5 μM) in the presence of RsbR (5 μM) and RsbS (5 μM) in Buffer A were initiated by addition 500 μM ATPγS. The reactions were quenched with 6 μL of 500 mM EDTA at 0 min, 5 min, 10 min, 20 min, 30 min, 45 min, 60 min, 90 min and 120min. Quenched reactions were heated at 60 °C for 5 min, prior to alkylation with 1 mM *para*-nitrobenzylmesylate (PNBM) for 1.5 hr. Proteins were separated on 4-20% Tris-glycine SDS-PAGE gels (Biorad) and then were transferred from SDS-PAGE gels to nitrocellulose transfer membranes (0.2 μm, BioRad) using the Trans-Blot Turbo Transfer System (BioRad) at the high molecular weight setting for 10 min. Thiophosphoserine was detected as previously described.[19] Primary antibody specific for alkylated thiophosphate ester (1:5000, Abcam 51-8) was added and incubated with the blot overnight at 4°C. Subsequently, secondary antibody goat anti-rabbit HRP (1:5000, BioRad) was incubated with the blot at 25°C for 1.5 hr. The blot was developed using Western Blotting Detection Reagent kit (BioRad) and Amplified Opti-4CN Substrate kit (BioRad) for colorimetric detection. The blot was imaged using Epson Perfection V600 photo scanner (Epson) at the Professional Setting. Kinetics experiments were performed at least in triplicate to ensure reproducibility and accuracy of the assay, and mean and standard deviation values were calculated for each time point. Negative control reactions were performed without addition of ATP-γ-S to ensure there was no

cross-activity with alkylated cysteines. Representative western blots are shown in Figure 2.7.

2.3.4 Western blot analysis

Intensities of western blot signals were analyzed using ImageJ (RSB). Signal intensity at each time point was expressed as a relative percentage to the most intense band on the same western blot.

2.3.5 O_2 dissociation rate

O_2 dissociation rates were measured as previously described.[17] The dissociation of O_2 from heme protein RsbR at 25 °C was monitored using an SX20 equipped with a diode array detector and temperature controlled bath, and fit globally using Pro-KII software (Applied Photophysics). Additional fitting analysis was performed using Igor Pro (Wavemetrics).

2.3.6 Stressosome complex structural analysis

Dynamic light scattering (DLS) experiments were carried out with a NanoPlus zeta/nano particle analyzer (Particulate Systems) at 25 °C. The particle size distribution was derived from a deconvolution of the measured intensity autocorrelation function of the sample by the general-purpose mode algorithm included in the software. DLS measurements were performed in buffer containing 50 mM Tris-HCl and 250 mM NaCl (pH =7) with 5% (v/v) glycerol; concentrations of all protein samples were 15 μM. All experiments were performed in triplicate to ensure reproducibility and accuracy of the assay.

2.3.7 RsbR autooxidation experiment

Autoxidation experiments were carried out with a Cary 100 UV-Vis spectrophotometer (Agilent Technologies) at 25 °C. Spectra of Fe^{II}-O_2 RsbR were taken every 15 min for 18 hours. Heme ligands for Fe^{II} and Fe^{III} RsbR (CO and KCN, respectively, which have diagnostic spectra) were added after two hours to determine the oxidation state of RsbR.

2.4 References

1. (a) Janda, J. M.; Newton, A. E.; Bopp, C. A., Vibriosis. *Clin Lab Med* **2015,** *35* (2), 273-88; (b) Travers, M. A.; Miller, K. B.; Roque, A.; Friedman, C. S., Bacterial diseases in marine bivalves. *J Invertebr Pathol* **2015**.

2. (a) Yildiz, F. H.; Schoolnik, G. K., Role of rpoS in stress survival and virulence of Vibrio cholerae. *J Bacteriol* **1998,** *180* (4), 773-84; (b) Jones, M. K.; Oliver, J. D., Vibrio vulnificus: disease and pathogenesis. *Infect Immun* **2009,** *77* (5), 1723-33.

3. (a) Marles-Wright, J.; Grant, T.; Delumeau, O.; van Duinen, G.; Firbank, S. J.; Lewis, P. J.; Murray, J. W.; Newman, J. A.; Quin, M. B.; Race, P. R.; Rohou, A.; Tichelaar, W.; van Heel, M.; Lewis, R. J., Molecular architecture of the "stressosome," a signal integration and transduction hub. *Science* **2008,** *322* (5898), 92-6; (b) Price, C. W.; Fawcett, P.; Ceremonie, H.; Su, N.; Murphy, C. K.; Youngman, P., Genome-wide analysis of the general stress response in Bacillus subtilis. *Mol Microbiol* **2001,** *41* (4), 757-74.

4. Marles-Wright, J.; Lewis, R. J., The stressosome: molecular architecture of a signalling hub. *Biochem Soci Trans* **2010,** *38* (4), 928-33.

5. Chen, C. C.; Yudkin, M. D.; Delumeau, O., Phosphorylation and RsbX-dependent dephosphorylation of RsbR in the RsbR-RsbS complex of Bacillus subtilis. *J bacteriol* **2004,** *186* (20), 6830-6.

6. (a) Gaidenko, T. A.; Price, C. W., Genetic evidence for a phosphorylation-independent signal transduction mechanism within the Bacillus subtilis stressosome. *PLoS One* **2014,** *9* (3), e90741; (b) Murray, J. W.; Delumeau, O.; Lewis, R. J., Structure of a nonheme globin in environmental stress signaling. *Proc Nat Acad Sci USA* **2005,** *102* (48), 17320-5.

7. (a) Kim, T. J.; Gaidenko, T. A.; Price, C. W., A multicomponent protein complex mediates environmental stress signaling in Bacillus subtilis. *J Mol Biol* **2004,** *341* (1), 135-50; (b) Kim, T. J.; Gaidenko, T. A.; Price, C. W., In vivo phosphorylation of partner switching regulators correlates with stress transmission in the environmental signaling pathway of Bacillus subtilis. *J Bacteriol* **2004,** *186* (18), 6124-32; (c) Chen, C. C.; Lewis, R. J.; Harris, R.; Yudkin, M. D.; Delumeau, O., A supramolecular complex in the environmental stress signalling pathway of Bacillus subtilis. *Mol Microbiol* **2003,** *49* (6), 1657-69.

8. Gaidenko, T. A.; Yang, X.; Lee, Y. M.; Price, C. W., Threonine phosphorylation of modulator protein RsbR governs its ability to regulate a serine kinase in the environmental stress signaling pathway of Bacillus subtilis. *J Mol Biol* **1999,** *288* (1), 29-39.

9. Eymann, C.; Schulz, S.; Gronau, K.; Becher, D.; Hecker, M.; Price, C. W., In vivo phosphorylation patterns of key stressosome proteins define a second feedback loop that

limits activation of Bacillus subtilis sigmaB. *Mol Microbiol* **2011,** *80* (3), 798-810.

10. Pane-Farre, J.; Lewis, R. J.; Stulke, J., The RsbRST stress module in bacteria: a signalling system that may interact with different output modules. *J Mol Microbiol Biotechnol* **2005,** *9* (2), 65-76.

11. (a) Guengerich, F. P., New trends in cytochrome p450 research at the half-century mark. *J Biol Chem* **2013,** *288* (24), 17063-4; (b) Poulos, T. L., Heme enzyme structure and function. *Chem Rev* **2014,** *114* (7), 3919-62; (c) Shimizu, T.; Huang, D.; Yan, F.; Stranava, M.; Bartosova, M.; Fojtikova, V.; Martinkova, M., Gaseous O2, NO, and CO in signal transduction: structure and function relationships of heme-based gas sensors and heme-redox sensors. *Chem Rev* **2015,** *115* (13), 6491-533; (d) Jain, R.; Chan, M. K., Mechanisms of ligand discrimination by heme proteins. *J Bio Inorg Chem* **2003,** *8* (1-2), 1-11.

12. (a) Phippen, B. L.; Oliver, J. D., Role of anaerobiosis in capsule production and biofilm formation in Vibrio vulnificus. *Infect Immun* **2015,** *83* (2), 551-9; (b) Fan, F.; Liu, Z.; Jabeen, N.; Birdwell, L. D.; Zhu, J.; Kan, B., Enhanced interaction of Vibrio cholerae virulence regulators TcpP and ToxR under oxygen-limiting conditions. *Infect Immun* **2014,** *82* (4), 1676-82.

13. (a) Hou, S.; Larsen, R. W.; Boudko, D.; Riley, C. W.; Karatan, E.; Zimmer, M.; Ordal, G. W.; Alam, M., Myoglobin-like aerotaxis transducers in Archaea and Bacteria. *Nature* **2000,** *403* (6769), 540-4; (b) Kitanishi, K.; Kobayashi, K.; Uchida, T.; Ishimori, K.; Igarashi, J.; Shimizu, T., Identification and functional and spectral characterization of

a globin-coupled histidine kinase from Anaeromyxobacter sp. Fw109-5. *J Bio Chem* **2011,** *286* (41), 35522-34.

14. Kang, C. M.; Vijay, K.; Price, C. W., Serine kinase activity of a Bacillus subtilis switch protein is required to transduce environmental stress signals but not to activate its target PP2C phosphatase. *Mol Microbiol* **1998,** *30* (1), 189-96.

15. Barry A. Springer, S. G. S., John S. Olson, George N. Jr. Phillips, Mechanisms of Ligand Recognition in Myoglobin. *Chem Rev* **1994,** *94* (3), 699-714.

16. Ohta, T.; Yoshimura, H.; Yoshioka, S.; Aono, S.; Kitagawa, T., Oxygen-sensing mechanism of HemAT from Bacillus subtilis: a resonance Raman spectroscopic study. *J Am Chem Soc* **2004,** *126* (46), 15000-1.

17. Burns, J. L.; Deer, D. D.; Weinert, E. E., Oligomeric state affects oxygen dissociation and diguanylate cyclase activity of globin coupled sensors. *Mol Biosyst* **2014,** *10* (11), 2823-6.

18. Kelley, L. A.; Mezulis, S.; Yates, C. M.; Wass, M. N.; Sternberg, M. J., The Phyre2 web portal for protein modeling, prediction and analysis. *Nat protoc* **2015,** *10* (6), 845-58.

19. Carlson, H. K.; Plate, L.; Price, M. S.; Allen, J. J.; Shokat, K. M.; Marletta, M. A., Use of a semisynthetic epitope to probe histidine kinase activity and regulation. *Anal Biochem* **2010,** *397* (2), 139-143.

Chapter 3: Study of 3',5'-cCMP as a Putative Mammalian Second Messenger- Progress Toward Identification of 3',5'-cCMP-related Enzymes in Mammalian Tissues

3.1 Introduction

Cyclic nucleotides such as adenosine 3', 5'-cyclic monophosphate (cAMP) and guanosine 3', 5'-monophosphate (cGMP) are second messengers that perform crucial roles in regulating cellular metabolism and mediating numerous biochemical processes in eukaryotic cells (Figure 3.1).[1] While the cyclic nucleotides 3',5'-cAMP and 3',5'-cGMP have been established as crucial mammalian signaling molecules for decades, a third naturally occurring pyrimidine cyclic nucleotide, cytidine 3', 5'-cyclic monophosphate (3',5'-cCMP) has been identified, but its biological function still remain unknown (Figure 3.1).[2]

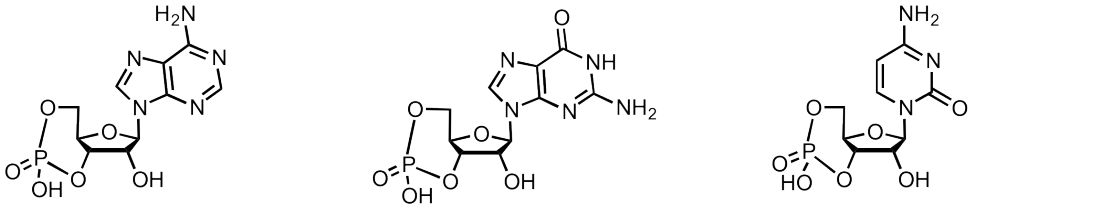

Figure 3.1 Structures of three cyclic 3',5'-nucleotide monophosphates, 3',5'-cAMP, 3',5'-cGMP and 3',5'-cCMP described in this chapter.

3',5'-cCMP was initially isolated from urine samples of acute leukemia patients and in rapidly dividing tissues.[2] Subsequently, putative proteins capable of synthesizing and hydrolyzing 3',5'-cCMP, cytidylate cyclase and 3',5'-cCMP-specific

phosphodiesterase (PDE) respectively, as well as 3',5'-cCMP dependent protein kinases were reported.[2c, d, 3] More recently, 3',5'-cCMP was shown to stimulate phosphorylation of Rab23, a negative regulator of the tumorigenic sonic hedgehog (shh) signaling pathway, which is one of the key regulators during animal development, which controls neural tube development.[4] However, while the potential role of cCMP in cellular differentiation and proliferation has been suggested over the past few decades, little is known about its physiological and biochemical roles in mammalian systems. Furthermore, research has revealed the promiscuity of purified soluble guanylyl cyclase (sGC) and its ability to synthesize 3',5'-cGMP, 3',5'-cAMP and 3',5'-cCMP at various rates, casting doubt on the authenticity of the previous isolated cytidylate cyclase.[5]

Although isolations of cytidylate cyclase, 3',5'-cCMP-specific PDE and 3',5'-cCMP-dependent kinase (PKA) have been previously reported, the amino acid and gene sequences of these proteins still remain unknown.[2c, d, 3, 6] Without previous knowledge about the identity of cytidylate cyclase and cCMP-specific phosphodiesterase (PDE), the initial step to study 3',5'-cCMP signaling pathway is to isolate enzymes involved in the 3',5'-cCMP signaling pathway. To date, there are multiple isoforms of adenylate cyclase and guanylate cyclase reported, both of which consist of soluble and membrane-bound isoforms.[1b, 7] Although the location of mammalian cytidylate cyclase has not been unequivocally reported, previously published research has observed turnover of CTP to 3',5'-cCMP in enzymes isolated from both the cytosolic and the membrane fraction, which has led the proposal of the presence of multiple isoforms of cytidylate cyclase, both soluble and membrane-bond.[8] Also, previous published analytical methods using

thin layer chromatography (t. l. c) and radioimmunoassay lack the sensitivity and specificity to detect and quantify 3',5'-cCMP. Moreover, lack of a standardized purification protocol and analytical method to study 3',5'-cCMP-related enzymes has made establishing the role of 3',5'-cCMP as a mammalian signaling molecule especially challenging.[3a, 8a]

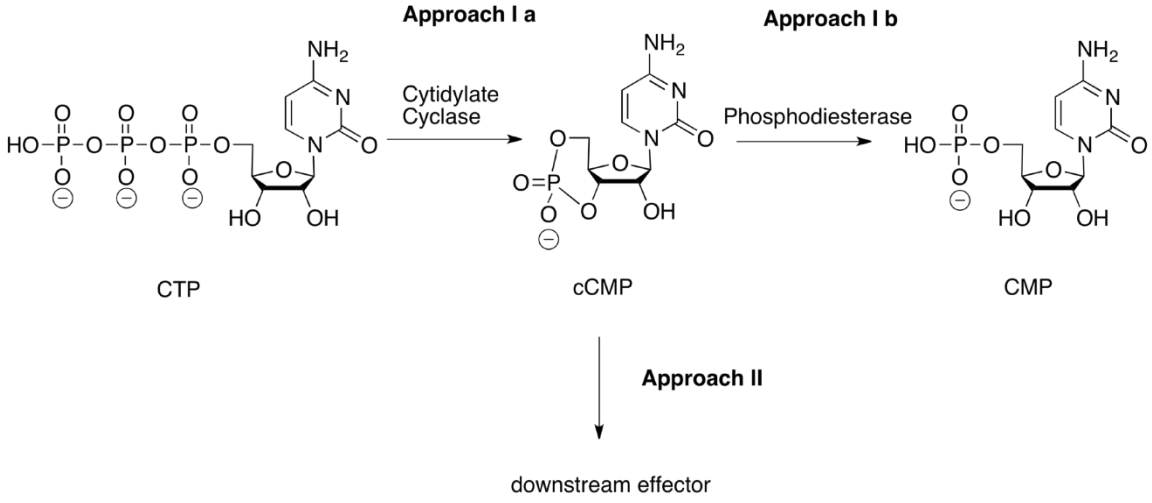

Figure 3.2 Outline of putative 3',5'-cCMP-related enzymes isolation and identification using enzyme fractionation and cCMP-affinity matrices approaches described in this chapter.

In this chapter, we aim to develop an efficient protocol to identify enzyme members of 3',5'-cCMP signaling pathways through two complementary approaches (Figure 3.2). In the first approach, we attempted to isolate and identify protein members in the pathways using modified previously published protocols (Figure 3.2 Approach Ia and Ib). Amino acid or gene sequence of putative mammalian cytidylate cyclase and

cCMP-specific PDE using tandem MS-based proteomics studies will be determined in order to establish molecular identifies of these enzymes. In the second approach, I identified potential cCMP-binding proteins through cCMP matrices affinity chromatography (Figure 3.2 Approach II). We have synthesized cCMP probes tethered to agarose, which were used to probe for cCMP-binding proteins in mammalian tissue homogenates. The identification of isolated proteins was attempted using MALDI (Matrix Assisted Laser Desorption/Ionization) mass spectrometry and published genome sequences.

3.2 Results and Discussion

3.2.1 Approach I: Identification of cCMP-Related Enzymes through Protein Purification

3.2.1.1 Partial Purification and Properties of Cytidylate Cyclase Activity

An outline of the optimized purification protocols for soluble and membrane-bound cytidylate cyclase is depicted in Figure 3.3 and 3.4 (refer to experimental section 3.4.2 for details).[9] To prepare soluble cytidylate cyclase, frozen rat livers were homogenized in pre-chilled homogenate buffer with 1 mM protease inhibitor AEBSF. The highest concentration of cCMP was identified in re-generating organs such as rat livers; therefore, rat livers were chosen for testing cytidylate cyclase activity. The low-speed centrifugation (Figure 3.3, step 2) was used to remove lipids and cellular debris. The subsequent high-speed centrifugation (Figure 3.3, step 3) was used to separate

insoluble protein from soluble protein, and both fractions were tested for enzyme activity. To purify membrane-bound cytidylate cyclase, a sucrose solution was used to solubilize membrane-bound protein (Figure 3.4). Both the supernatant containing solubilized membrane-bound protein and pellet were used to test for cytidylate cyclase activity.

Initially, cytidylate cyclase activity assay was analyzed using HPLC. The intrinsic retention time for each compound based on the authentic standard was used for identifying putative cNMPs. In order to achieve the best results, a series of optimization experiments were performed to achieve the highest cytidylate cyclase activity. These optimizations include varying concentrations of substrate, cofactor $MnCl_2$ and purified enzyme mixture. Enzyme fractions putatively containing soluble (Figure 3.3 step 3) and membrane-bound (Figure 3.4 step 4) cyticylate cyclase were used to optimize the analytical protocol. The initial concentrations of $MnCl_2$ and CTP in the cytidylate cyclase reaction were 40 mM and 1 mM respectively, however, incubating both soluble and membrane-bound fractions with starting material and the metal co-factor yielded only the hydrolyzed product cytidine instead of the cyclized product 3',5'-cCMP. Previous research reports the highest cytidylate cyclase activity in partially purified rat organ fraction is achieved with $\leq$ 5 mM Mn^{2+}, and the enzymatic activity level dramatically decreases when Mn^{2+} is higher than 10 mM.[10] However, decreasing $MnCl_2$ concentration to 4 mM, the reaction still produced solely the hydrolyzed product cytidine. Increasing concentration of the starting material CTP 5 fold and 10 fold, resulted in isolation of the starting material CTP. The concentration of enzyme in each reaction is another important factor determines reaction rates. Incubating various volumes of soluble and membrane-

bound fractions with 4 mM $MnCl_2$ and 1 mM CTP, reactions still yielded only the hydrolysis product cytidine. Since a previously published protocol has isolated an active membrane-bound cytidylate cyclase from the membrane fraction solubilized by Triton-X100, cytidylate cyclase activity was carried out using similar reaction conditions as described above, but with re-solubilized enzyme in the pellet fraction following both purifications protocols. Unfortunately, these reactions also yielded only the hydrolyzed product cytidine.

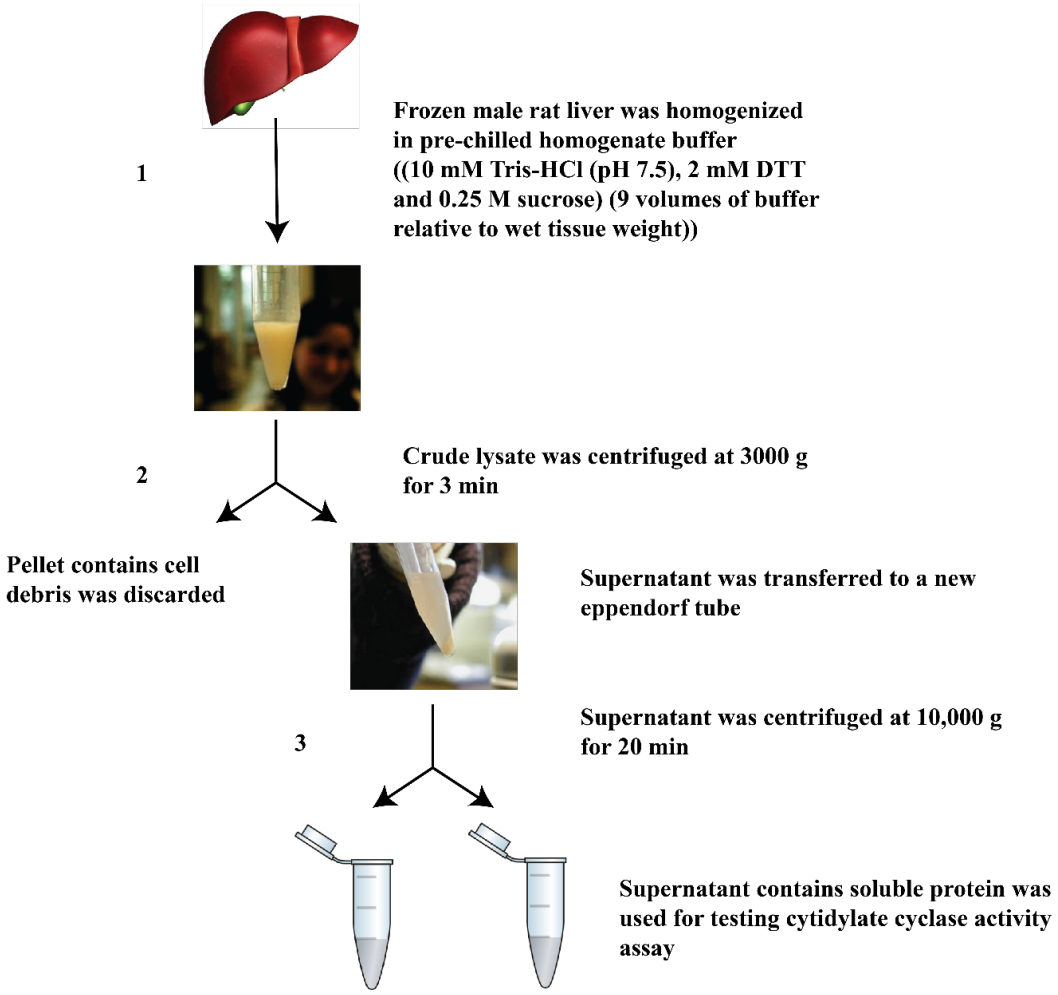

Figure 3.3 Workflow chart of soluble cytidylate cyclase purification from rat livers.

Control experiments detecting adenylate cyclase (AC) and soluble guanylyl cyclase (sGC) activities in rat liver were performed to ensure the reliability of our purification and analytical protocols. However, only the starting material ATP in the AC activity assays, and the hydrolyzed product guanosine in the sGC activity assays have been identified using HPLC. Cytidylate cyclase identification and enzymatic activity assays were unfruitful using the current purification and analytical method, likely either because cytidylate cyclase was inactivated during purification, or the presence of a phosphodiesterase in the partial purified cytidylate cyclase fraction that hydrolyzed cNMPs to the corresponding hydrolyzed products.

The unsuccessful isolation of enzymatic activity based on a previously published protocol has also led us to question whether the sensitivity of HPLC is sufficient to detect cNMPs in those enzyme assays. Therefore, mass spectroscopy, a technique that provides a higher degree of specificity and sensitivity, was adapted to detect putative cNMP products in this study. Cytidylate cyclase activity assay was analyzed on a Thermo LTQ-FTMS. The exact masses of various cNMP and NMP standards are reported in Table 3.1. Mass spectrometry-based techniques have been a game-changing tool for detecting putative cNMPs product in purified enzymatic activity assays.

The putative 3',5'-cCMP was identified in the reaction mixture incubating 80 uL of soluble enzyme fraction (Figure 3.4) with 4 mM $MnCl_2$ and 1 mM CTP using electrospray ionization mass spectrometry (ESI-MS), which indicates the presence of a soluble cytidylate cyclase or a promiscuous adenylate or guanylate cyclase. Therefore, further fractionation is needed to purify and isolate the putative cytidylate cyclase.

1

Frozen male rat liver was homogenized
in pre-chilled homogenate buffer
((50 mM Tris-HCl (pH 7.5), 9 volumes of buffer
relative to wet tissue weight)

2

Crude lysate was centrifuged at 500 g
for 5 min

Pellet contains cell
debris was discarded

Supernatant was dialyzed in
homogenate buffer for four hr

3

0.25 M sucrose solution was added
to he dialysate to solubilize membrane-
bond protein

4

The mixture was centrifuged at 100,000 g
for 90 min

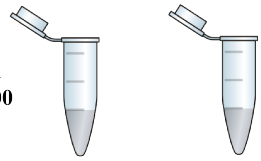

Pellet containing insoluble protein
was dissolved in 0.3% Triton X-100

Supernatant contains soluble protein was
used for cytidylate cyclase activity assay

5

Solublized pellet fraction was centrifuged
at 100,000 g for 1hr

Insoluble fraction was used for
cytidylate cyclase activity assay

Figure 3.4 Workflow chart of membrane-bound cytidylate cyclase purification from rat livers.

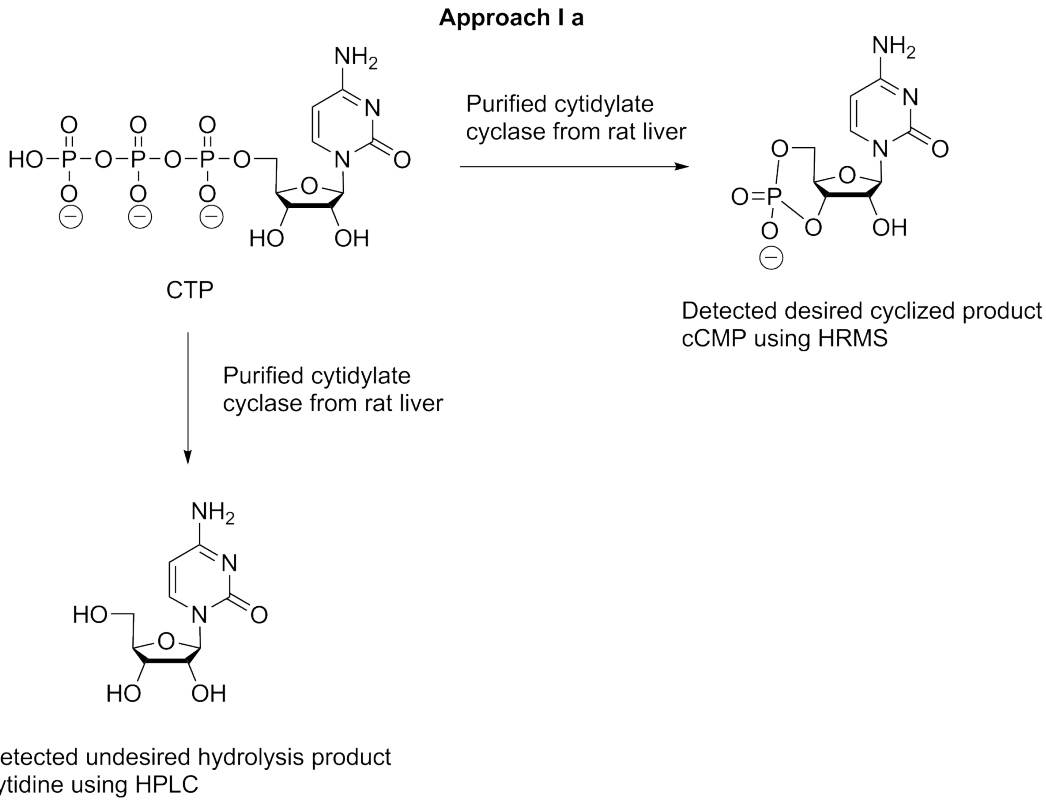

Figure 3.5 In Approach Ia, two distinct products from purified cytidylate cyclase activity assays were detected using different analytical methods, HPLC and HRMS. Cyclized product 3',5'-cCMP was detected using HRMS, indicating that mass spectrometry-based analytical method with improved sensitivity should be adapted to identify cNMPs in this chapter.

Table 3.1 Exact masses of authentic nucleotides and cyclic nucleotides analyzed on a LTQ-FTMS.

	cCMP	**cAMP**	**CMP**	**AMP**	**cytidine**	**adenosine**
Exact Mass (*m/z*)	305.04129	329.05252	323.05186	347.06309	243.08552	267.09676
$[M+H]^+$ (*m/z*)	306.04129	330.05252	324.05186	348.06309	244.08552	268.09676

$[M + H]^+$ = protonated molecular mass.

As shown on the spectrum, we also have isolated a variety of small molecules from the complex soluble enzyme fraction incubation mixture (Figure 3.6). Moreover, matrix effects result from co-eluting matrix components, such as endogenous phospholipids, can greatly affect ionization of the analyte-of-interest in LC-MS/MS analyses, resulting in ion suppression.[11] Therefore, an efficient sample preparation protocol and a liquid chromatography-based separation prior to MS analysis are needed to reduce matrix effect. Moreover, utilizing tandem mass spectrometry (MS/MS), which offers further information about specific ions, will provide comprehensive structural analysis on analyte-of-interest, thereby allowing unequivocal identification of putative cNMP products.

A control experiment detecting adenylate cyclase (AC) activity in rat liver was performed to ensure the reliability of our purification and analytical protocols. Putative 3',5'-cAMP product was also isolated in the reaction mixture using ESI-MS (Figure 3.7). It agrees with previous published results on presence of adenylate cyclase in rat liver.

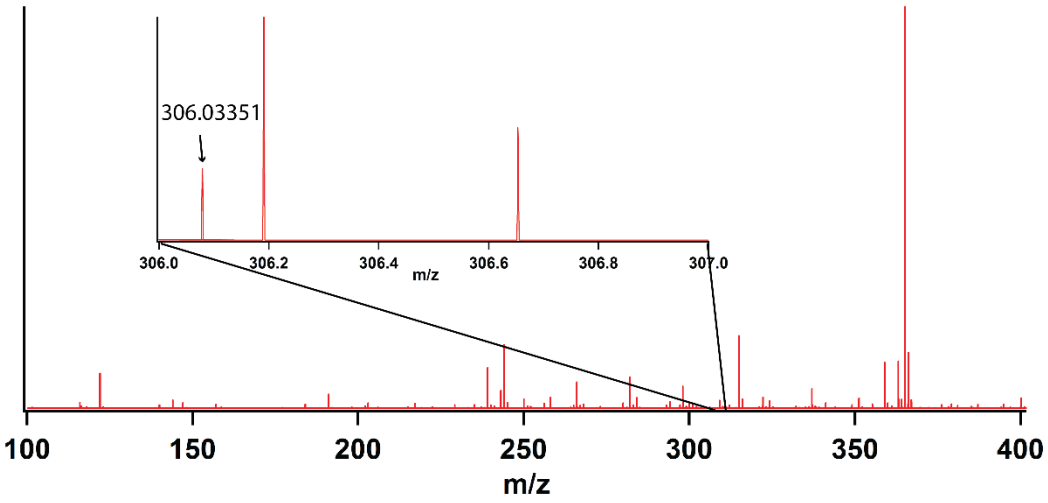

Figure 3.6 Positive-ion high-resolution mass spectrum of soluble cytidylate cyclase reaction mixture after termination of reaction. Expanded spectrum of putative cCMP product ($[M+H]^+$, *m/z* 306.03351) is in the inset.

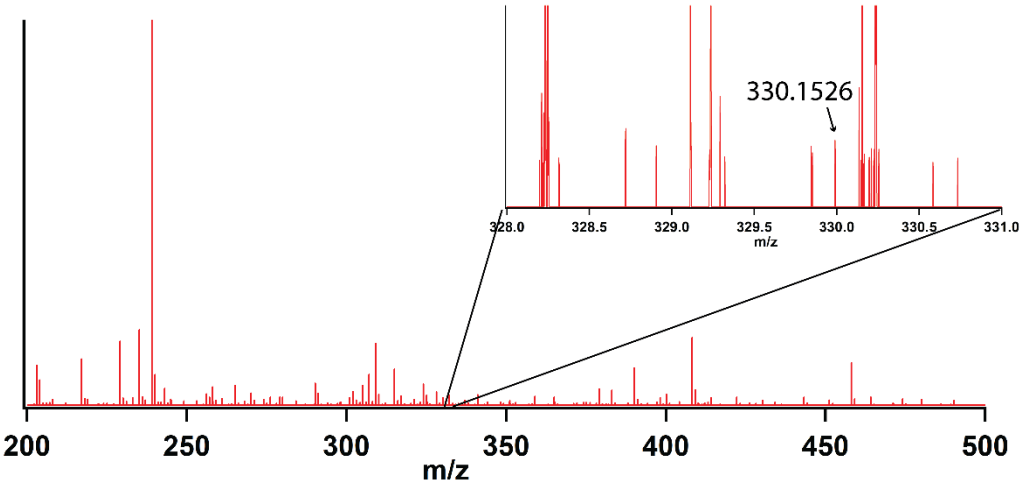

Figure 3.7 Positive-ion high-resolution mass spectrum of soluble adenylate cyclase incubation mixture after termination of reaction. Expanded spectrum of putative cAMP product ($[M+H]^+$, *m/z* 330.1526) is in the inset.

Results show that a mass spectrometry-based technique is a much more sensitive and suitable analytical method for detecting putative cNMP products. Using the current protocol, we have identified putative 3',5'-cCMP product synthesized in rat brains; the cytidylate cyclase activity could result from the presence of a novel cytidylate cyclase or an active non-specific cyclase. Future work includes developing an efficient protocol to further fractionate the cytosolic fraction, in order to isolate and characterize the potential cytidylate cyclase in rat livers. Determining the amino acid sequence of the novel mammalian cytidylate cyclase will not only help us understand the molecular structure of the protein, but also establish the physiological role of 3',5'-cCMP as a naturally occurring signaling molecule in mammals. An improved sample preparation protocol and LC-based separation method prior to MS or MS/MS analysis is important to reduce matrix effects and improve sensitivity of the analytical method.

3.2.1.2. Partial Purification and Properties of cCMP-Specific Phosphodiesterase (PDE) Activity

An outline of the optimized purification protocol for 3',5'-cCMP-specific PDE in rat liver is depicted in Figure 3.8 (refer to experimental section 3.4.3 for details).[6] Following a previously published protocol, ammonium sulfate fractionation was used to purify PDE in the rat liver.[6] Ammonium sulfate precipitation is a method used to purify proteins based on their solubility in the presence of a high concentration of salt. This type

of fractionation has a stabilizing action on some enzymes, and has been proven to be a very effective means of fractionating protein. [12]

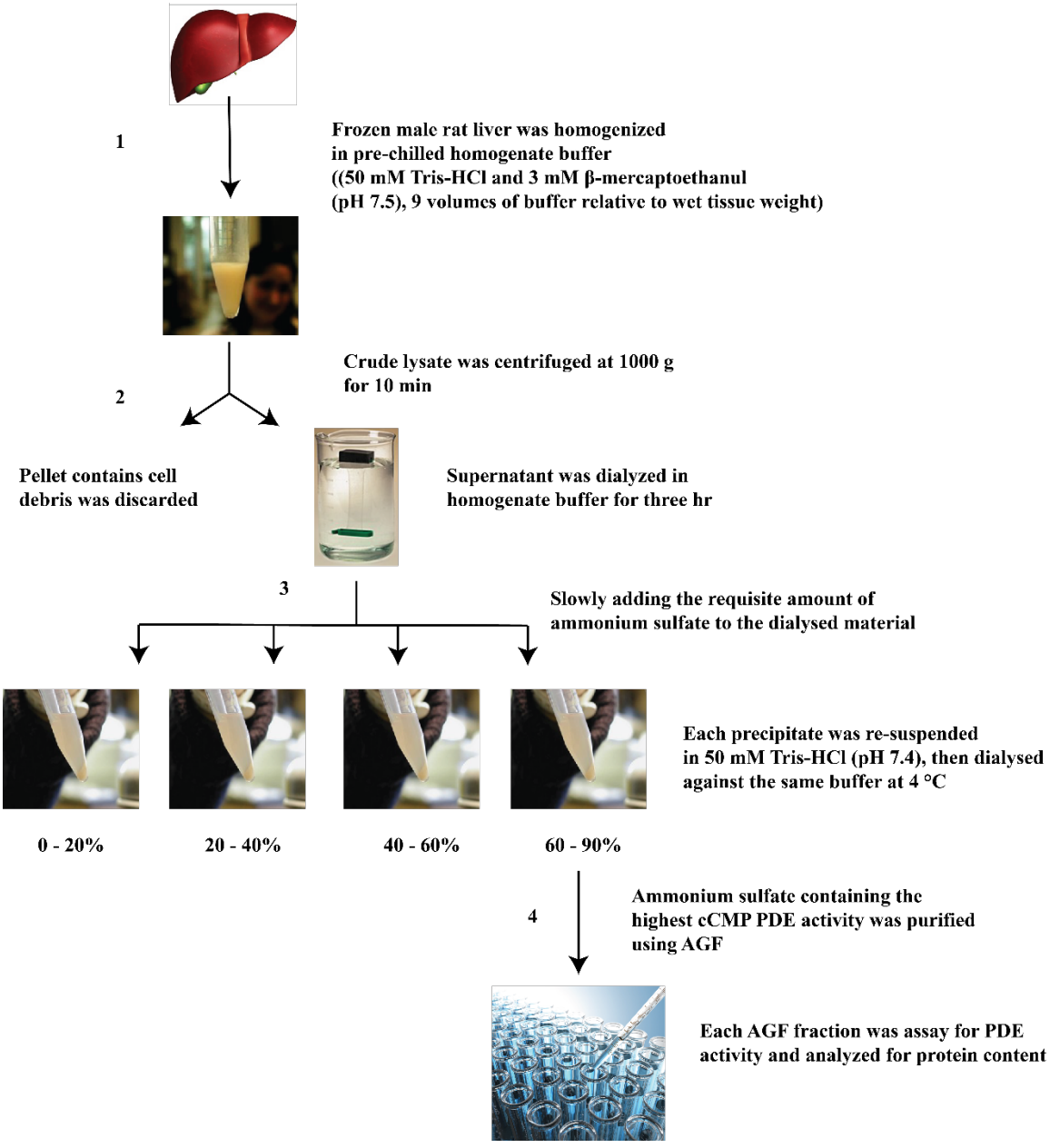

Figure 3.8 Workflow chart of cCMP-specific PDE purification from rat livers.

Previously published research has partially purified 3',5'-cCMP-specific PDE that has a molecular weight of 28 kDa from ammonium sulfate fractionation fraction 60-90% in rat liver.[6] The fraction containing the highest cCMP PDE activity was then purified on analytical gel filtration (AGF) to further purify the desired enzyme. Intriguingly, fraction 43 after AGF shows a band with molecular weight at around 28 kDa, which is the same as previously identified 3',5'-cCMP PDE (Figure 3.9). It suggests that fraction 43 may contain the desired 3',5'-cCMP PDE. cCMP PDE-containing fraction 43 was incubated with 10 mM starting material cCMP and 10 mM $FeSO_4 \bullet 7H_2O$ to test for PDE activity. Putative CMP product from these activity assays was analyzed on HPLC. As a control experiment, similar PDE activity assay was also carried out using the crude lysate fraction to ensure putative enzyme maintain its activity throughout the protocol. However, the crude lysate mixture yielded the hydrolyzed product cytidine, while fraction 43 produced only the starting material 3',5'-cCMP. It suggests that the current protocol is not yet sufficient in maintaining cCMP-specific PDE activities. It is also possible that cCMP PDE may be present, but the concentration of the putative CMP product was close to the detection limit on HPLC.

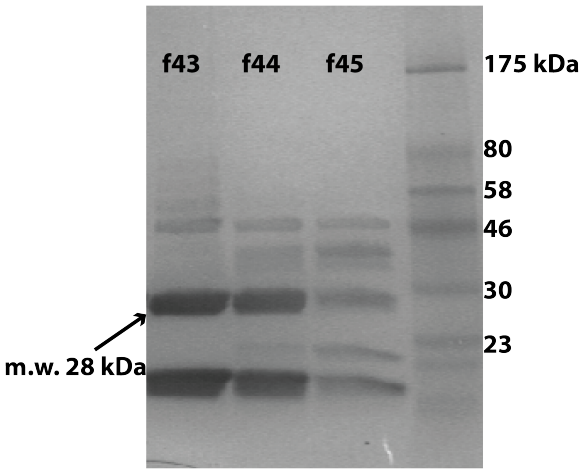

Figure 3.9 SDS-PAGE analysis of analytical gel filtration (AGF) fractions that may contain a putative cCMP PDE. Fraction 43 contains a protein with molecular weight at around 28 kDa, which is the same as previously reported cCMP-specific PDE.

These results suggest that the putative 3',5'-cCMP PDE has lost its activity during purification. Future work includes developing a more gentle and time-conserving protocol to preserve and isolate 3',5'-cCMP-specific PDE in mammalian tissues. In addition, mass spectrometry-based techniques are better analytical methods for detecting CMP. Obtaining the amino acid sequence of the putative cCMP-specific PDE in the future will not only provide molecular identify of the protein, but also will help to establish the physiological role of 3',5'-cCMP as a mammalian signaling molecule.

3.2.2 Approach II: 3',5'-cCMP Matrices for the Affinity Purification of cCMP-binding Protein

Affinity matrix chromatography makes use of specific binding interactions between proteins and ligand bound to solid support. A particular ligand is chemically immobilized on a solid support, and then after other sample components are washed away, the bound protein is eluted from the support, resulting in its purification from the original sample. We have synthesized 3',5'-cCMP resin by coupling immobilized diaminodipropylamine (DADPA) (Figure 3.10, B) to cCMP at two different positions. 2'- and 3'-hydroxyl groups of 3',5'-cCMP can be activated by NHS esters or carbodiimides for the subsequent conjugation to the free amine of the immobilized DADPA linker through amine-reactive reactions. Immobilizing the DADPA agarose at 2'-hydroxyl and the phosphate positions of 3',5'-cCMP yielded 3',5'-cCMP-2'-OH and 3',5'-cCMP-phosphate probes, respectively (Figure 3.10, A). Linking agarose at two different positions increases the accessibility of the affinity ligands to proteins, thereby increases the likelihood of obtaining 3',5'-cCMP-binding proteins. Tethering 3',5'-cCMP to the MS $(PEG)_4$ agarose linker will elongate the spacer arm, which reduces possible steric hindrance, possibly permitting greater binding of proteins (Figure 3.10, C). A control probe, 3',5'-cAMP-phosphate agarose, was also synthesized to test for non-specific binding and promiscuity of the 3',5'-cCMP-binding proteins.

Following a previously published method, 3',5'-cCMP-phosphate probe was synthesized by coupling DADPA agarose with an activated cCMP (Scheme 3.1, **2**).[13]

Coupling 3',5'-cCMP salt **1** with 4-bromocrotonic acid installs the carboxyl group required for the subsequent coupling reaction on 3',5'-cCMP. EDC (1-Ethyl-3-(3-dimethylaminopropyl) carbodiimide• HCl) reacts with the carboxyl group to form an amine-reactive o-acylisourea intermediate. The resulting intermediate reacts with the DADPA agarose to yield the desired 3',5'-cCMP-phosphate probe. A control probe, 3',5'-cAMP-phosphate probe was synthesized in a similar fashion to test for non-specific binding.

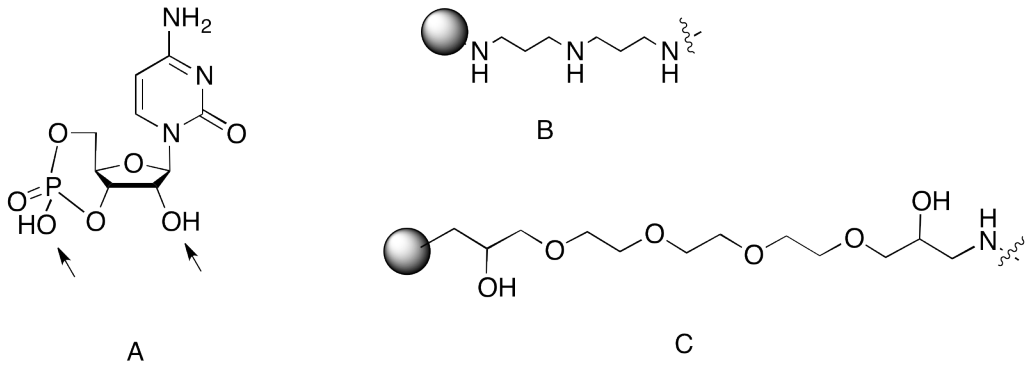

Figure 3.10 Structures of synthesized 3',5'-cCMP matrices for the affinity purification of cCMP-binding protein. A. Proposed sites of modifications of cCMP. B. Side chain DADPA agarose to be coupled to cCMP probe. C. Side chain MS $(PEG)_4$ agarose linker.

Two isomers of the intermediate **2** (Figure 3.11) are likely to form as a result of the coupling reaction between 3',5'-cCMP (Scheme 3.1, **1**) and 4-bromocrotonic acid.

Scheme 3.1 Synthesis of 3',5'-cCMP-phosphate resin.

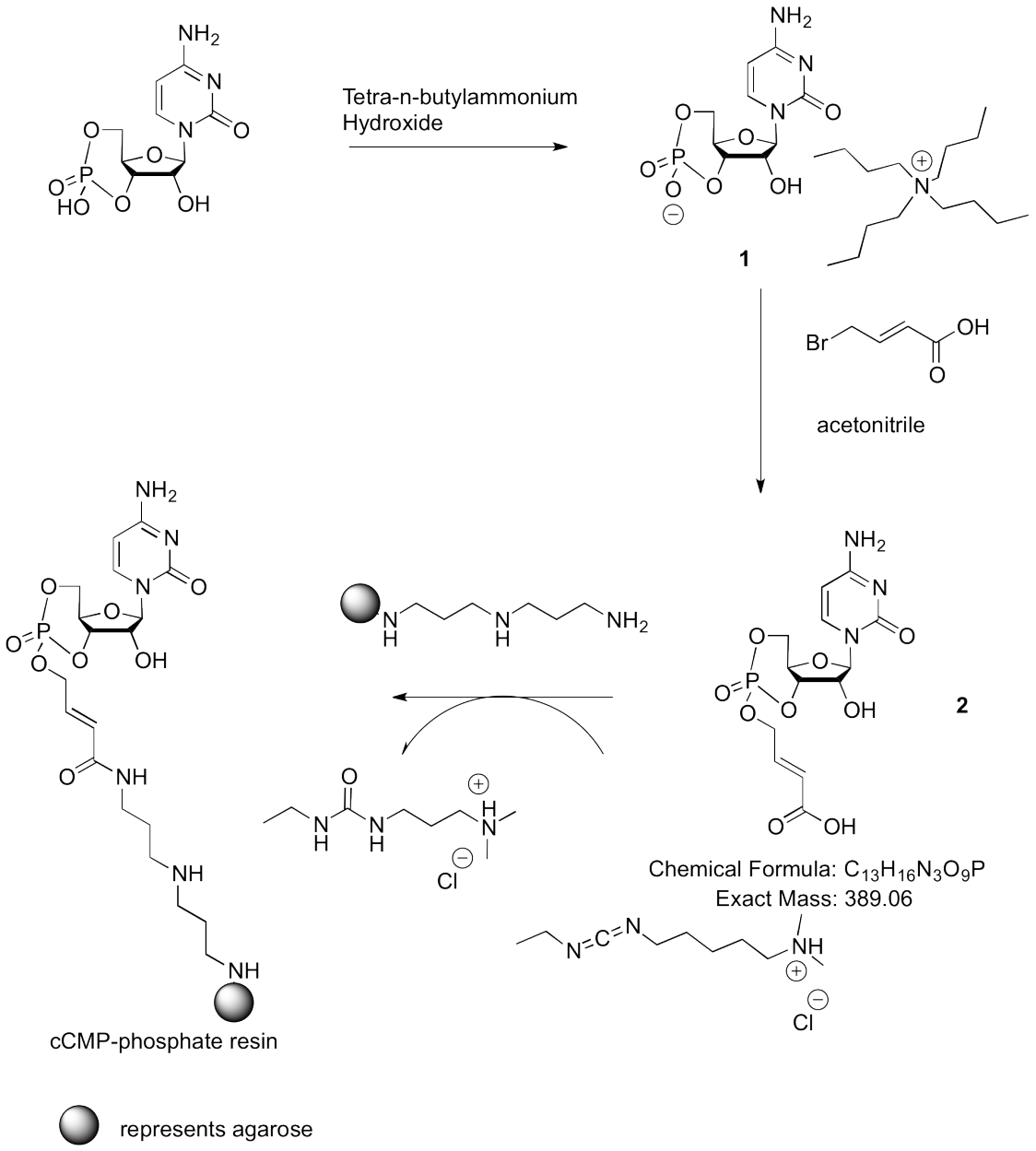

Although the unfavorable 1,3-diaxial interactions in the axial isomer due to steric hindrance between the acid group and both 3' and 5'-hydrogens favor the equatorial or

axial isomer, the more dominant electronic gauche effect overcomes the steric effects, suggesting majority of the product should be the axial isomer (Figure 3.11).[13] We have not successfully obtained the isomeric ratio of the two isomers using our current chromatography conditions. This could be because the crotonic acid group is not bulky enough to differentiate between the two isomers. Both ^{1}H NMR and HRMS results show that **2** is the major product of this coupling reaction alone with tetra-n-butylammonium salt. Since the presence of by-product salt does not greatly affect the subsequent coupling reaction, the crude mixture containing desired intermediate both isomers of **2** was used for the next step.

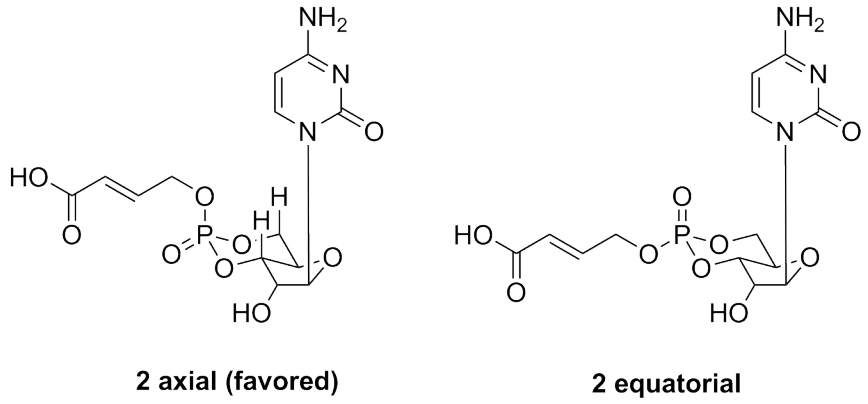

Figure 3.11 Axial and equatorial isomers of intermediate **2** in Scheme 3.1 (certain bond lengths have been elongated to show steric collision). The axial isomer of **2** is favored due to gauche effect.[13]

Following a previously published method, synthesis of the 2'-OH-cCMP probe is depicted in Scheme 3.1.[14] N, N'-dicyclohexyl-4-morpholinecarboxamidinum 3',5'-cCMP

salt **3** was formed before coupling with 1, 1'-carbonyldiimidazole mainly due to the low solubility of 3',5'-cCMP in DMF. The carbonyldiimidazole-activated 3',5'-cCMP **4** was coupled with the immobilized DADPA to yield 2'-OH-cCMP probe.

Scheme 3.2 Synthesis of 2'-OH cCMP resin.

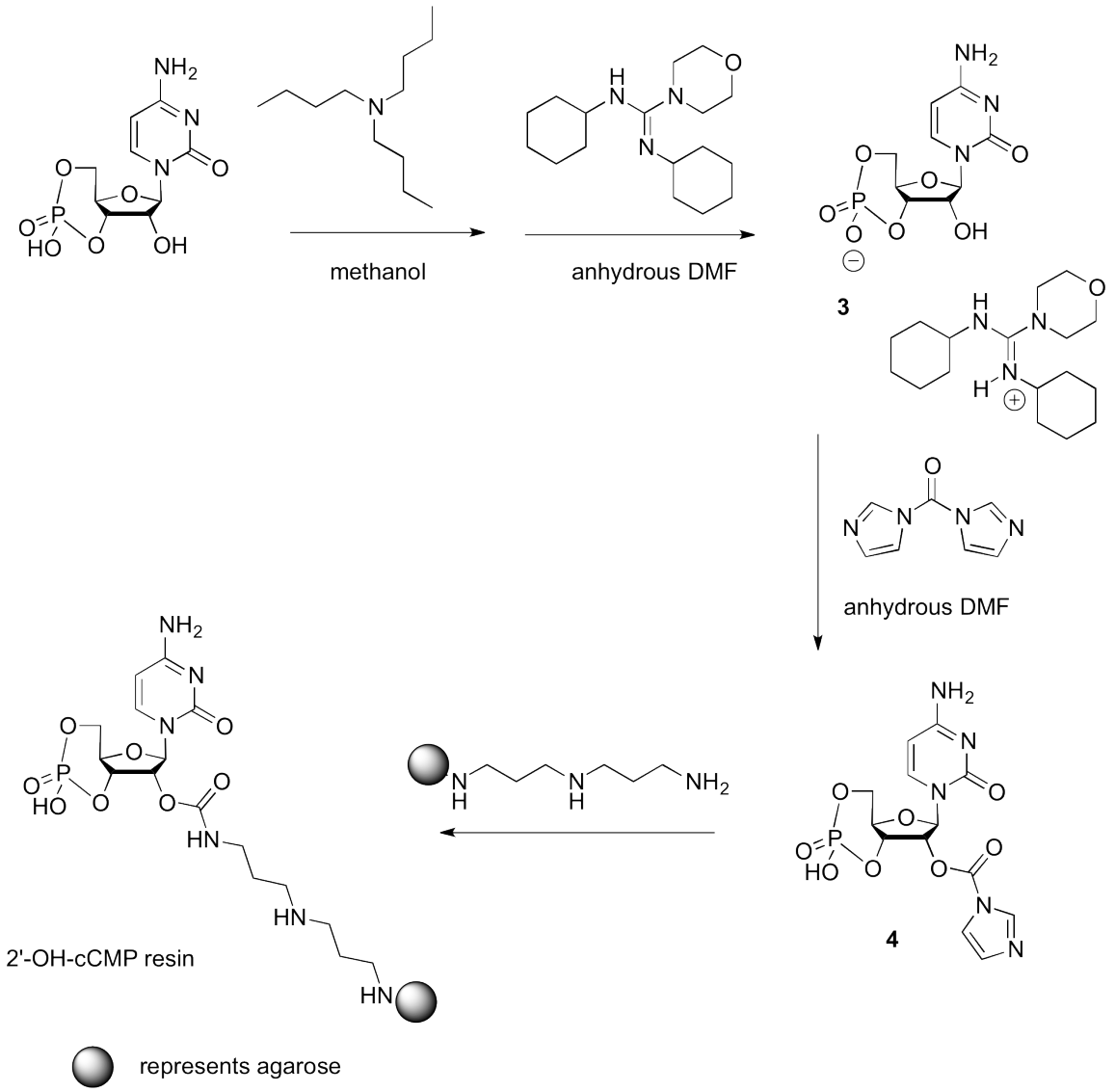

The synthesized cCMP-phosphate resin, 2'-OH-cCMP resin and a control cAMP-phosphate resin were incubated with rat brain in order to isolate 3',5'-cCMP-binding proteins (Figure 3.12).

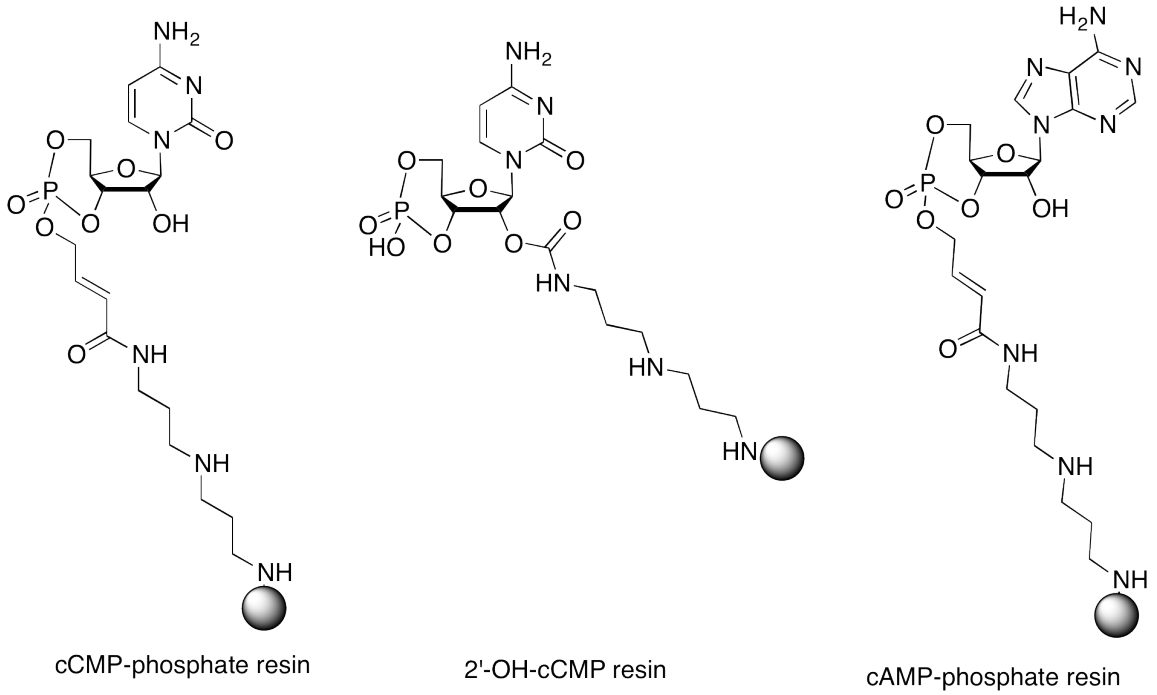

Figure 3.12 Structures of the synthesized cCMP/cAMP-affinity resins.

SDS-PAGE gel shows the isolated 3',5'-cCMP-binding proteins from the soluble fraction of rat brains isolated using synthesized 3',5'-cCMP-affinity probes (Figure 3.13). Proteins at bands 1, 2 and 3 on the SDS-PAGE gel were isolated using the 2'-OH-cCMP probe (Figure 3.13, Lanes 4 and 5). The intensities of bands 1, 2 and 3 are enhanced in 2'-OH cCMP agarose lanes (Lanes 4 and 5), as compared with the total protein present in the crude lysate fraction (Lane 9). A competing reaction was performed by introducing 2 mM 3',5'-cCMP in the incubation mixture (Lanes 1, 3 and 6). cCMP-binding proteins

show interaction with free 3',5'-cCMP, and reductions of band intensities in control experiments indicate isolation of 3',5'-cCMP-binding proteins. Results show increasing intensities of bands 2 and 3 in the competing reaction, likely because protein in either band was isolated by the 2'-OH-cCMP resin through non-specific binding, due to the fact that these proteins do not interact with free cCMP; or because the presence of 2'-OH-cCMP resin interferes with proteins in bands 2 and 3 interaction with free cCMP. Protein in band 1 that was competed away by 3',5'-cCMP (Lanes 3, 4 and 5) could potentially be a cCMP-binding protein, because it interacts with both the synthesized probe and its native substrate 3',5'-cCMP. The proteins isolated by cCMP-phosphate resins only show faint bands at around 46 to 58 kDa (Lanes 7 and 8). On the other hand, a competing reaction performed by introducing 2 mM cCMP into the incubation mixture shows multiple bands; it could be because the isolated cCMP-phosphate-binding proteins were activated in the presence of free cCMP (Lane 6). The control cAMP-phosphate probe also isolated a potential cAMP-binding protein at around 40 kDa (Lane 2).

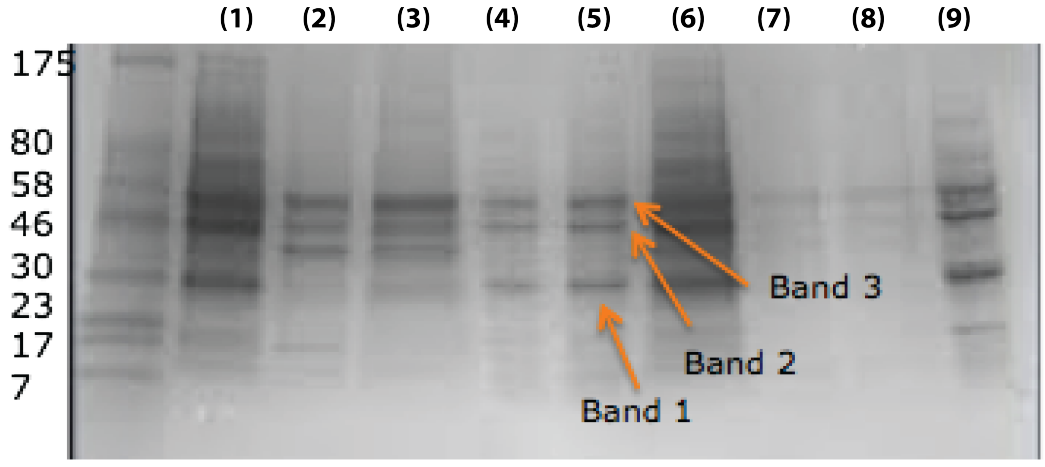

Figure 3.13 SDS-PAGE analysis of isolated cCMP-binding proteins from rat brains using various synthesized cCMP resins. Lane 1, control cAMP-phosphate resin + 2 mM cAMP; lane 2, control cAMP-phosphate resin; lane 3, 2'-OH-cCMP resin + 2 mM cCMP; lane 4, 2'-OH-cCMP resin, lane 5, 2'-OH-cCMP resin; lane 6, cCMP-phosphate resin + 2 mM cCMP; lane 7, cCMP-phosphate resin; lane 8, cCMP-phosphate resin; lane 9, rat brain crude lysate.

Bands 1, 2 and 3 containing potential putative cCMP-binding proteins were extracted from the SDS-PAGE gel for the subsequent tryptic digest MALDI analysis.

The MALDI-MS data was searched in the SwissProt database 2012.09.06, which contains sequences of rat proteins (Table 3.2). The MOWSE (MOlecular Weight SEarch) score, used in peptide mass fingerprinting, is a score based on peptide frequency distribution from the OWL non-redundant Database, and is used to evaluate the significance of the correlation analysis.[15] There is no particular threshold for a reliable MOWSE score- the higher the score is, the more likely the putative protein matches an identified protein in the database. Intriguingly, results show that protein in band 2 shares 8% (10/124 matches) sequence similarity to a THO complex subunit 5 (Thoc5) homolog. Thoc5 is one of the subunits of the THO complex, which functions to rectify aberrant structures that arise during transcription and is required for cell proliferation.[16] Preliminary data suggest the potential role of 3',5'-cCMP in cellular proliferation through regulation of the THO complex.

Table 3.2 Results of the in-gel MALDI analysis of potential cCMP-binding proteins extracted from bands 1, 2 and 3 in Figure 3.13. Predicted proteins with the highest MOWSE scores are reported here (prospector.ucsf.edu).

Band 1			
MOWSE Score	**% Matching**	**Species**	**Protein name**
462	5	Rat	Exocyst complex component 5
414	4	Rat	Single-strand selective monofunctional uracil-DNA glycosylase
Band 2			
MOWSE Score	**% Matching**	**Species**	**Protein name**
32114	8	Rat	THO complex subunit 5 homolog
14912	6	Rat	Zinc finger protein DZIP1L
Band 3			
MOWSE Score	**% Matching**	**Species**	**Protein name**
2403	10	Rat	Neurotrypsin
302	10	Rat	Rho guanine nucleotide exchange factor 2

Table 3.3 shows the matched peptide sequences of the isolated binding proteins with previously established protein THO complex subunit 5 homolog. Our preliminary MALDI-MS based 3',5'-affinity chromatography results suggest that 3',5'-cCMP could be binding and interacting with the THO protein complex. Furthermore, MALDI-MS/MS on individual peptides will be performed to confirm the results. Future work includes optimizing the in-gel tryptic digest MALDI analysis conditions in order to improve the

sequence coverage of extracted proteins and identify cCMP-binding proteins with greater confidence.

Table 3.3 Matched peptide sequence of the putative protein extracted from band 2 in figure 3.13 with THO complex subunit 5 homolog. The matched peptides cover 29.3% of the protein. (prospector.ucsf.edu)

MH^+ Submitted (*m/z*)	MH^+ Matched (*m/z*)	Matched peptide sequences
520.2609	520.2799	(K)EMLK(R)
2309.1780	2309.2024	(K)DIVEAGLAGDTNLYYLALIER(G)
2518.1069	2518.2018	(R)LCVLLDVYLETESHDDSVEGPK(E)
2611.3433	2611.1334	(K)EQPQHTVMADHSQSASHMETTMK(L)
2753.5054	2753.3312	(K)AEITMGDPHQQTLARLDWELEQR(K)
2839.5723	2839.3793	(R)LNSIMQASLPVQEYLFMPFDQAHK(Q)
2942.4329	2942.5444	(K)VDAYHLQLQNLLYEVMHLQKEITK(C)
2995.0476	2995.3035	(K)ALFKPPEDSQDDESDSDAEEEQTTRR(R)
3062.8193	3062.5768	(K)QFASLEHGIVPVTSECQYLFPAKVVSR(L)
3276.3525	3276.5617	(R)LCVLLDVYLETESHDDSVEGPKEFPQEK(M)

2.3. Conclusion

For many years, progress made in isolation of 3',5'-cCMP-related enzymes has been

slow due to the lack of efficient purification methods and sensitive analytical tools to identify and isolate enzyme members of 3',5'-cCMP signaling pathways. In this chapter we report a preliminary mass spectrometry-based technique that is suitable for detecting putative cNMP products. In the first approach, we have identified putative cCMP product synthesized in purified rat liver fraction, which could be an indication of the presence of a novel cytidylate cyclase or an active non-specific cyclase in rat. Future work includes developing an efficient protocol to further fractionate the cytosolic fraction, in order to isolate and characterize the putative mammalian cytidylate cyclase. Results show that the putative cCMP-specific PDE may be present, but the purification procedure has destroyed its activity. Future work includes developing a more gentle and rapid protocol to preserve the active cCMP-specific PDE in mammalian tissues. cCMP affinity chromatography results from the second approach suggest that we may have isolated THO complex subunit 5 from rat brains, using synthesized 3',5'-cCMP resins. THO complex subunit 5 is involved in cellular proliferation by controlling transcription and mRNA export, suggesting 3',5'-cCMP may be involved in regulation of the THO complex activity. Improving the coupling efficiency between 3',5'-cCMP intermediates and immobilized DADPA is crucial to synthesize cCMP resins effectively. In addition, various analogs of cCMP agarose such as amine-cCMP agarose will be synthesized in order to improve the accessibility of the affinity ligands to proteins, thereby increasing the likelihood of obtaining a variety of cCMP-binding proteins (Scheme 3. 3).

Scheme 3.3. Synthesis of amine-cCMP agarose for isolation of cCMP-binding proteins.

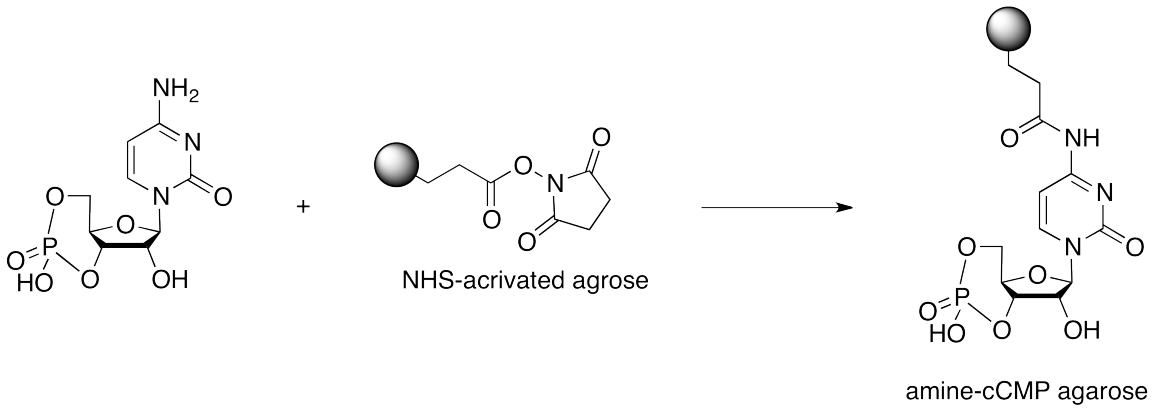

Identifying proteins involved in the cCMP signaling pathway will not only provide starting point for establishing physiological relevance of cCMP in mammals, but also provide a platform for studying the role of cCMP in mammalian signaling transduction, with a possible role in cancer biology.

3.4 Materials and Methods

3.4.1 Materials

Organs from Sprague-Dawley rats (brain, spleen, lung, kidney, heart and liver) were purchased from Innovative Research Inc. (Novi, MI, USA). According to the supplier, frozen organs were flash-frozen immediately after harvest and were stored at −80 °C upon receipt. Adenosine 3',5'-cyclic monophosphate hydrate (3',5'-cAMP) was purchased from TCI America (Portland, OR, USA). Cytidine 3',5'-cyclic monophosphate (3',5'-cCMP) was purchased from BioLog (Bremen, Germany). Guanosine 3',5'-cyclic monophosphate sodium salt (3',5'-cGMP), theophylline, 4-(2-Aminoethyl)

benzenesulfonyl fluoride hydrochloride (AEBSF), 1, 1'-carbonyldiimidazole, TCEP Tris(2-carboxyethyl)phosphine (TCEP) and Iodoacetamide (IAA) were purchased from Sigma-Aldrich (St. Louis, MO, USA). Ethylenediaminetetraacetic acid, disodium salt, dihydrate (EDTA) was purchased from EMD Millipore (Gibbstown, NJ, USA). Dithiothreitol (DTT), 1-Ethyl-3-(3-dimethylaminopropyl) carbodiimide• HCl (EDC), Immobilized diaminodipropylamine (DADPA), HPLC-grade acetonitrile and methanol were obtained from Thermo Fisher Scientific (Rockford, IL, USA). 4-bromocrotonic acid was purchased from TCI America. N',N'-dicyclohexyl-4-morpholinecarboxamidine was purchased from VWR.

3.4.2 Partial purification of cytidylate cyclase

3.4.2.1 Soluble cytidylate cyclase preparation

Soluble cytidylate cyclase was fractionated using a previously published protocol with modifications.[8a] A frozen male rat liver was homogenized using a hand homogenizer (OMNI TIP^{TM} Homogenizing Kits) in pre-chilled homogenate buffer (10 mM Tris-HCl buffer, 2 mM DTT and 0.25 M sucrose (pH 7.5), 9 volumes relative to tissue weight) containing 1 mM protease inhibitor AEBSF in conical tubes. Crude lysate was centrifuged at 1000 *g* for 3 min; a small portion of the crude lysate was tested for cytidylate cyclase activity and the rest of the supernatant was transferred to a new conical tube. The homogenate was centrifuged at 10,000 *g* for 20 min to separate the soluble proteins in the supernatant from the membrane-bond proteins. Centrifugation procedures

were maintained at 4 ºC for stability of the protein. The supernatant containing soluble protein was tested for cytidylate cyclase activity.

3.4.2.1 Membrane-bound cytidylate cyclase preparation

Membrane-bound cyclase was fractionated using a previously published protocol with modifications.[8b] A frozen male rat liver was homogenized using a hand homogenizer (OMNI TIP^{TM} Homogenizing Kits) in pre-chilled homogenate buffer (50 mM Tris-HCl (pH 7.4), 9 volumes relative to tissue weight) containing 1 mM protease inhibitor AEBSF in conical tubes. The homogenate was centrifuged at 500 *g* for 5 min; a small portion of the crude lysate was tested for cytidylate cyclase activity, and the rest of the supernatant was dialyzed in the homogenate buffer for four hours. 0.25 M sucrose solution was added to the dialysate, followed by ultracentrifugation at 100,000 *g* for 90 min to re-suspend membrane-bound proteins. The supernatant containing membrane-bound proteins was tested for cytidylate cyclase assay. Homogenate buffer containing 0.3% Triton X-100 was added to the pellet, vortexed to re-suspend membrane-bound proteins, and the resulting mixture was centrifuged at 100,000 *g* for 1 hr. Centrifugation procedures were maintained at 4 ºC for stability of the protein. The resulting supernatant was tested for cyclase activity.

3.4.3 Partial purification of cCMP-specific PDE

cCMP-specific phosphodiesterase was fractionated based on a previously published protocol using ammonium sulfate fractionation technique.[6] A frozen male rat

liver was homogenized using a homogenizer (OMNI TIP^{TM} Homogenizing Kits) in pre-chilled homogenate buffer (50 mM Tris-HCl and 3 mM β-mecaptoethanol (pH 7.5), 9 volumes relative to tissue weight). The homogenate was centrifuged at 4 ºC at 1000 *g* for 10 min. Centrifugation procedures were maintained at 4 ºC for stability of the protein. The supernatant was dialysed at 4 ºC against 12 volume of homogenate buffer for 3 hours. The dialysed material was fractionated by slowly adding the requisite amount of ammonium sulfate at 4 ºC to produce fractions: 0-20%, 20-40%, 40-60% and 60-90%. The precipitates were re-suspended in the minimum volume of 50 mM Tris-HCl buffer (pH 7.4) then dialysed overnight against 12 volume of the same buffer at 4 ºC. The re-suspended 60%-90% fraction, which was previously reported to have the highest observed PDE activity, was further purified using analytical gel filtration. Each re-suspended precipitate and analytical gel filtration fraction was assayed for PDE activity and analyzed for protein content.

3.4.4 Cytidylate cyclase activity assay

Cyclase preparations (80 μL) were incubated in 50 mM Tris-HCl buffer, pH 7.4 in a total volume of 100 μL containing 1 mM CTP and 4 mM $MnCl_2$ at room temperature for 10 min. Control studies were prepared exactly as above except that 1 mM ATP or GTP were used to test for substrate specificity of the putative cyclase and to test for contaminating adenylate and guanylate cyclases. The reaction was quenched with 100 μL of 150 mM EDTA (pH 4) and heated at 90 ºC for 3 minutes. The reaction mixture was

cooled on ice for 1 min and centrifuged at 2000 *g* for 20 min. The supernatant containing putative cNMP products was analyzed on HPLC or MS.

3.4.5 cCMP PDE activity assay

PDE preparations (38 µL) were incubated in 50 mM Tris-HCl buffer, pH 7.4 in a total volume of 100 µL containing 10 mM cCMP and 10 mM $FeSO_4 \bullet 7H_2O$ at room temperature for 20 min. Control studies were prepared exactly as above except that 10 mM cAMP or cGMP were used as to test for substrate specificity of the putative PDE and to test for contaminating 3',5'-cAMP and 3',5'-cGMP specific PDEs. The reaction mixture was heated at 90 ºC for 2 minutes, cooled on ice for 2 min, and centrifuged at 13,000 *g* for 3 min. The supernatant containing putative NMP products was analyzed via HPLC or MS.

3.4.6 HPLC optimized conditions

HPLC experiments were performed using an Infinity 1260 HPLC system (Agilent Technologies, Germany) equipped with a quaternary pump, a degasser, and a temperature controlled autosampler. Samples were separated using a reverse phase (C-18) column (250× 4.6 mm, Agilent Technologies). 20 µL of sample was analyzed by HPLC during each run. Buffer A contained 150 mM sodium phosphate (pH 5.2) and buffer B contained 60% buffer A and 40% acetonitrile. Putative cNMP and NMP products were eluted using a linear gradient from 0 to 100% buffer B in 30 min at 1 mL/min. Three independent HPLC runs were performed for each sample.

3.4.7 HRMS optimized conditions

HRMS experiments were performed using a Thermo Electron LTQ-FTMS system equipped with a diode array detector controlled by Xcalibur and DCMSlink software (Thermo Scientific). The samples were ionized by positive ion electrospray in the LTQ-FTMS using 5 kV voltage on the needle, with a capillary voltage of 35 V, capillary temperature of 275 °C, and tube lens voltage of 110 V. Detection was done in the FT portion of the LTQ-FTMS.

3.4.8 Size exclusion chromatography optimized conditions

Size exclusion chromatography experiments were performed using a BioLogic DuoFlow Medium-Pressure Chromatography System (Bio-Rad) equipped with a 26/600 Superdex 200 prep grade size exclusion column (GE Healthcare Life Sciences). Re-suspended 60%-90% ammonium sulfate fraction was separated using the elution solvent containing 50 mM Tris-HCl, 50 mM NaCl and 1 mM DTT (pH 7.5) at 1 mL/min.

3.4.9 Synthesis of intermediate 2 in Scheme 3.1

A mixture of 4-bromocrotonic acid (0.3 mmol, 20 mg) and cCMP tert-butylammonium salt **1** pre-formed by stirring cCMP (20 mg) with tetra-n-butylammonium hydroxide (1.5 mL) overnight was refluxed in acetonitrile (2 mL) in the dark for 5 hours. The solvent was evaporated in vacuo, and the residue was washed with 2 mL of water, dried and dissolved in chloroform/methanol. The mixture was purified by

flash chromatography. Elution using chloroform/methanol (19:1 to 4:1 v/v) yielded **2** (over 100% yield due to the presence of t-butylammonium salt). ^{1}H NMR spectrum indicates **2** as the major product of this reaction along with other possible side products. HRMS (ESI): exact mass calculated for $C_{14}H_{16}N_5O_8P$ ($[M+H]^+$): 413.0736, mass found: 413.0667.

3.4.10 cCMP-phosphate probe synthesis

Immobilized DADPA resin/gel slurry (0.7 mL) was centrifuged at 500 *g*, the supernatant was discarded and pellet was washed with H_2O. The slurry was centrifuged at 500 *g*, the supernatant was discarded and the pellet containing DADPA resin was used for subsequent coupling reaction. Intermediate **2** (Scheme 3.1) was dissolved in 0.5 mL of coupling buffer containing 0.1 M MES (2-(*N*-Morpholino) ethanesulfonic acid) buffer and 0.9% NaCl, pH 4.7. Solution containing intermediate **2** was added to the pre-washed DADPA resin and the mixture was gently stirred end-over-end for several minutes to pre-mix. EDC (15 mg) was added to 0.1 mL coupling buffer, and the EDC solution was added immediately to the resin slurry. The resulting mixture was stirred end-over-end for 3 hours at room temperature. The resin was washed three times with water and three times with MeOH. Concentration of un-reacted intermediate **2** in the supernatant was analyzed using UV-Vis spectrometry. The pellet containing cCMP-phosphate probe was re-suspended in 0.7 mL water and stored at 4 °C. The coupling reaction yielded 35% cCMP-phosphate probe.

3.4.11 Synthesis of N, N'-dicyclohexyl-4-morpholinecarboxamidinium cCMP salt 3 in Scheme 3.2

Tributylamine (0.11mL, 0.2 mmol) was added to a suspension of cCMP (25 mg, 0.076 mmol) in methanol (1 mL). The mixture was refluxed until it became homogeneous, and the solvent was evaporated under reduced pressure. The residue was dissolved in anhydrous DMF (1 mL) and N, N'-dicyclohexyl-4-morpholinecarboxamidine (22.42 mg, 0.076 mmol) was added to the mixture. The mixture was warmed gently until it became homogenous, the solvent was evaporated under reduced pressure, and the residue was dried by repeated vacuum evaporation of anhydrous DMF and then kept under vacuum overnight over P_2O_5 to give **3**.

3.4.12 Synthesis of imidazole-activated cCMP 4 in Scheme 3.2

A solution of N, N'-dicyclohexyl-4-morpholinecarboxamidinium cCMP salt **5** (0.15mmol) was dissolved in anhydrous DMF (1.5mL). The solution was stirred with 1,1'-carbonyldiimidazole (0.75 mmol) at room temperature for 2 hr. The reaction mixture was treated with methanol to quench excess 1,1'-carbonyldiimidazole and the solvent was evaporated in vacuo to give **4** (over 100% yield due to the presence of salt). ^{1}H NMR spectrum indicates **4** as the major product of this reaction alone with other possible side products. HRMS (ESI): exact mass calculated for $C_{13}H_{14}N_5O_8P$ ($[M+H]^+$): 399.0580, mass found: 399.2158.

3.4.13 Synthesis of 2'-OH-cCMP probe

Immobilized DADPA resin/gel slurry (0.7 mL) was centrifuged at 500 *g*. The supernatant was discarded and pellet was washed with H_2O. The slurry was centrifuged at 500 *g*, the supernatant was discarded and the pellet containing DADPA resin was used for the subsequent coupling reaction. Intermediate **4** (Scheme 3.2) was dissolved in 0.5 mL of coupling buffer containing 0.1 M MES (2-(*N*-Morpholino) ethanesulfonic acid) buffer and 0.9% NaCl, pH 4.7. Solution containing intermediate **4** was added to the pre-washed DADPA resin and the mixture was gently stirred end-over-end at room temperature for 72 hr. The resin was washed three times with water and three times with MeOH. Concentration of un-reacted cCMP in the supernatant was analyzed using UV-Vis spectrometry. The pellet containing cCMP-phosphate probe was re-suspended in 0.7 mL water and stored at 4 °C. The coupling reaction yielded 36% 2'-OH-cCMP probe.

3.4.14 Determination of coupling efficiency of cNMPs with DADPA resin using spectrophotometric analysis

Measurements of un-reacted cNMPs described above were accomplished by Agilent UV-Vis spectrophotometer (Agilent Technologies Cary 100). For all measurements the background absorbance of 50% water and 50% methanol was determined and corrected. To obtain absorbance spectra, samples of cAMP (λ_{max}=270 nm, ε= 9000 M^{-1} cm^{-1}) and cCMP (λ_{max}=260 nm, ε= 12600 M^{-1} cm^{-1}) were scanned from 320 nm to 600 nm. The amount of cNMPs coupled to the DADPA resin can then be calculated.

3.4.15 Preparation of enzyme fraction for cCMP affinity chromatography

A frozen male rat brain was homogenized using a hand homogenizer (OMNI TIP^{TM} Homogenizing Kits) in pre-chilled homogenate buffer (50 mM Tris-HCl (pH 7.4), 9 volumes relative to tissue weight) containing 1 mM protease inhibitor AEBSF in conical tubes. The homogenate was centrifuged at 500 *g* for 10 min to remove cellular debris. The supernatant was centrifuged at 100,000 *g* for 45 min. The resulting supernatant containing soluble protein was used to isolate cCMP-binding proteins. Homogenate buffer containing 0.3% Triton X-100 was added to the residue pellet and vortexed to dissolve membrane-bound proteins in the pellet. The resulting mixture was centrifuged at 100,000 *g* for 1 hr. Centrifugation procedures were maintained at 4 ºC for stability of the protein. The supernatant was used for cCMP-affinity chromatography experiments.

3.4.16 cCMP matrices for the affinity purification of cCMP-binding protein in rat brains

Enzyme fractions were pre-incubated with clean DADPA resin at 4 °C for 1 hour prior to the binding experiments to eliminate non-specific binding. Various analogs of synthesized cCMP probes (70 µL) were incubated with pre-incubated enzyme fractions (330 µL) and stirred end-over-end at 4 °C for overnight. Competing reactions were performed by introducing 2 mM cCMP in the incubation mixture. cCMP-binding proteins that interact with cCMP probes should also recognize cCMP as a substrate. The reaction mixture was centrifuged at 1,000 *g* for 3 mins and the agarose beads were washed three

times with 500 µL of wash buffer containing 10 mM NaCl. The cCMP probes containing cCMP-binding proteins were heated for 10 min at 90 °C, and protein content was analyzed by SDS-PAGE Gel.

3.4.17 Preparation of in-gel tryptic digest samples

Protein-containing gel lanes 1, 2 and 3 were cut into 1× 1 mm pieces and destained with acetonitrile. Subsequently, gel pieces were reduced by 50 mM TCEP (Tris[2-carboxyethyl]phosphine), then alkylated by 50 mM IAA (Iodoacetamide) to avoid cross-linking product. Trypsin was then added at a concentration of 10 ng/µL in 25 mM of ammonium bicarbonate and the protein digest was performed at 30 °C overnight with shaking. The supernatant of each digestion was desalted and concentrated using ZipTip® Pipette Tips with 0.6 µL C-18 resin before spotted onto a MALDI target plate (AB Sciex, Darmstadt, Germany).

3.4.18 MALDI-MS optimized conditions

MALDI-MS using Applied Biosystems (4700 Proteomics Analyzer) equipped with 355 nm laser. Samples were analyzed using MS Reflective Positive Mode. Error tolerance was set to 100 ppm for precursor masses. α-cyano-4-hydroxycinnamic acid in water/acetonitrile (1:1 ratio) was used as sample matrices. A trypsin fragment at 842.51 *m/z* ($[M+H]^+$) was used as an internal calibration standard.

3.4.19 Statistical analysis

Peptide identifications and assignments of post-translational modification were performed at peptide N-terminal Gln to pyroGlu, Oxidation of M and protein N-terminus acetylation was specified as variable modifications. All data sets were searched using the following constraints: only tryptic peptides with up to one missed cleavage site were allowed; ±100 ppm mass tolerance for peptide precursor mass search.

3.5 References

1. (a) Sutherland, E. W., Studies on the mechanism of hormone action. *Science* **1972,** *177* (4047), 401-8; (b) Lucas, K. A.; Pitari, G. M.; Kazerounian, S.; Ruiz-Stewart, I.; Park, J.; Schulz, S.; Chepenik, K. P.; Waldman, S. A., Guanylyl cyclases and signaling by cyclic GMP. *Pharmacol Rev* **2000,** *52* (3), 375-414.

2. (a) Bloch, A., Cytidine 3',5'-monophosphate (cyclic CMP). I. Isolation from extracts of leukemia L-1210 Cells. *Biochem Biophy Res Co* **1974,** *58* (3), 652-9; (b) Bloch, A., Isolation of cytidine 3',5'-monophosphate from mammalian tissues and body fluids and its effects on leukemia L-1210 cell growth in culture. *Adv Cyclic Nucl Res* **1975,** *5*, 331-8; (c) Kuo, J. F.; Brackett, N. L.; Shoji, M.; Tse, J., Cytidine 3':5'-monophosphate phosphodiesterase in mammalian tissues. Occurrence and biological involvement. *J Biol Chem* **1978,** *253* (8), 2518-21; (d) Cech, S. Y.; Ignarro, L. J., Cytidine 3',5'-monophosphate (cyclic CMP) formation in mammalian tissues. *Science* **1977,** *198* (4321), 1063-5.

3. (a) Cech, S. Y.; Ignarro, L. J., Cytidine 3',5'-monophosphate (cyclic CMP) formation by homogenates of mouse liver. *Biochem Biophy Res*

Co **1978,** *80* (1), 119-25; (b) Cheng, Y. C.; Bloch, A., Demonstration, in leukemia L-1210 cells, of a phosphodiesterase acting on 3':5'-cyclic CMP but not on 3':5'-cyclic AMP or 3':5'-cyclic GMP. *J Biol Chem* **1978,** *253* (8), 2522-4; (c) Helfman, D. M.; Shoji, M.; Kuo, J. F., Purification to homogeneity and general properties of a novel phosphodiesterase hydrolyzing cyclic CMP and cyclic AMP. *J Biol Chem* **1981,** *256* (12), 6327-34.

4. (a) Briscoe, J.; Therond, P. P., The mechanisms of Hedgehog signalling and its roles in development and disease. *Nat Rev Mol Cell Bio* **2013,** *14* (7), 416-29; (b) Bond, A. E.; Dudley, E.; Tuytten, R.; Lemiere, F.; Smith, C. J.; Esmans, E. L.; Newton, R. P., Mass spectrometric identification of Rab23 phosphorylation as a response to challenge by cytidine 3',5'-cyclic monophosphate in mouse brain. *Rapid Commun Mass Spec* **2007,** *21* (16), 2685-92.

5. Beste, K. Y.; Burhenne, H.; Kaever, V.; Stasch, J. P.; Seifert, R., Nucleotidyl cyclase activity of soluble guanylyl cyclase alpha1beta1. *Biochem* **2012,** *51* (1), 194-204.

6. Newton, R. P.; Salih, S. G., Cyclic CMP phosphodiesterase: isolation, specificity and kinetic properties. *Int J Biochem* **1986,** *18* (8), 743-52.

7. (a) Sunahara, R. K.; Dessauer, C. W.; Gilman, A. G., Complexity and diversity of mammalian adenylyl cyclases. *Annu Rev Pharmacol* **1996,** *36*, 461-80; (b) Hurley, J. H., Structure, mechanism, and regulation of mammalian adenylyl cyclase. *J Biol Chem* **1999,** *274* (12), 7599-602; (c) Kuhn, M., Structure, regulation, and function of mammalian membrane guanylyl cyclase receptors, with a focus on guanylyl cyclase-A. *Circ Res* **2003,** *93* (8), 700-9.

8. (a) Mori, S.; Yanagida, M.; Kubotsu, K.; Yamamoto, I., Characterization of detergent dispersed cytidylate cyclase of rat brain. *Sec Mess Phosphoprot* **1990,** *13* (1), 1-12; (b) Newton, R. P.; Groot, N.; van Geyschem, J.; Diffley, P. E.; Walton, T. J.; Bayliss, M. A.; Harris, F. M.; Games, D. E.; Brenton, A. G., Estimation of cytidylyl cyclase activity and monitoring of side-product formation by fast-atom bombardment mass spectrometry. *Rapid Commun Mass Spec* **1997,** *11* (2), 189-94.

9. Yamamoto, I.; Takai, T.; Mori, S., Cytidylate cyclase activity in mouse tissues: the enzymatic conversion of cytidine 5'-triphosphate to cytidine 3',5'-cyclic monophosphate (cyclic CMP). *Biochem Biophys Acta* **1989,** *993* (2-3), 191-8.

10. Ziegelberger, G.; van den Berg, M. J.; Kaissling, K. E.; Klumpp, S.; Schultz, J. E., Cyclic GMP levels and guanylate cyclase activity in pheromone-sensitive antennae of the silkmoths Antheraea polyphemus and Bombyx mori. *J Neurosci* **1990,** *10* (4), 1217-25.

11. Chambers, E.; Wagrowski-Diehl, D. M.; Lu, Z.; Mazzeo, J. R., Systematic and comprehensive strategy for reducing matrix effects in LC/MS/MS analyses. *J Chromatogr B Analyt Technol Biomed life Sci* **2007,** *852* (1-2), 22-34.

12. Dixon M, W. E., *Enzymes*. A subsidiary of Harcourt Brace Jovanovish Publishers Longman Group: New York San Francisco, 1979.

13. Eckardt, T.; Hagen, V.; Schade, B.; Schmidt, R.; Schweitzer, C.; Bendig, J., Deactivation behavior and excited-state properties of (coumarin-4-yl)methyl derivatives. 2. Photocleavage of selected (coumarin-4-yl)methyl-caged adenosine cyclic 3',5'-monophosphates with fluorescence enhancement. *J Org Chem* **2002,** *67* (3), 703-10.

14. Corrie, J. E.; Pizza, C.; Makwana, J.; King, R. W., Preparation and properties of an affinity support for purification of cyclic AMP receptor protein from Escherichia coli. *Protein Expres Purif* **1992,** *3* (5), 417-20.

15. Pappin, D. J.; Hojrup, P.; Bleasby, A. J., Rapid identification of proteins by peptide-mass fingerprinting. *Curr Bio* **1993,** *3* (6), 327-32.

16. Larochelle, M.; Lemay, J. F.; Bachand, F., The THO complex cooperates with the nuclear RNA surveillance machinery to control small nucleolar RNA expression. *Nucleic Acids Res* **2012,** *40* (20), 10240-53.

Chapter 4: Study of 3',5'-cCMP as a Putative Mammalian Second Messenger- A Facile and Sensitive Mass Spectrometry-Based Method for Quantification of Cyclic Nucleotide Monophosphates in Mammalian Organs

4.1 Introduction

Cyclic nucleotides adenosine 3',5'-cyclic monophosphate (3',5'-cAMP) and guanosine 3',5'-cyclic monophosphate (3',5'-cGMP) are essential mammalian metabolites that function primarily within the cell as secondary messengers. 3',5'-cAMP and 3',5'-cGMP have been investigated for decades and have been found to perform crucial roles in regulating cellular metabolism and mediating actions of numerous mammalian hormones and neurotransmitters.[1] The existence of additional cyclic nucleotides, including cytidine 3',5'-cyclic monophosphate (3',5'-cCMP), inosine 3',5'-cyclic monophosphate (3',5'-cIMP) and 2',3'-cyclic nucleotide monophosphates (2',3'-cNMPs), in mammalian tissues and cell lines has previously been reported.[2] However, while their potential roles in tumorigenesis, cellular signal transduction and post-injury mechanisms have been suggested, their signalling pathways have yet to be elucidated.[3]

Of the atypical cyclic nucleotides, 3',5'-cCMP has been the best studied, having previously been found in pmol/g concentration ranges in various mammalian tissues.[2b] Furthermore, 3',5'-cCMP was found to occur at increased concentrations in the brain and in dividing tissues (such as regenerating livers). Putative proteins involved in cCMP signalling pathways were also reported 20–30 years ago, but have yet to be identified and fully characterized.[4] In addition to cCMP, 3',5'-cIMP has been identified as an endogenous product released from a variety of rat organs using fast atom bombardment mass spectrometry.[2c] Recently, 3',5'-cIMP has been shown to be synthesized from ITP by purified soluble guanylyl cyclase (sGC) and by sGC in porcine coronary arteries.[5] Furthermore, CadD, an enzyme found in the pathogenic bacterium *Leptospira interrogans*, has been recently reported as a cAMP specific deaminase, resulting in the

production of 3',5'-cIMP.[3b] This conversion has suggested the possibility that cells also sense 3',5'-cIMP levels.[3b, 6]

In addition to 3',5'-cNMPs, recent reports have detailed the identification and putative roles of the 2',3'-regioisomers. 2',3'-cAMP was first detected in perfused rat kidney using liquid chromatography coupled with tandem mass spectrometry (LC-MS/MS).[7] Additional studies have suggested that tissue injury triggers mRNA degradation, leading to production of 2',3'-cAMP that is converted through the action of the enzyme 2',3'-cyclic nucleotide phosphodiesterase to endogenous adenosine, which upon binding to various adenosine receptors can protect against acute organ injury, as well as have profound effects on the cardiovascular system.[3c, 8] Recently, 2',3'-cAMP and cGMP have been shown to correlate with leaf wounding stress in *Arabidopsis*, further suggesting that these nucleotides may be important in post-injury mechanisms.[9] 2',3'-cCMP and 2',3'-cGMP also were reported in two mammalian cell lines (HEK293T and HuT-78), however their role is unknown.[2a] Such observations imply that multiple 2',3'-cNMPs may be involved in various cellular pathways, including mechanisms to protect against tissue injury.

Despite the progress that has been made to establish the role of cNMPs in signalling pathways, quantitation of mammalian tissue distributions has been challenging. Previous studies have reported problems with identifying cNMPs due to interference from tissue components and lack of an efficient extraction protocol for analyzing extremely low concentrations of cNMPs in mammalian organs [10]. Since the 1970s, various procedures for measurement of extracted cNMPs in organs have required initial separation by thin layer chromatography (t. l. c.) or ion exchange resin (e.g. dowex resin).[10a, 11]

However, those protocols were time-consuming and resulted in low sensitivity, which made rapid analysis of large numbers of tissue samples that contain low concentrations of cNMPs problematic.

Radioimmunoassay techniques have also been used due to the improved sensitivity and simplified quantification protocol, but the use of radioactive isotopes can introduce difficulties, as radioactive materials can cause health issues, if not handled properly.[12] To date, most reports measure relative levels of either cAMP or cGMP following an external stimulus using commercially available enzyme-linked immunosorbent assays (ELISAs), rather than absolute concentrations.[13] Using ELISAs has significant advantages, including safety of handling, minimal training requirements and ease of waste disposal. Unfortunately, despite the adequate sensitivity and cost, cross-reactivity may occur with the secondary antibody, resulting in over-estimation of the analyte-of-interest.[14] Additionally, ELISA assays can only provide relative quantitative, but not absolute quantitative results. High performance liquid chromatography (HPLC) and mass spectroscopy provides a means of unambiguous identification of analyte-of-interest, and have quickly been adapted to provide unequivocal evidence of cCMP catalyzed by purified putative enzymes. The application of fast-atom bombardment (FAB) mass spectrometry with collision-induced dissociation (CID)/mass-analysed ion kinetic energy (MIKE) spectroscopy gained popularity in identifying cNMPs due to its capability in detecting involatile and/or thermally labile molecules in the early 90's.[15] However, FAB, using a "hard ionization" technique, usually generates high chemical background and lower sensitivity, as compared to the modern "soft ionization" electrospray ionization mass spectrometry (ESI-MS).[15] ESI tends to produce mass spectra with little or no

fragmentations, which is advantageous due to that the parent molecular ion is always present. Therefore, a sensitive modern and high-throughput method to analyze low concentrations of multiple cNMPs in tissues should find utility in both research and clinical laboratories.

Using LC-MS/MS techniques provides the advantages of high sensitivity, high-throughput data analysis, and widespread instrumentation.[16] It has been quickly adapted as a main method for quantitative metabolomics and nucleotideomics in the past decade.[16a-c] Furthermore, LC-MS/MS has found significant utility in studying biomarkers in clinical laboratories.[17] However, current LC-MS/MS protocols for extraction of cNMPs from mammalian tissues have typically quantified only one to two cNMPs, rather than monitoring a wide range of cNMP levels.[18] Previous work has observed the negative impact of matrix effects in organ extraction samples analyzed by LC-MS/MS, specifically phospholipids in biological extracts that can be ionized competitively with the analytes-of-interest, decreasing the sensitivity and reproducibility of the method.[19] However, in most published organ extraction protocols, a solution to solve such matrix effects has not been offered.[20]

Since previous studies suggest that both 3',5'- and 2',3'-cNMPs may be biologically important, an efficient and sensitive protocol has been developed and validated for extraction and quantification of multiple cNMPs simultaneously in various systems (organs, cell lines, *etc.*) using instrumentation available in the majority of research institutions. By utilizing standard instrumentation and a readily available internal standard (IS), this procedure should be useful for a wide variety of researchers and will facilitate further investigations into the physiological roles of cNMPs.

4.2 Results and Discussion

4.2.1 Optimization of LC-MS/MS Analytical Method

Development of the current method to extract and quantify cNMPs from mammalian tissues began with optimization of the separation and detection protocols by LC-MS/MS. The LTQ mass spectrometer in a Thermo LTQ-FTMS system was used for all analyses, as similar systems are typically available to researchers through departmental or university instrument cores due to their popularity and because of their ease of use and utility in protein studies. Many existing protocols studying metabolomics use a combination of ultra-performance liquid chromatography (UPLC) coupled with a triple quadrupole MS for greater sensitivity and precision.[18b, 21] However, these instruments often are not readily available to non-specialist investigators.

Initial work focused on optimizing the separation of various cNMP isomers so that unique retention times can be used as identifiers for each cNMP. Different types of LC columns such as HILIC, fluoro phenyl, and C-18 were tested due to their abilities to separate polar compounds and acidic compounds that contain aromatic substituents.[22] Following testing of various columns, a reverse phase C-18 column was chosen due to its stability, as well as reproducibility and peak shapes when separating seven cNMPs. Positive electrospray ionization (ESI) was used to fragment cNMPs in the mass spectrometer using a 0.1% formic acid buffer to enhance protonation of the cNMP species. Positive ion MS/MS in the LTQ yielded much greater sensitivity compared to other ion modes tested (Table 4.1).

Table 4.1 Comparison of ionization methods for LC-MS/MS analysis of cNMPs. Data for four cNMPs (ratios of peak areas of cNMP to internal standard) are listed. Positive ion mode exhibits improved sensitivity, particularly at lower cNMP concentrations.

	A(2',3'-cAMP)/ A(IS81)	**A(3',5'-cAMP)/ A(IS81)**	**A(2',3'-cGMP)/ A(IS81)**	**A(3',5'-cGMP)/ A(IS81)**
Positive ion: 2.5 μM	3.07	2.15	1.87	3.35
Negative ion: 2.5 μM	1.52	1.90	1.99	1.27
Positive ion: 1 μM	1.65	1.03	1.24	1.78
Negative ion: 1 μM	0.68	0.82	0.93	0.56
Positive ion: 0.5 μM	0.82	0.51	0.60	0.86
Negative ion: 0.5 μM	0.35	0.43	0.48	0.27

Using solely the FTMR analysis, 3',5'-cAMP and 2',3'-cAMP yield identical mass fragmentations, which makes differentiating the 2',3'- and 3',5'-regioisomers difficult (Figure 4.1). Therefore, chromatographic separations of all seven cNMPs and the IS (8-Br-cAMP) was achieved by liquid chromatography, prior to using the mass spectrometer to distinguish analytes based on mass to charge ratio. Figure 4.2 depicts the reconstructed ion chromatograms of the different protonated cNMPs. The 2',3'- and 3',5'-isomers of each cNMP are visualized by fragment ions corresponding to the protonated base, which were used for peak integration.

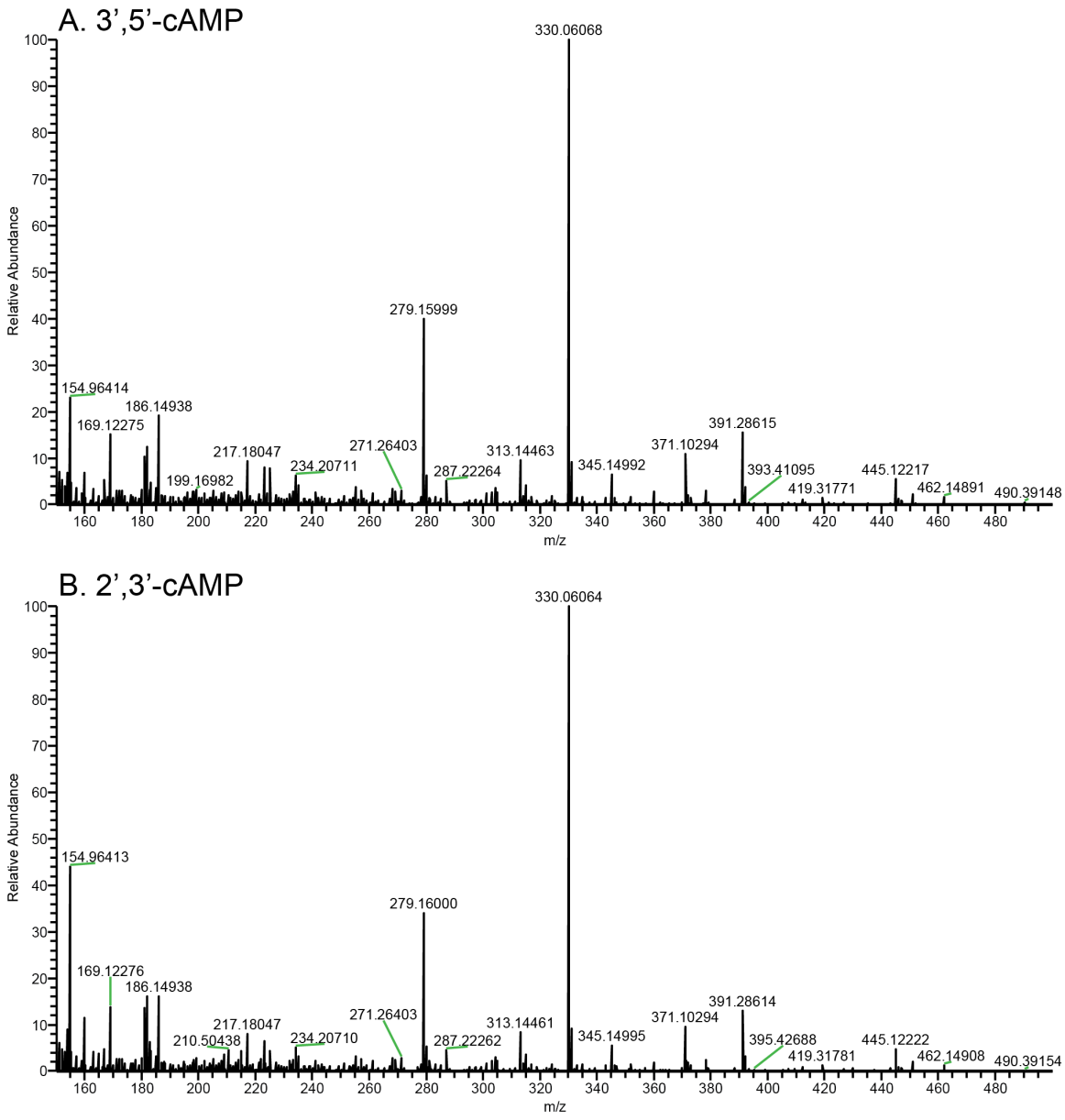

Figure 4.1 FT-MS of 3',5'-cAMP (A) and 2',3'-cAMP (B). While FT-MR analysis of cNMPs results in excellent sensitivity, the regioisomers yield identical mass spectra and cannot be distinguished.

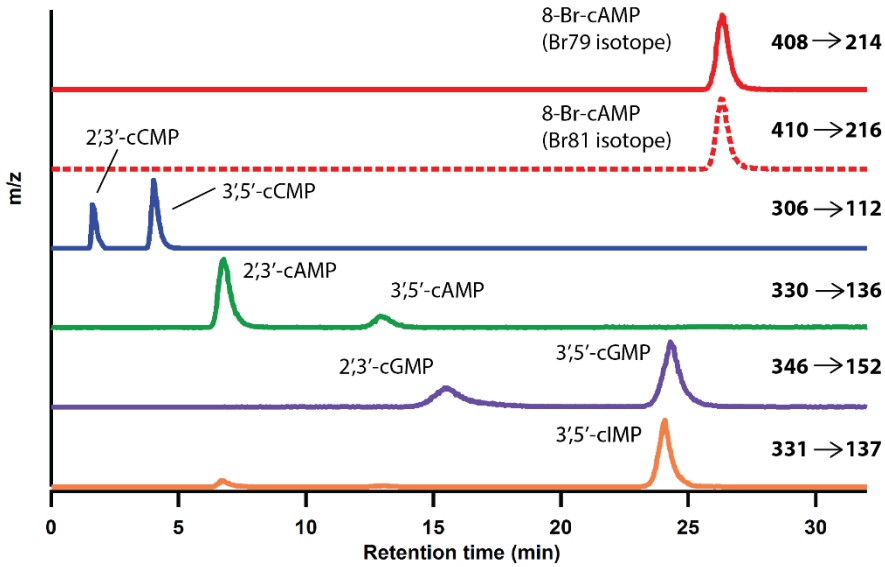

Figure 4.2 Reconstructed ion chromatogram of authentic cNMPs using Xcalibur software. From top to bottom, transition 408 → 214 *m/z* was monitored and reconstructed for ^{79}Br-cAMP (Top, red trace) and transition 410 → 216 *m/z* was monitored and reconstructed for ^{81}Br-cAMP (dotted red trace); transition 306 → 112 *m/z* was monitored and reconstructed for 2',3'-cCMP and 3',5'-cCMP (blue trace); transition 330 → 136 *m/z* was monitored and reconstructed for 2',3'-AMP and 3',5'-cAMP (green trace); transition 346 → 152 *m/z* was monitored and reconstructed for 2',3'- cGMP and 3',5'-cGMP (purple trace); transition 331 → 137 *m/z* was monitored and reconstructed for 3',5'-cIMP (orange trace).

Previously, due to the structural similarity of purine and pyrimidine cyclic nucleotides, clear separation by LC was difficult achieve.[23] Optimization of the LC-MS/MS system to fully separate all cNMPs also can be difficult to accomplish, as has been observed in a number of publications that utilize LC-MS/MS systems.[2a, 20] As shown in Table 4.2, although cGMP and cIMP are structurally similar, the current

method can readily separate the two analogues due to the difference in protonated precursor ion $[M + H]^+$ mass to charge ratio (15 *m/z*). The improved peak shapes on the reconstructed ion chromatogram (Figure 4.2) yielded separation of cGMP and cIMP (RTs of cGMP and cIMP are 24.3 and 24.1 min, respectively, Table 4.2), allowing for accurate identification.

8-Bromoadenosine 3',5'-cyclic monophosphate (8-Br-cAMP) was employed as an internal standard (IS) in the present method to quantify extracted cNMPs. 8-Br-cAMP was chosen because it is readily commercially available, relatively inexpensive, and not naturally present in mammalian cells. In addition, the cyclic phosphate group of 8-Br-cAMP is shared with the cNMPs, resulting in similar ionization efficiencies. Moreover, the two naturally occurring isotopes of bromine allow for unequivocal identification and quantification of 8-Br-cAMP in extracted samples.

Table 4.2 Mass spectrometric parameters for the measured transitions of cyclic nucleotide monophosphates (cNMPs) and internal standard (8-Br-cAMP; IS).

Parameters	**2',3'-cAMP**	**3',5'-cAMP**	**2',3'-cCMP**	**3',5'-cCMP**	**2',3'-cGMP**	**3',5'-cGMP**	**3',5'-cIMP**	**8-^{79}Br-cAMP**	**8-^{81}Br-cAMP**
$[M + H]^+$ (*m/z*)	330.1	330.1	306.1	306.1	346.1	346.1	331.0	408.0	410.0
Production (*m/z*)	136.1	136.1	112.1	112.1	152.1	152.1	137.1	214.0	216.0
Ret. time (min)	6.8	12.9	1.6	4.0	15.6	24.3	24.1	26.3	26.3
LOD (fmol)	273	153	171	455	94	487	219	NA	NA
LOQ (fmol)	910	510	570	1517	313	1623	730	NA	NA

$[M + H]^+$ = protonated molecular mass; NA = not applicable; LOD = limit of detection; LOQ = limit of quantitation.

4.2.2 LC-MS/MS Method Calibration and Limits of Detection

Limits of detection (LOD) using the developed LC-MS/MS protocol for 2',3'-cAMP, 3',5'-cAMP, 2',3'-cCMP, 3',5'-cCMP, 2',3'-cGMP, 3',5'-cGMP and 3',5'-cIMP were calculated [24] as 273 fmol, 153 fmol, 171 fmol, 455 fmol, 94 fmol, 487 fmol and 219 fmol, respectively (Table 4.2). For all samples, in order to minimize intra-assay variability, each sample was measured in 2–3 separate runs. The average and standard deviation (or range) were calculated and reported for each sample. A set of standards to generate calibration curves was included at the beginning of each LC sequence to account for any day-to-day variability in ionization efficiency or retention times of cNMPs.

4.2.3 Optimization of Extraction Method

Difficulty with organ extractions has previously been reported due to low levels of cNMPs and interference from the complex organ matrix.[10a, 19] In addition, published protocols typically have focused on identifying or quantifying only a small number of cNMPs in cells and often are not adapted to analyze organ extracts.[2a, 16d, 18b] The lack of an efficient extraction and analysis protocol to study multiple cNMPs has made establishing tissue distributions of all cNMPs very challenging. As cNMPs are of interest as both established and putative signalling molecules, it is crucial to develop a versatile extraction protocol using standard instrumentations that many researchers can employ in order to establish the role of cNMPs in mammalian tissues, as well as in other systems.

An outline of the optimized extraction protocol is depicted in Figure 4.3. In order to achieve the best results, a series of optimization experiments were performed to maximize internal standard (IS) recovery and cNMP signal intensities in LC-MS/MS.

Frozen rat organs were homogenized in pre-chilled extraction buffer containing the phosphodiesterase (PDE) inhibitors EDTA and theophylline (Figure 4.3, step 1). Different combinations and ratios of organic and aqueous solvent were evaluated and the reported extraction mixture (acetonitrile/methanol/water 1:2:2, v/v/v) yielded the best analyte recovery. A solubility test was conducted to ensure extracted cNMPs were dissolved in the extraction mixture. Solubilities of the IS and seven cNMPs are greater than or equal to 1 mM in extraction mixture. As a previous publication indicates, cAMP and cGMP levels in mammalian cells are well below the micromolar range, the chosen extraction mixture will therefore dissolve all extracted cNMPs.[2b, 4a, 18b]

Following homogenization, the crude lysate was heated (Figure 4.3, step 2) to denature enzymes that could bind, synthesize, or hydrolyze cNMPs, thereby decreasing the possibility of altered basal levels. Thermal stability of the seven cNMPs and IS were tested under the heat denaturation conditions and all were found to be thermally stable. cNMP concentrations were 87%–141% compared to the reference samples, indicating that heating does not degrade cNMPs (Table 4.3). Moreover, a stability test of cAMP in water exposed to the extraction conditions did not result in formation of cIMP, suggesting that 2',3'-cIMP and 3',5'-cIMP detected in rat organs were not degradation products of 3',5-cAMP and 2',3'-cAMP. A similar test was also conducted in crude organ lysate and addition of 3',5'-cAMP to an organ extract did not cause an increase in 3',5'-cIMP levels, indicating that 3',5'-cIMP, and likely 2',3'-cIMP, detected in organ samples were not deaminated products of 3',5'- and 2',3'-cAMP (Table 4.4).[25] Low-speed centrifugation following step 2 was used to remove lipids, cell walls and denatured proteins from extracted small molecules in the supernatant. Results have shown that low centrifugation

at ~3000× *g* is sufficient to remove most insoluble material, as the supernatant (Figure 4.3, step 3) generated after treatment appears to be clear, except for liver samples, which are particularly complex. Homogenization, heating and centrifugation were performed in the same conical tube to minimize loss of extracted cNMPs.

Table 4.3 Thermal stability test (μM). Samples dissolved in water were treated at 60°C for 10 min.

	2',3'-cAMP	**3',5'-cAMP**	**2',3'-cCMP**	**3',5'-cCMP**	**2',3'-cGMP**	**3',5'-cGMP**	**3',5'-cIMP**	**8-Br-cAMP**
Sample conc.	46.4	50.3	48.6	60.8	40.5	54.7	30.3	45.8
Conc. after treating with heat	59.4	48.1	69	70.6	35.2	62.7	42.1	50.4
% to reference sample	128%	95.6%	141%	116%	87%	114%	138%	110%

Table 4.4 Deaminase activity test (pmol/ g wet tissue), concentrations are reported as mean ± range (each sample was analyzed twice on LC-MS/MS). Liver A and B were from one liver. 40 pmol of 3',5'-cAMP was added to liver B.

	3',5'-cAMP	**2',3'-cIMP**	**3',5'-cIMP**
Liver A	3.90 ± 0.82	1.85 ± 0.19	1.76 ± 0.02
Liver B	1844.14 ± 106.63	2.34 ± 0.17	2.28 ± 0.40

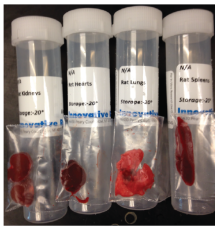

1

Frozen rat organs were homogenzized using a tissue homogenizer in pre-chilled acetonitrile/methanol/water buffer (1:2:2, v/v/v; 3 ml extraction buffer/g wet tissue)

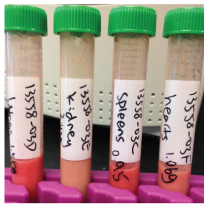

2

Crude lysate was heated for 10 min at 60°C, cooled on ice for 10 min, centrifuged at 2427 *g* for 90 min

2a

Supernatant was transferred to a round bottom flask

2c

The washed sample was centrifuged at 2427 *g* for 30 min. The supernant was combined with supernatant 2a

2b

The pellet and the sides of the tubes were washed 2-3 times with 2 ml water each time

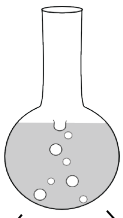

3

Organic solvent of the combined supernatant was removed using a rotary evaporator

3a

Aqueous layer was ransferred to a high-speed centrifuge tube

3b

Rinsed twice with 1 ml of water

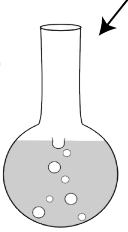

3c

Transferred to a high-speed centrifuge tube

4

High-speed centrifugation at 18,000-20,000 *g* to remove remaining particulates

4a

Supernatant was transferred to a glass vial. IS (67 pmol/ g wet tissue) was added to each sample, which was then lyophilized over-night to remove water

5

LC-MS/MS quantification

Lyophilized powder waas dissolved in 50 mM phosphate buffer (pH=7.4) (~100 µl/ g wet tissue). Mixed throughly until extracted compounds were fully dissolved

Figure 4.3 Workflow chart of cNMPs extraction from rat organs. Brain, spleen and heart samples require high-speed centrifugation (step 4) at 18,000× *g*. Liver, lung and kidney samples require high-speed centrifugation (step 4) at 20,000× *g*.

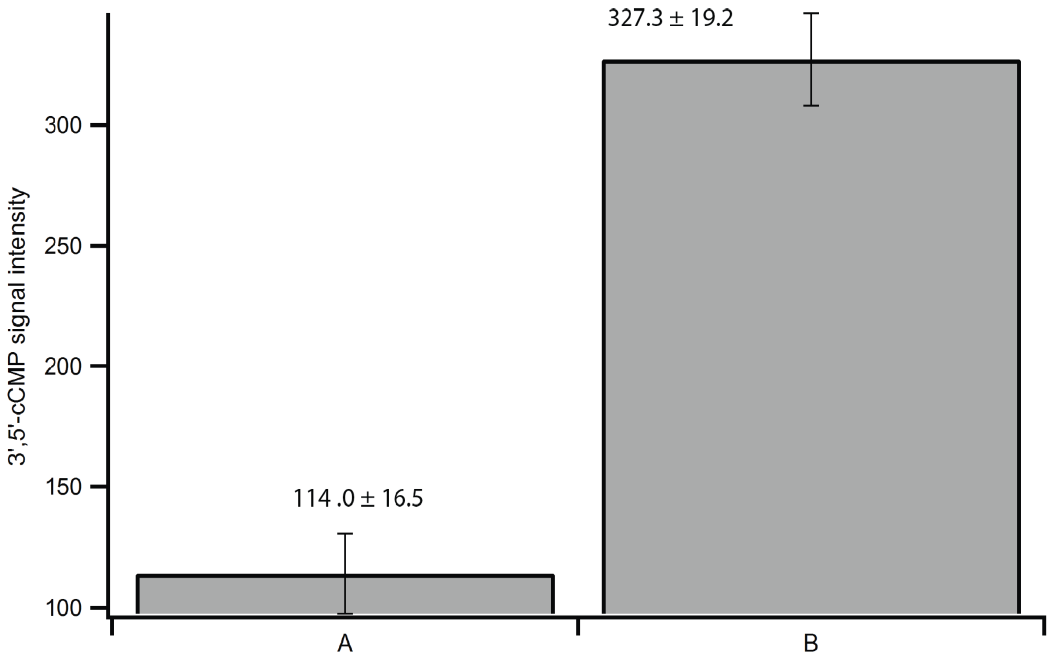

Figure 4.4 LC-MS/MS signal intensity of 3',5'-cCMP in rinsing tests. Crude lysate from a brain extract was split into two portions A and B, heat extractions were performed independently. (**A**) Sample was treated without extensive rinsing of tube walls; (**B**) sample was treated with extensive rinsing of tube walls (Figure 4.3, step 2b).

Rinsing of the sides of the tube walls and pellet during step 2b in Figure 4.3 was performed to ensure transfer of any residual cNMPs on the tube walls or pellet. Figure 4.4 shows that 3',5'-cCMP recovery improved by over three fold when tube walls were washed extensively, suggesting that cNMPs can stick to the tube walls or to fine

particulate matter removed during centrifugation. 8-Br-cAMP is less soluble than most natural cNMPs, and all cNMPs tend to stick to the tube walls and/or particles within the tubes, making the rinsing steps (Figure 4.3, steps 2b and 3b) crucial for complete recovery of extracted cNMPs and IS.

The combined supernatants from steps 2a–2c were concentrated using a rotary evaporator to remove organic solvent, as organic solvents often resulted in melting of the mixture on the freeze-dryer. Depending on the lyophilizer/free-dryer used, this step can be eliminated and the supernatant can be concentrated without use of the rotary evaporator. As discussed above, an extra rinse (Figure 4.3, step 3b) was included when transferring the aqueous layer to a high-speed centrifuge tube (Figure 4.3, step 3a–3c) to ensure complete recovery of extracted cNMPs.

The high-speed centrifugation step was employed to remove remaining particulate material, thereby improving separation on the LC column and sensitivity of the LC-MS/MS. Results in Figure 4.5 show that IS recovery was improved to ~90% by utilizing a high-speed centrifugation step in sample preparation. As previously mentioned, steps to eliminate matrix effects by removing cellular debris were crucial for improving sensitivity. High-speed centrifugation eliminated the remaining particulates in the sample, which resulted in improved sensitivity. Filtering samples using a number of different brands of syringe filters to remove remaining matrix components also was tested; however, including a filtering step did not decrease the prevalence of sample components that limited sensitivity and clogged the column. Additionally, the signal intensity of the IS on LC-MS/MS is crucial in quantifying putative cNMP levels, since the IS signal and concentration of the cNMP analytes are inversely proportional, low IS

signal will lead to over-estimation of cNMP concentration. Treating brain, spleen and heart samples with high-speed centrifugation at 18,000× *g* is sufficient to achieve the reported percent recovery. However, due to the nature of the organs, centrifugation at 20,000× *g* or higher is required for liver, lung and kidney samples. Finally, the clear supernatant extracted from each organ was transferred to a glass vial, followed by addition of the IS and lyophilization over-night to remove water (Figure 4.3, step 4a). The lyophilized powder containing extracted cNMPs was re-dissolved in 50 mM phosphate buffer (pH = 7.4) (~10 µL/g wet tissue) before analysis by LC-MS/MS.

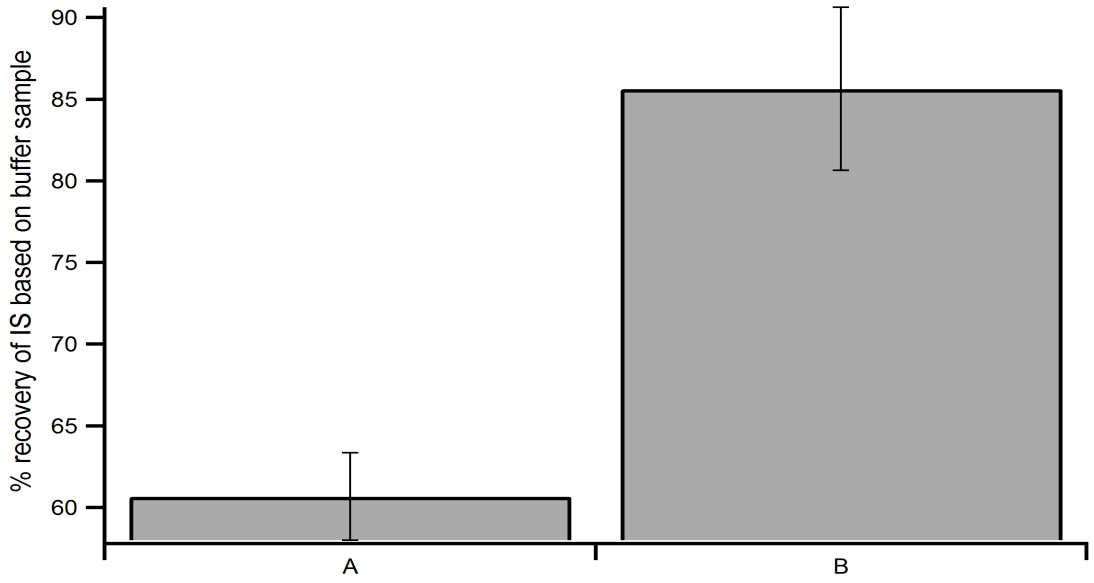

Figure 4.5 Percent recovery of IS signal in samples without and with high-speed centrifugation. Heat extractions were performed independently. (**A**) Sample was treated without high-speed centrifugation step; (**B**) sample was treated with the high-speed centrifugation step (Figure 4.3, step 4).

4.2.4 Method Validation and Reproducibility Tests

In order to validate the present extraction protocol,[26] extraction replicates using a frozen brain were performed. Sample A in Figure 4.6 shows the basal level of 3',5'-cCMP detected in the brain sample, which was below the LOD. To samples B and C, 60 pmol of 3',5'-cCMP were added at various points during extraction protocol to determine if the developed method is able to isolate all of the cNMPs within biological samples. Addition of 60 pmol 3',5'-cCMP to the crude lysate (Figure 4.3, step 1) or with IS (Figure 4.3, step 4a) resulted in 105% ± 12% and 118% ± 28% recovery of the added 3',5'-cCMP, respectively. These results demonstrate that the present extraction protocol is efficient in recovering extracted cNMPs. Also, addition of IS at various points during the extraction protocol does not affect the outcome of the extraction procedures (Table 4.5).

To test the reproducibility of the protocol, the optimized method was performed using rat brains. A frozen brain was split into three portions, which were extracted and quantified independently (refer to Experimental section 4.3.10). As shown in Table 4.7, the relative standard deviation of each calculated cNMP concentration ranges from 2.1%–20.0%. It is worth noting that the relative standard deviation may have suffered, particularly for 3',5'-cCMP, due to the extremely low concentration in each organ portion. The relative standard deviations for the calculated concentrations that are several fold above the LOD (2',3'-cAMP, 3',5'-cAMP and 3',5'-cGMP) are less than or equal to 10% (Table 4.6).

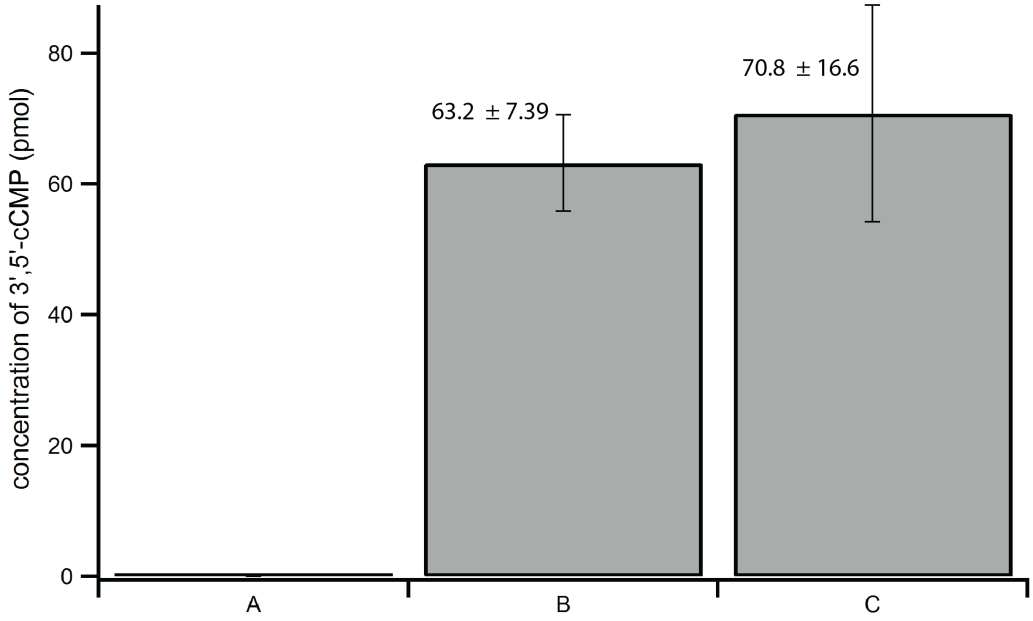

Figure 4.6 Method validation test shows recovered 3',5'-cCMP (added 60 pmol 3',5'-cCMP) following addition at various time points during the extraction protocol. A brain crude lysate was split into three portions A, B and C, and heat extractions were performed independently (refer to Experimental section 4.9). (**A**) Basal level of 3',5'-cCMP; (**B**) 60 pmol of 3',5'-cCMP was added with the crude lysate (Figure 4.3, step 1); (**C**) 60 pmol of 3',5'-cCMP was added with IS (Figure 4.3, step 4a). Data in tabulated form can be found in Table 4.6.

Table 4.5 Comparison of extraction efficiency of the internal standard (IS; 8-Br-cAMP) at different addition times. A rat brain was homogenized, split into two equal parts, and IS was added either to crude lysate (Fig. 4.3, step 2) or following centrifugation (Fig. 4.3, step 4). 3',5'-cAMP was quantified to provide a reference. No significant difference in peak areas was detected.

Sample	Internal Standard	3',5'-cAMP
IS addition to crude lysate	123458 ± 6715	272637 ± 12635
IS addition post-heating	140722 ± 7070	267800 ± 13043

Table 4.6 Intra-run precision and accuracy data in tabulated form. Extractions and measurements were performed in rat brains (see Fig. 4.6).

	Measured (pmol)	Precision (RSD in %)	Accuracy (%)
3',5'-cCMP (60 pmol)	63.3 ± 7.4	11.7%	105.4%
3',5'-cCMP (60 pmol)	70.8 ± 16.6	23.5%	117.9%

Table 4.7 Reproducibility of the method. A rat brain was split into three portions, and cNMPs were extracted and quantified independently. Results are reported in pmol/g of tissue.

Sample	2',3'-cAMP	3',5'-cAMP	2',3'-cCMP	3',5'-cCMP	2',3'-cGMP	3',5'-cGMP	3',5'-cIMP
Portion 1	9.9 ± 0.2	88.7 ± 12.3	1.2 ± 0.9	0.9 ± 0.7	2.5 ± 0.01	10.1 ± 2.3	2.6 ± 0.9
Portion 2	9.6 ± 0.3	92.3 ± 2.9	ND	0.6 ± 0.4	1.8	8.7 ± 0.3	2.3 ± 0.3
Portion 3	9.7 ± 0.2	87.9 ± 4.8	1.3	0.6 ± 0.4	1.8 ± 0.5	8.3 ± 0.7	3.1 ± 0.3
Average	9.7 ± 0.2	89.6 ± 2.3	1.3 ± 0.1	0.7 ± 0.1	2.0 ± 0.4	9.0 ± 0.9	2.7 ± 0.4
Inter-run Precision	2.1	2.6	7.7	14.3	20.0	10.0	14.8

N/D—Not detected, concentration below LOD; Precision—relative standard deviation in %

4.2.5 Applications

The existence of additional cyclic nucleotides beyond the paradigmatic second messengers 3',5'-cAMP and cGMP has been reported in the literature for a number of years.[2a, 2c, 3c, 27] Therefore, the optimized extraction and quantification protocol was used to detect levels of previously identified, as well as novel, cyclic nucleotides in mammalian organs. Using t. l. c., previous work has found that the concentration of mammalian 3',5'-cGMP is several fold lower than that of 3',5'-cAMP in mammalian organs (488 pmol/g extracted 3',5'-cAMP and 119 pmol/g extracted 3',5'-cGMP in rat heart; 11.8 pg/mg extracted 3',5'-cAMP and 5.2 pg/mg extracted 3',5'-cGMP in rabbit pancreas; all measurements listed as per gram of organ weight).[10a, 18b] The concentration of 3',5'-cCMP in rat organs also has been previously determined using radioimmunoassay[2b] and 3',5'-cIMP and 2',3'-cAMP have been detected in various rat organs.[2c, 7] Therefore, a panel of rat organs, including brain, spleen, heart, kidney, lung and kidney, was chosen to validate previous studies and to establish tissue distribution of cNMPs in major rat organs. As shown in Figures 4.7 and 4.10, eight cNMPs were detected and quantified in the majority of rat organs studied. The ability to analyze eight cNMPs simultaneously in a single run demonstrates the efficiency of the developed method. The concentrations of 3',5'-cGMP, 3',5'-cAMP and 3',5'-cCMP (Figure 4.7, Table 4.9) agree with the previously reported values within less than an order of magnitude.[2b, 10a, 18b] In addition, the range of cNMP levels detected in organs from different rats confirms the biological variability between animals that has previously been reported.

In addition to 3',5'-cAMP and cGMP, 2',3'-cAMP has previously been detected in rat kidney and neurons, while 2',3'-cGMP has been detected and quantified in cellular systems.[2a, 7] This report details the first measurements of 2',3'-cGMP in rat tissues, which should aid in the study of its putative role in post-injury mechanisms (Figure 4.8, 4.9 and 4.10). In addition, 3',5'-cIMP has been previously reported as an endogenous product found in a variety of rat organs using t. l. c. and fast atom bombardment mass spectrometry.[2c] The present study confirms that 3',5'-cIMP is an endogenous molecule produced in the heart, kidney, spleen and liver (Figure 4.7 and Table 4.8). As a recent publication has suggested a possible role of 3',5'-cIMP in cellular signal transduction, quantification of 3',5'-cIMP in healthy tissues will be useful in establishing relevant physiological concentrations.[3b, 6] 2',3'-cIMP also was detected in a number of the rat organs studied, although its role *in vivo* has yet to be proposed (Figure 4.10 and Table 4.4). We believe the present extraction protocol will help identify and quantify 3',5'- and 2',3'-cIMP levels in various disease states and promote further study of their potential roles as signalling molecules.

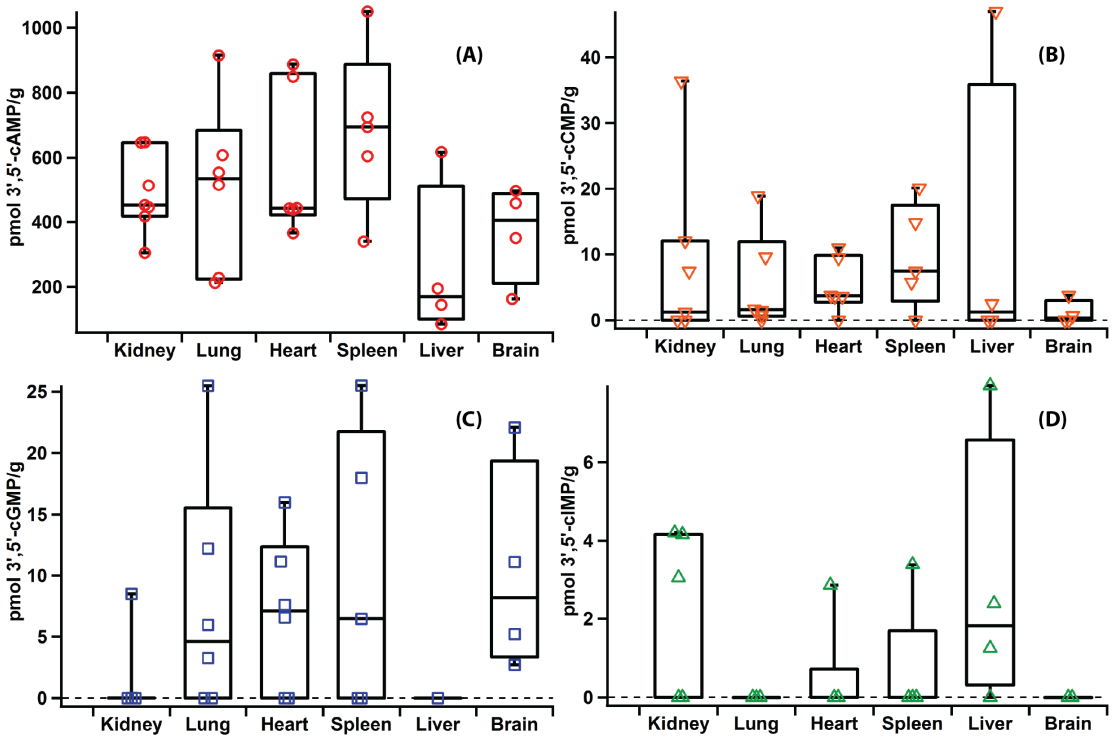

Figure 4.7 Levels of extracted 3',5'-cNMPs (pmol/g wet tissue) in rat organs. Each point represents the level measured in a replicate from a different rat. (**A**) 3',5'-cAMP (**B**) 3',5'-cCMP (**C**) 3',5'-cGMP (**D**) 3',5'-cIMP. Whisker top: 90 percentile, box top: 75 percentile, box middle: 50 percentile, box bottom: 25 percentile and whisker bottom: 10 percentile.

Table 4.8 Measured concentrations of 8 cNMPs in various rat organs reported as mean ± SD (pmol/ g wet tissue). Each cNMP was calculated using 4-7 individual organs as replicates, each sample was analyzed in 2-3 separate runs.

	2',3'-cAMP	**3',5'-cAMP**	**2',3'-cCMP**	**3',5'-cCMP**	**2',3'-cGMP**	**3',5'-cGMP**	**2',3'-cIMP**	**3',5'-cIMP**
Rat 1	8.73	497.03 ± 243.75	N/D	N/D	N/D	2.71	0.90 ± 0.52	N/D
Rat 2	N/D	162.61	2.50*	N/D	6.48 ±	5.22 ±	N/D	N/D

		± 31.21			1.19	1.79		
Rat 3	11.50	351.00 ± 24.84	2.63	0.67 ± 0.09	17.49 ± 11.86	22.09 ± 4.82	N/D	N/D
Rat 4	N/D	458.28 ± 67.80	N/D	3.75 ± 0.01	22.09 ± 0.63	11.12 ± 4.05	0.17 ± 0.37	N/D
Ave brain	10.11 ± 1.96	367.23 ± 149.75	2.57 ± 0.07	2.21 ± 1.54	15.35 ± 8.02	10.29 ± 8.62	0.54 ± 0.37	N/D

	2',3'-cAMP	**3',5'-cAMP**	**2',3'-cCMP**	**3',5'-cCMP**	**2',3'-cGMP**	**3',5'-cGMP**	**2',3'-cIMP**	**3',5'-cIMP**
Rat 1	N/D	849.05 ± 10.44	8.73	N/D	4.17	N/D	N/D	N/D
Rat 2	N/D	442.14 ± 46.57	4.57 ± 0.27	3.60 ± 0.04	13.63 ± 6.16	7.61 ± 3.04	BQL	N/D
Rat 3	N/D	365.55 ±43.38	4.22	3.62 ±0.10	7.27 ±4.04	6.58 ±1.98	N/D	N/D
Rat 4	28.35	887.34 ± 156.06	N/D	10.96 ±0.75	28.06 ± 7.03	15.98 ± 12.12	BQL	N/D
Rat 5	7.30	439.40 ± 69.43	N/D	9.49 ± 1.12	20.90 ± 4.48	11.16 ±4.60	0.07 ± 0.03	2.86
Female rat 1	32.84 ± 29.36	443.07 ± 62.82	N/D	3.76 ± 4.06	5.63 ± 0.03	N/D	N/D	N/D
Ave heart	22.83 ± 13.63	571.09 ±232.33	5.84 ±2.51	6.29 ± 3.63	13.30 ± 9.52	10.33 ± 4.25	0.07	2.86

Rat 1	15.67 ± 20.89	515.52 ± 48.28	291.44 ± 425.18	N/D	6.67 ± 3.74	5.98	N/D	N/D
Rat 2	N/D	212.66 ± 4.98		18.89 ± 0.81	4.74 ± 1.42	3.28 ± 0.61	N/D	N/D
Rat 3	N/D	914.96 ± 130.83	7.35 ± 1.47	9.60 ± 0.97	25.42 ± 1.46	25.49 ± 12.15	N/D	N/D
Rat 6	19.58 ± 2.42	554.21 ± 50.42	68.73 ± 6.94	0.78	N/D	12.24	N/D	N/D
Rat 7	17.42	227.84 ± 114.58	N/D	1.45	N/D	N/D	N/D	N/D
Female rat 2	29.21 ± 2.97	607.29 ± 106.08	2.04	1.69 ± 1.00	27.73 ± 2.64	N/D	N/D	N/D
Ave lung	20.48± 6.04	505.58 ±	92.39 ± 136.11	6.48 ± 7.81	16.14± 12.11	11.75 ± 9.90	N/D	N/D

		262.05						
Rat 1	20.31 ± 11.65	417.72 ± 13.15	187.15 ± 24.26	N/D	12.66	N/D	N/D	3.05 ± 1.83
Rat 2	28.60 ± 11.02	646.05 ± 143.88	14.80 ± 11.99	36.68 ± 6.37	11.61	N/D	BQL	N/D
Rat 3	21.88 ± 12.04	647.25 ± 372.78	6.58 ± 0.66	7.45	N/D	N/D	N/D	N/D
Rat 4	17.96 ± 7.53	452.31 ± 190.19	3.94 ± 1.97	12.06	2.38	0.02	BQL	4.16
Rat 6	46.08 ± 11.72	305.35 ± 59.38	N/D	N/D	3.81 ± 1.22	N/D	N/D	4.16
Rat 7	56.20 ± 4.84	513.95 ± 63.81	438.16 ± 262.27	N/D	10.99 ± 0.19	N/D	N/D	N/D
Female rat 2	72.68 ± 48.38	445.49 ± 43.87	10.88 ± 5.03	1.22	9.64 ± 2.00	8.50 ± 6.14	N/D	N/D
Ave kidney	37.67 ± 21.06	489.73 ± 124.08	110.25 ± 175.77	14.35 ± 15.53	8.51 ± 4.33	4.26 ± 6.00	BQL-N/D	3.79 ± 0.64

	2',3'-cAMP	**3',5'-cAMP**	**2',3'-cCMP**	**3',5'-cCMP**	**2',3'-cGMP**	**3',5'-cGMP**	**2',3'-cIMP**	**3',5'-cIMP**
Rat 1	21.80 ± 3.47	724.48 ± 14.16	114.56 ± 79.19	N/D	11.84	N/D	N/D	3.39
Rat 2	30.07 ± 15.39	339.83 ± 7.73	9.33 ± 2.07	5.74 ± 0.10	17.07 ± 5.51	6.47 ± 1.24	N/D	N/D
Rat 3	79.60 ± 32.62	1050.12 ± 290.46	191.18 ± 91.08	20.14 ± 4.66	47.20 ± 7.28	25.50 ± 5.48	BQL	N/D
Rat 4	11.52 ± 2.86	694.34 ± 84.05	N/D	7.43 ± 0.37	26.54 ± 3.39	17.98 ± 2.01	0.05 ± 0.01	N/D
Female rat 1	214.65 ± 109.03	604.31 ± 249.78	123.48 ± 117.42	14.81	N/D	N/D	N/D	N/D
Ave spleen	71.53 ± 84.17	682.62 ± 255.24	109.63 ± 75.11	11.10 ± 7.87	25.66 ± 15.59	16.65 ± 9.59	0.05	3.39

Rat 8	N/D	144.31	15.62	N/D	N/D	N/D	1.7	N/D
Rat 9	N/D	195.03	64.70	N/D	N/D	N/D	N/D	1.25
Rat 10	12.63	617 ±	6.10 ±	46.96 ±	7.07 ±	N/D	2.5	7.95

Rat 11	6.23	192.93 84.97 ± 23.22	1.54 1.19 ± 0.17	7.08 2.48	1.39 N/D	N/D	N/D	2.39
Ave liver	9.43 ± 3.2	260.46 ± 242.26	21.90 ± 29.16	24.72 ± 22.24	7.07 ± 1.40	N/D	2.1 ± 0.4	3.86 ± 3.59

* Only one injection was evaluated for numbers without standard deviation

N/D – Not detected, concentration below LOD

BQL – below quantification limit; detected, but level too low to quantify

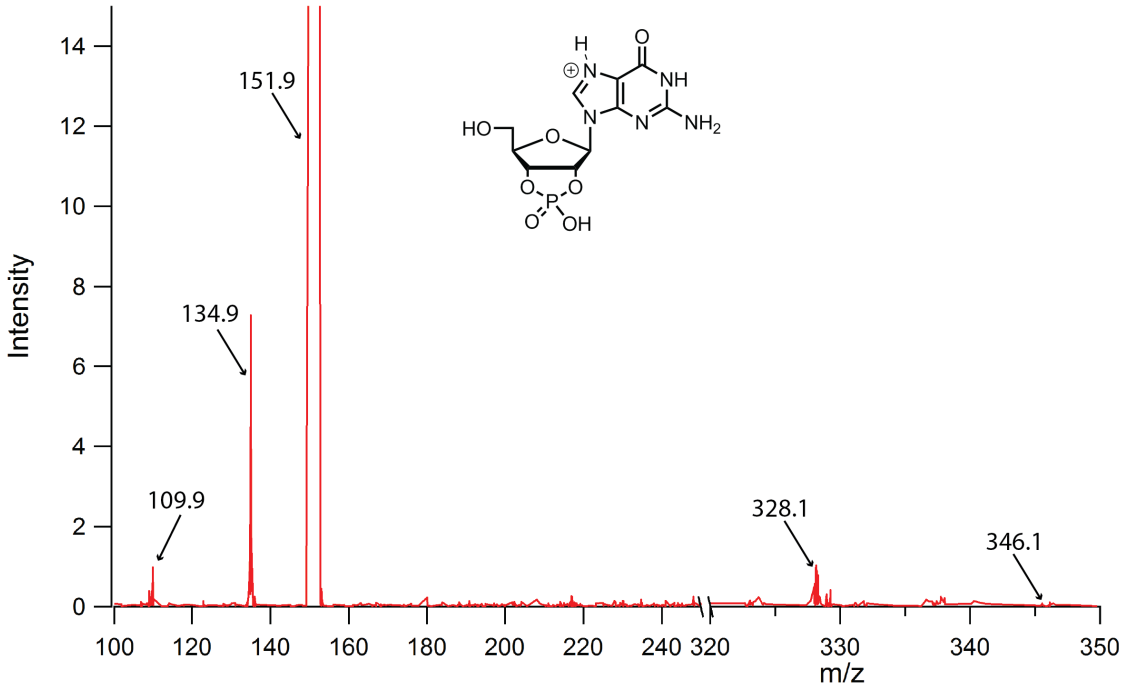

Figure 4.8 MS/MS spectrum of authentic 2',3'-cGMP.

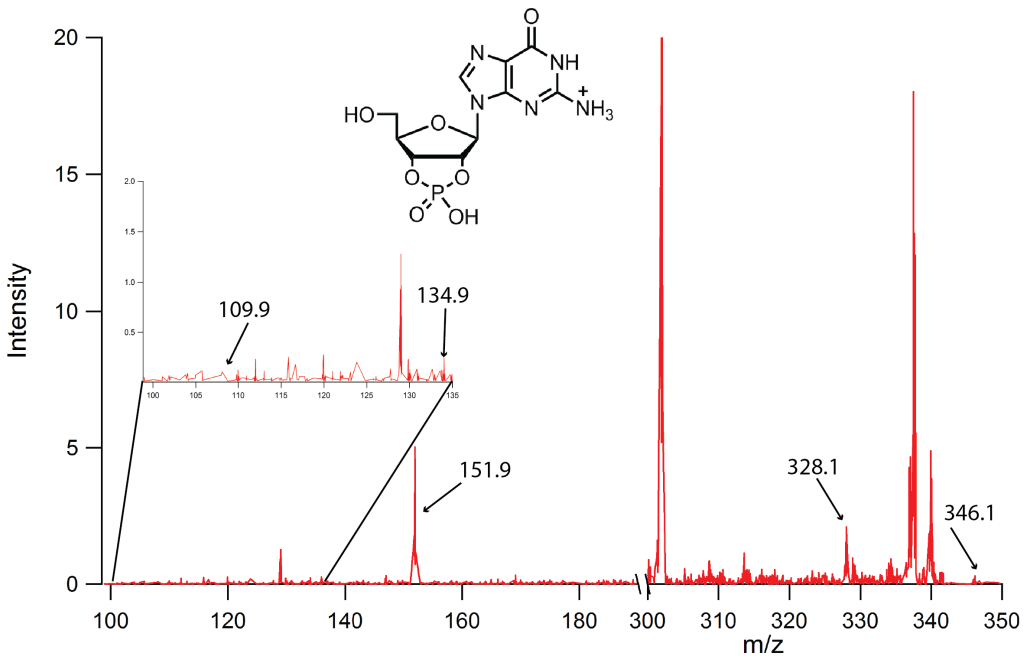

Figure 4.9 MS/MS spectrum of extracted 2',3'-cGMP in rat heart.

It is worth mentioning that the concentrations of 2',3'-cCMP, 3',5'-cCMP, 2',3'-cIMP and 3',5'-cIMP in brain, heart and liver samples are close to the LOD of the method, and therefore are associated with relatively high standard deviations (Figures 4.7 and 4.10, Table 4.8). While the higher deviations potentially could be due to variability in the method, the validation experiment described above suggests that bio-variability between animals and organs plays a larger role than variability due to the method. For low abundance cNMPs, the precision of calculated concentrations can be improved by increasing the injection volume or concentration of samples. However, caution should be used when attempting to produce extremely concentrated samples as cNMPs can be lost if the entire extract is not completely dissolved. In addition, analysis of samples using a triple quadrupole MS instrument would likely improve sensitivity and the described

method can be readily adapted if researchers have access to such an instrument. Improving sensitivity through either method will be important for future studies analyzing small organs such as rat spleen and heart (~0.7 g and ~0.8 g, respectively), as the total amounts of cNMPs in smaller organs are close to the LOD.

During the analysis of cNMP tissue distributions, a peak proposed to correspond to 2',3'-cIMP was identified. An authentic standard of 2',3'-cIMP was synthesized [28] and used to verify the identity of the extracted compound based on molecular weight, fragmentation pattern, and retention time. As can be seen in Figure 4.11, both authentic and extracted 2',3'-cIMP elute at 2.4 min, supporting our identification of 2',3'-cIMP in mammalian organs (Figure 4.11). The other peaks in the extracted 2',3'-cIMP chromatogram include 3',5'-cIMP and 3',5'-cAMP that has incorporated a single ^{13}C, which results in the same low resolution mass as cIMP.

Additionally, the high resolution spectrum of extracted 2',3'-cIMP yielded *m/z* of 331.0455 (authentic 2',3'-cIMP = 331.04525) and, based on the fragmentation of authentic 2',3'-cIMP (Figure 4.12) and on previously published fragmentation patterns of 2',3'-cGMP,[29] the predicted product ion corresponding to the protonated inosine base $[BH_2]^+$ was observed at *m/z* 136.9 (authentic 2',3'-cIMP, $[BH_2]^+$ = 136.9, Figure 4.12). 2',3'-cIMP was detected, although often below the limit of quantitation, in extracts from brain, kidney, spleen, heart, and liver (Table 4.8). Therefore, we believe that we have detected 2',3'-cIMP in a panel of mammalian organs.

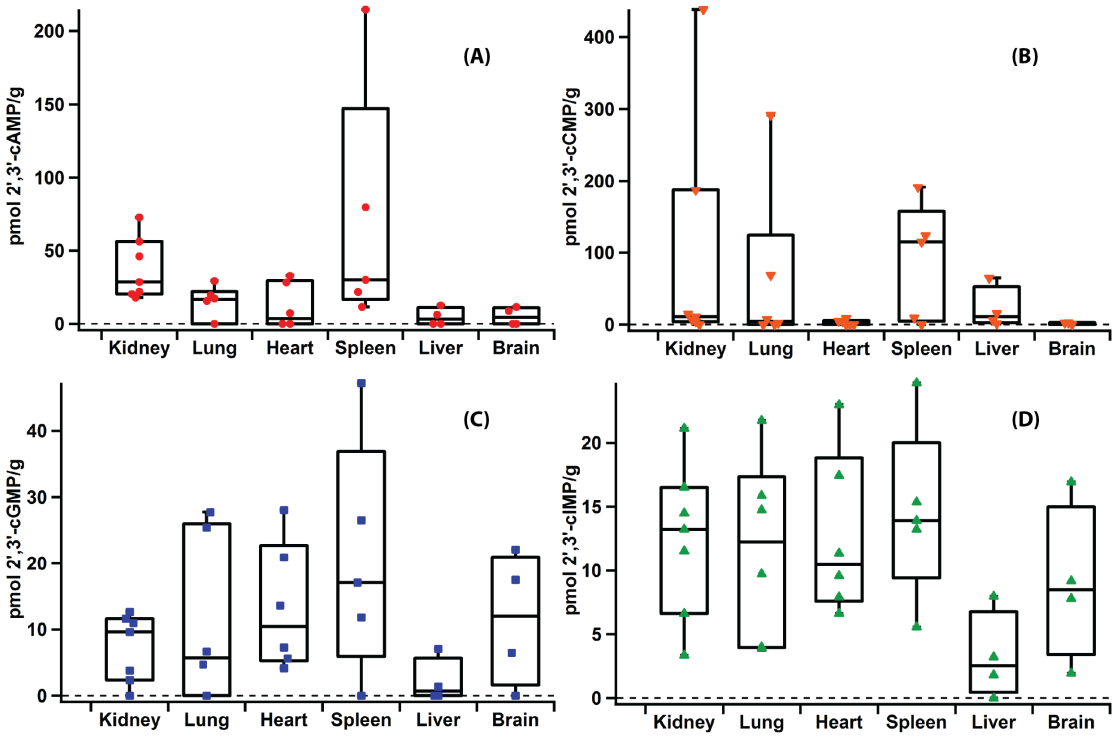

Figure 4.10 Levels of extracted 2',3'-cNMPs (pmol/g wet tissue) in rat organs. Each point represents the level measured in a replicate from a different rat. (**A**) 2',3'-cAMP; (**B**) 2',3'-cCMP; (**C**) 2',3'-cGMP; (**D**) 2',3'-cIMP. Whisker top: 90 percentile, box top: 75 percentile, box middle: 50 percentile, box bottom: 25 percentile and whisker bottom: 10 percentile.

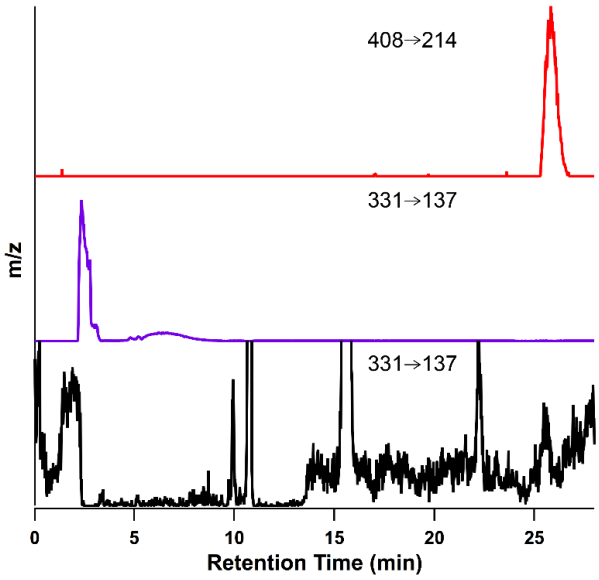

Figure 4.11 Reconstructed ion chromatogram of IS (top, red trace), authentic 2',3'-cIMP (purple trace), and extracted 2',3'-cIMP (bottom, black trace) from male rat brain using Xcalibur software. Transition 331 → 137 *m/z* was monitored and reconstructed for extracted 2',3'-cIMP.

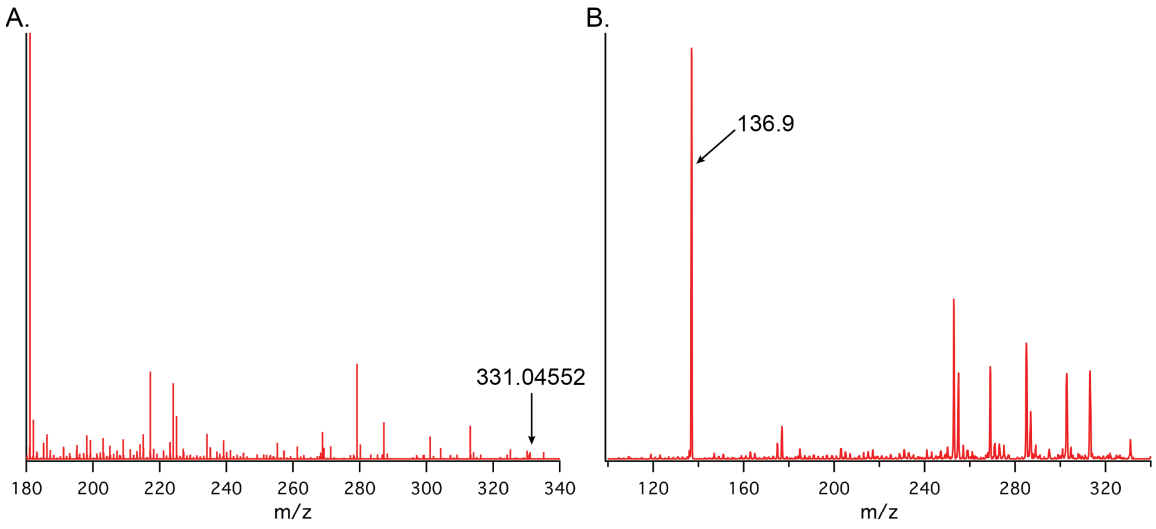

Figure 4.12 High resolution MS (**A**) and MS/MS (**B**) spectra of 2',3'-cIMP extracted from rat brain. Authentic 2',3'-cIMP: 331.04525; extracted: 331.04552. Authentic 2',3'-cIMP $[BH_2]^+$: 136.9; extracted: 136.9.

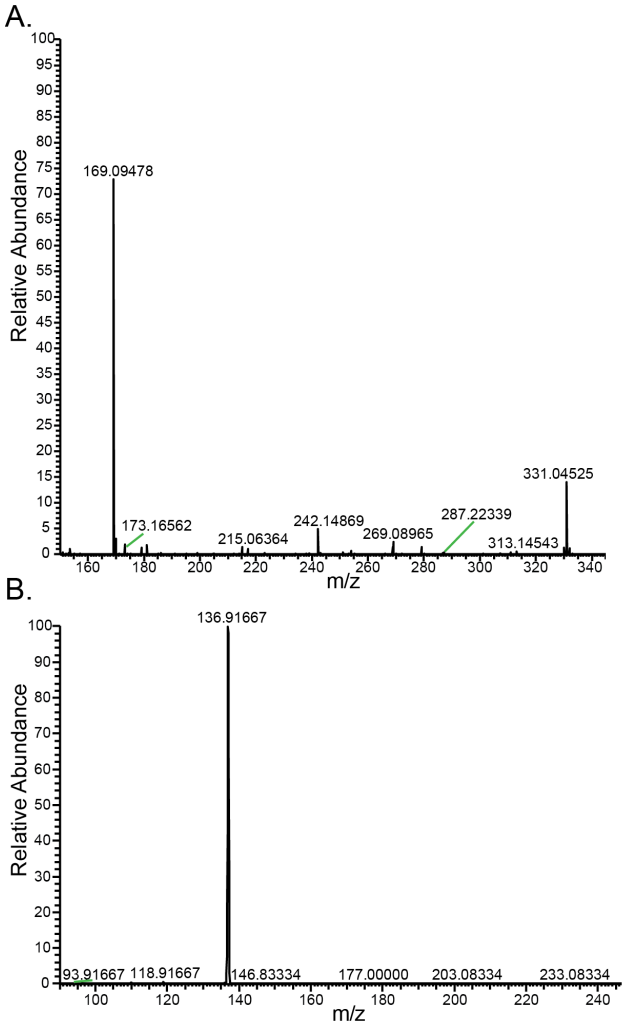

Figure 4.13 High resolution MS (A) and MS/MS (B) spectra of authentic 2',3'-cIMP. 2',3'-cIMP calculated: 331.04515; observed: 331.04525. $[BH_2]^+$ calculated: 137.04635; observed: 136.91667.

Based on the precedence of enzymatic production of 3',5'-cIMP from 3',5'-cAMP, 2',3'-cIMP also may be formed enzymatically *in vivo* through the deamination of 2',3'-cAMP.[3b] If so, deamination of 2',3'-cAMP may play a role in modulating levels of 2',3'-cAMP to alter the downstream effects of the mammalian 2',3'-cAMP-adenosine pathway.[3c] To our knowledge, this study presents the first detection of 2',3'-cIMP and the first quantification of 3',5'-cIMP in a panel of mammalian organs, laying the groundwork for future studies of the biochemistry and physiology of both cIMP isomers.

4.2.6 Versatility of the Method

To further extend the method, its utility was tested on mammalian cells. NIH-3T3 cells were studied using the developed LC-MS/MS protocol. As shown in Table 4.9, most cNMPs, except 3',5'-cCMP, 2',3'-cIMP and 3',5'-cIMP, were detected and quantified in this particular cell line. Extracted samples from cell lines were much cleaner and required fewer washing and transfer steps (due to the decreased volume) compared to organ extractions and the data showed improved sensitivity and reproducibility. On-going experiments have found that the present method also can be used to quantify levels of cNMPs in *Escherichia coli* samples.

Table 4.9 Measured concentrations of eight cNMPs in NIH-3T3 cell line reported as mean ± SD (pmol/10^6 cells). Each cNMP concentration was calculated from three separated samples (1, 2 and 3), and each sample was analyzed in two separate runs.

Replicate	2',3'-cAMP	3',5'-cAMP	2',3'-cCMP	3',5'-cCMP	2',3'-cGMP	3',5'-cGMP	2',3'-cIMP	3',5'-cIMP
1	5.1 ± 0.3	4.8 ± 0.1	1.3 ± 0.1	N/D	2.1 ± 0.1	N/D	N/D	N/D
2	N/D	167.1 ± 35.0	N/D	N/D	32.0 ± 2.3	17.2 ± 0.3	N/D	N/D
3	N/D	99.8 ± 0.2	1.8	N/D	19.9 ± 0.2	8.0 ± 3.7	N/D	N/D
Average	5.1	90.6 ± 81.6	1.6 ± 0.3	N/D	18.0 ± 15.0	12.6 ± 4.6	N/D	N/D

N/D—not detected, concentration below LOD.

4.2.7 Discussion

The aim of this work was to develop an efficient and versatile LC-MS/MS protocol that can detect and quantify multiple cNMPs concurrently in biological and cellular samples using standard instrumentation. There are several key steps that were discovered in developing the current protocol. First, cNMPs tend to stick to the centrifuge tube walls during extraction, regardless of whether glass or plastic tubes are used; therefore, an extensive rinsing step is key to ensuring complete recovery of extracted cNMPs. Secondly, matrix effects resulted in unfavourable competitive ionization with the analytes-of-interest, which is common in complex biological samples. However, introduction of a high-speed or ultra-centrifugation step to remove remaining particulate can greatly reduce the matrix effect and increase sensitivity. Despite high-speed centrifugation, liver samples were found to clog the ion transfer tube on the LC-MS/MS; cleaning the tube after every 4–5 samples also can help to maintain high sensitivity during high throughput sample analysis. In addition, large numbers of sample runs (~50–70) lead to the build-up of extracted compounds from organs on the column. This problem is easily solved by washing with organic solvents (e.g., acetonitrile or DMF) or

switching buffer systems (e.g., triethanolamine HCl, pH 5.5) to remove the remaining material. Lastly, while the results of the current work were achieved using a quadrupole ion trap, this method could easily be adapted to a triple quadrupole detector, which would further increase the sensitivity of the current method.

One advantage of the present extraction protocol is that unlike quantification protocols using isotopically labelled cNMPs or expensive/synthetically challenging nucleotide analogues as the internal standard, affordable and commercially available 8-Br-cAMP was employed as an IS to allow for quantification of cNMPs and to account for any losses during sample preparation. 8-Br-cAMP was chosen because it is not naturally present in mammalian cells, is readily commercially available, and is relatively inexpensive (particularly in comparison to previously described internal standards).[2a, 18b] Due to the structural similarity between the internal standard and the cNMP analytes, the ionization efficiency of 8-Br-cAMP is similar to the natural cNMPs.

The optimized extraction and quantification protocol was used to detect levels of previously identified, as well as novel cyclic nucleotides in mammalian organs. The quantification of additional atypical nucleotides should aid in identifying their roles *in vivo*. 2',3'-cAMP and cGMP have been shown to correlate with stress in perfused kidney and in *Arabidopsis* following leaf wounding, suggesting that these nucleotides may be important in post-injury mechanism.[9] Furthermore, the potential roles of 3',5'-cCMP, cIMP, cUMP, cTMP and cXMP as secondary messengers have been proposed for decades and are still under investigation.[2a, 2c, 10b, 27] Previous studies have revealed the broad substrate specificity of purified soluble guanylyl cyclase (sGC) and its ability to synthetize a variety of atypical cNMPs at various rates; however, little is known about their

physiological and biochemical roles in mammalian systems.[5b, 30] The developed protocol allows for the detection and quantification of a large panel of cNMPs, which will provide a powerful tool in analyzing cNMPs levels in mammalian systems.

4.2.8 Conclusions

In summary, we have described a sensitive, efficient and versatile method using standard instrumentation to extract and quantify cNMPs in mammalian tissues and cellular systems. The optimized LC-MS/MS protocol can separate and quantify all eight cNMPs studied. By utilizing the present method, we have established the tissue distributions of a panel of cNMPs, allowing for future studies on their cellular roles. Using commercially available 8-Br-cAMP greatly reduced the cost of experiments, relative to the use of isotopically labelled standards, thereby making the protocol economically feasible for a wide variety of researchers. Furthermore, this study allows for quantification of eight cNMPs simultaneously, which provides the opportunity to compare levels of multiple cNMPs in the same system and examine the relationship between tissue levels of cNMPs and organ function. Since the signalling networks for some cNMPs may be intertwined (e.g., 3',5'-cIMP is likely a deamination product of 3',5'-cAMP in cells)[7], correlation of cNMPs levels in various rat organs, and their alterations in disease states, will provide insights into additional potential signalling pathways.

4.3 Experimental

4.3.1 Materials

Organs from Sprague-Dawley rats (brain, spleen, lung, kidney, heart and liver) were purchased from Innovative Research Inc. (Novi, MI, USA). According to the supplier, all organs were flash-frozen immediately after harvest and were stored at −80 °C upon receipt. Adenosine 2',3'-cyclic monophosphate (2',3'-cAMP) was purchased from MP Biomedicals (Solon, OH, USA). Adenosine 3',5'-cyclic monophosphate hydrate (3',5'-cAMP) was purchased from TCI America (Portland, OR, USA). Cytidine 2',3'-cyclic monophosphate monosodium salt (2',3'-cCMP) was purchased from Carbosynth (Berkshire, UK). Cytidine 3',5'-cyclic monophosphate (3',5'-cCMP) and guanosine 2',3'-cyclic monophosphate (2',3'-cGMP) were purchased from BioLog (Bremen, Germany). Guanosine 3',5'-cyclic monophosphate sodium salt (3',5'-cGMP), inosine 3',5'-cyclic monophosphate sodium salt (3',5'-cIMP), 8-bromoadenosine 3',5'-cyclic monophosphate (8-Br-cAMP), theophylline and 3-isobutyl-1-methylxathanine (IBMX) were purchased from Sigma-Aldrich (St. Louis, MO, USA). Ethylenediaminetetraacetic acid, disodium salt, dihydrate (EDTA) was purchased from EMD Millipore (Gibbstown, NJ, USA). HPLC-grade acetonitrile and methanol were obtained from Thermo Fisher Scientific (Rockford, IL, USA). Dulbecco's Modification of Eagle's Medium (DMEM), Cosmic Calf Serum (CCS), L-glutamine, penicillin G and streptomycin were purchased from Mediatech Inc. (Manassas, VA, USA).

4.3.2 Calibration Curves

Stock solutions of all cNMPs and internal standard 8-Br-cAMP were quantified using a UV-visible spectrophotometer (Cary Series, Agilent Technology, Santa Clara, CA, USA). Calibration curves were constructed by plotting the ratio of peak area for each

cNMP/internal standard (IS) against the ratio of concentration of each cNMP/IS in each standard sample. Concentration of IS in each calibration curve is 1 μM, while concentrations of the cNMPs ranged from 0.05–2.5 μM. The concentration range for the calibration curve was chosen because it encompasses the typical concentrations of cNMPs within the experimental samples that are injected on the LC-MS/MS (section 4.6). Calibration curves were generated using a linear regression model.

4.3.3 NIH-3T3 Cell Growth

NIH-3T3 cells were cultured in DMEM supplemented with 10% (v/v) CCS, L-glutamine (2.1 mM), penicillin G (100 IU mL^{-1}) and streptomycin (100 μg mL^{-1}) were incubated with 5% (v/v) CO_2 at 37 °C. Cells were passaged at 90%–100% confluency.

4.3.4 cNMP Extraction from Rat Organs

Frozen Sprague-Dawley rat organs (brain, spleen, lung, kidney, heart and liver) were homogenized using a tissue homogenizer (TH, OMNI International, Kennesaw, GA, USA) in pre-chilled acetonitrile/methanol/water buffer (1:2:2, v/v/v; 3 mL extraction buffer/g wet tissue) containing the phosphodiesterase inhibitors EDTA and theophylline (1 mM each) in conical tubes (Celltreat Scientific Products, Shirley, MA, USA). The crude lysate was heated in a water bath for 10 min at 60 °C, cooled on ice for 10 min, centrifuged at 2427× *g* for 90 min and the supernatant transferred to a round bottom flask.

The pellet from the first centrifugation and the sides of the conical tube were washed twice with 2 mL of water each time for brain, spleen, lung, kidney and heart samples and centrifuged at 2427× *g* for 30 min to isolate the supernatant. The supernatant

from the wash was combined with the supernatant from the first centrifugation. One additional rinse with 2 mL of water was required for liver due to its size. Combined supernatants containing the extracted cNMPs were transferred to a round bottom flask (Chemglass Life Sciences, Vineland, NJ, USA) and the organic solvent was concentrated using a rotary evaporator (IKA^{TM}, RU10 Basic, Wilmington, NC, USA) at 35 °C and the concentrated solution transferred to centrifuge tubes. The round bottom flask was rinsed twice with 1 mL of water each time to ensure complete transfer of cNMPs to the high-speed centrifuge tubes.

High-speed centrifugation of the cNMP solution following rotary evaporation was performed for 30 min at 20,000× *g* for liver and 18,000× *g* for other organs to remove any remaining particulates. The supernatant after high-speed centrifugation was transferred to a glass vial (Wheaton, Millville, NJ, USA) and 67 pmol/g wet tissue of internal standard (IS), 8-Br-cAMP was added. The sample was frozen in liquid N_2 and lyophilized (Flexi-Dry^{TM}, FTS Systems, Warminster, PA, USA) overnight to remove water.

4.3.5 cNMP Extraction from NIH-3T3 Cell Line

The pellet of NIH-3T3 cells was re-suspended in 125 µL pre-chilled extraction buffer (125 µL/10^6 cells) containing EDTA and theophylline (1 mM each). IS (20 pmol 8-Br-cAMP/ 10^6 cells) was added to the sample, which was then subjected to 10 cycles of flash-freezing in liquid N_2, followed by thawing on ice, until the cells appeared lysed by visual inspection. The lysate was heated at 80 °C for 10 min, cooled on ice for 10 min, and centrifuged at 13,000× *g* for 30 min at room temperature to precipitate cellular

debris. The supernatant was removed for analysis, and then the pellet and sides of the tube were washed twice with 100 μL of water, centrifuged at 13,000× *g* for 30 min and the supernatants from each centrifugation step were combined. The combined supernatants were lyophilized over-night to remove water.

4.3.6 LC-MS/MS Sample Preparation

Liquid chromatography-tandem mass spectrometry (LC-MS/MS) samples were prepared by re-dissolving lyophilized powder from each extraction in 50 mM phosphate buffer (pH = 7.4) (~100 μL/g wet tissue and 20 μL/10^6 cells). Re-dissolved samples were thoroughly mixed on a vortex mixer (Analog Vortex Mixer, VWR, Radnor, PA, USA) and then placed in an ultrasonic cleaner (Branson Model 2510, Fisher Scientific, Pittsburgh, PA, USA) for 3 min to fully dissolve all extracted compounds. The vortexing and sonicating steps were repeated two more times to yield clear LC-MS/MS samples.

4.3.7 LC-MS/MS Optimized Conditions

LC-MS/MS experiments were performed using a Thermo Electron LTQ-FTMS system equipped with a Shimadzu autosampler (SIL20AC, Shimadzu, Columbia, MD, USA) and a Dionex Ultimate 3000 dual gradient pump and diode array detector controlled by Xcalibur and DCMSlink software (Thermo Scientific). Samples were separated using a reverse phase (C-18) column (15 mm × 2.1 mm, 2.7 μm, Ascentis Express; guard column (0.5 cm × 2.1 mm, 2.7 μm, Ascentis Express, Sigma Aldrich). 20 μL of sample were analyzed by LC-MS/MS system during each run. Buffer A contained

0.1% formic acid in water and buffer B contained 0.1% formic acid in methanol. The optimized LC protocol (Buffer A/B) for separating cNMPs is as follows: 0–4 min, 0% B; 4–15 min, 0%–1.5% B; 15–20 min, 1.5%–8% B; 20–25 min, 8% B; 25–28 min, 8%–15% B; 28–35 min, 15% B; 35–45 min, 0% B with a flow rate of 0.3 mL/min. After 4 tissue samples, the column was washed using acetonitrile (Buffer C) to ensure removal of all retained cellular compounds. The wash protocol is as follows: 0–2 min, 0%–100% B, 0% C; 2–10 min, 100% B, 0% C; 10–12 min, 100%–0% B, 0%–100% C; 12–20 min, 0% B, 100% C; 20–25 min, 0% B, 100%–0% C; 25–40 min, 0% B, 0% C with a flow rate of 0.3 mL/min. Three independent LC-MS/MS runs were performed for each sample.

The samples were ionized by positive ion electrospray in the LTQ-FTMS using 5 kV voltage on the needle, with a capillary voltage of 35 V, capillary temperature of 275 °C, and tube lens voltage of 110 V. The tandem mass spectra were obtained in the ion trap of the LTQ-FTMS with an isolation window of 1 amu and normalized collision energy of 35 eV, with an activation Q of 0.250 and activation time of 30 milliseconds. Detection was done in the ion trap of the LTQ-FTMS.

4.3.8 Statistical Analysis

Xcalibur software (Thermo Scientific) was used to integrate the area under the reconstructed selected ion chromatograms of the product ions. Xcalibur was also used to obtain the retention time and MS/MS spectrum of each analyte. IGOR Pro software (version 6.0.1.9, WaveMetrics, Lake Oswego, OR, USA) was used to analyze calibration curves and calculate organ concentrations. Organ concentrations are reported as mean ±

standard deviation and are based on 4–7 independent extractions. Data were corrected to pmol/g wet tissue or pmol/10^6 cells to normalize between organs and cells.

4.3.9 Method Validation Test

A frozen rat brain (1.22 g wet tissue) was homogenized in 4 mL pre-chilled acetonitrile/methanol/water buffer (1:2:2, v/v/v), as described above. The crude lysate was split into three equal portions (~1 mL each, samples 1–3) and transferred to individual tubes. The centrifuge tube was washed with 1.2 mL water; the wash was split equally into each tube (0.4 mL each). 100 pmol IS (8-Br-cAMP) was added to each sample. 60 pmol of 3',5'-cCMP was added to sample 2 following homogenization, while 60 pmol of 3',5'-cCMP was added to sample 3 after heating. LC-MS/MS quantitation was performed independently on each sample (refer to Experimental sections 4.6 and 4.7).

4.3.10 Method Reproducibility Test

A frozen rat brain (1.55 g wet tissue) was homogenized in 5 mL pre-chilled acetonitrile/methanol/water buffer, as described above (refer to heat extraction from rat organs section). The crude lysate was split into 3 equal portions (~2 mL each) and transferred to individual tubes. The centrifuge tube was washed with 1.2 mL water, which was split equally into each tube (0.4 mL each). Heat extraction and LC-MS/MS experiments were performed independently on each sample (refer to Experimental sections 4.4, 4.6 and 4.7).

4.3.11 Synthesis of 2',3'-cIMP

2',3'-cIMP was synthesized by deamination of 2',3'-cAMP, as previously described.[28] A solution of $NaNO_2$ (26 mg) in 100 μL water was added to 50 mg of 2',3'-cAMP (MP Biomedical) in glacial acetic acid (0.8 mL). The solution was stirred at room temperature for 6 hrs. Three equal portions of $NaNO_2$ (60 mg total) were added over the 6 h period and the reaction was allowed to continue stirring for an additional 30 h (36 h total). After 36 h, the reaction was evaporated *in vacuo* to dryness. The product was purified by anion exchange chromatography using DEAE cellulose resin in carbonate form and eluted with a gradient of 0.005 M ammonium bicarbonate (pH 7.8) to 0.1 M ammonium bicarbonate (pH 7.0). The high resolution MS (calculated: 331.04515, observed: 331.04525), ^{1}H, ^{13}C, and ^{31}P NMR, and UV spectra confirmed the 2',3'-cIMP structure.

4.5 References

1. (a) Sutherland, E. W., Studies on the mechanism of hormone action. *Science* **1972,** *177* (4047), 401-8; (b) Lucas, K. A.; Pitari, G. M.; Kazerounian, S.; Ruiz-Stewart, I.; Park, J.; Schulz, S.; Chepenik, K. P.; Waldman, S. A., Guanylyl cyclases and signaling by cyclic GMP. *Pharmacol Rev* **2000,** *52* (3), 375-414.

2. (a) Bahre, H.; Kaever, V., Measurement of 2',3'-cyclic nucleotides by liquid chromatography-tandem mass spectrometry in cells. *J Chromatogr B* **2014,** *964*, 208-11; (b) Newton, R. P., Cytidine 3',5'-Cyclic-Monophosphate - a 3rd Cyclic-Nucleotide Secondary Messenger. *Nucleos Nucleot* **1995,** *14* (3-5), 743-747; (c) Newton, R. P.; Kingston, E. E.; Hakeem, N. A.; Salih, S. G.; Beynon, J. H.; Moyse, C. D., Extraction,

purification, identification and metabolism of 3',5'-cyclic UMP, 3',5'-cyclic IMP and 3',5'-cyclic dTMP from rat tissues. *Biochem J* **1986,** *236* (2), 431-9.

3. (a) Bond, A. E.; Dudley, E.; Tuytten, R.; Lemiere, F.; Smith, C. J.; Esmans, E. L.; Newton, R. P., Mass spectrometric identification of Rab23 phosphorylation as a response to challenge by cytidine 3',5'-cyclic monophosphate in mouse brain. *Rapid Commun Mass Spectrom* **2007,** *21* (16), 2685-92; (b) Goble, A. M.; Feng, Y.; Raushel, F. M.; Cronan, J. E., Discovery of a cAMP deaminase that quenches cyclic AMP-dependent regulation. *ACS Chem Biol.* **2013,** *8* (12), 2622-9; (c) Jackson, E. K., The 2',3'-cAMP-adenosine pathway. *Am J Physiol Renal Physiol* **2011,** *301* (6), F1160-7.

4. (a) Newton, R. P.; Salih, S. G.; Salvage, B. J.; Kingston, E. E., Extraction, Purification and Identification of Cytidine 3',5'-Cyclic-Monophosphate from Rat-Tissues. *J Biochem* **1984,** *221* (3), 665-673; (b) Murphy, B. E.; Stone, J. E., Changes in the concentration of cytidine 3',5' monophosphate (cyclic CMP) in regenerating rat liver. *Proc Soc Exp Biol Med.* **1980,** *163* (3), 301-4; (c) Newton, R. P.; Hakeem, N. A.; Salvage, B. J.; Wassenaar, G.; Kingston, E. E., Cytidylate cyclase activity: identification of cytidine 3',5'-cyclic monophosphate and four novel cytidine cyclic phosphates as biosynthetic products from cytidine triphosphate. *Rapid Commun Mass Spectrom* **1988,** *2* (6), 118-26; (d) Kuo, J. F.; Brackett, N. L.; Shoji, M.; Tse, J., Cytidine 3':5'-monophosphate phosphodiesterase in mammalian tissues. Occurrence and biological involvement. *J Biol Chem.* **1978,** *253* (8), 2518-21; (e) Gaion, R. M.; Krishna, G., Cytidylate cyclase: the product isolated by the method of Cech and Ignarro is not cytidine 3',5'-monophosphate. *Biochem Biophys Res Commun* **1979**, 86 (1), 105-11.

5. (a) Chen, Z.; Zhang, X.; Ying, L.; Dou, D.; Li, Y.; Bai, Y.; Liu, J.; Liu, L.; Feng, H.; Yu, X.; Leung, S. W.; Vanhoutte, P. M.; Gao, Y., Cyclic IMP-Synthesized by sGC as a Mediator of Hypoxic Contraction of Coronary Arteries. *Am J Physiol Heart Circ Physiol* **2014**; (b) Beste, K. Y.; Burhenne, H.; Kaever, V.; Stasch, J. P.; Seifert, R., Nucleotidyl Cyclase Activity of Soluble Guanylyl Cyclase alpha(1)beta(1). *Biochemistry-Us* **2012,** *51* (1), 194-204.

6. Seifert, R., Is cIMP a second messenger with functions opposite to those of cGMP? *Naunyn Schmiedebergs Arch Pharmacol.* **2014**.

7. Ren, J.; Mi, Z.; Stewart, N. A.; Jackson, E. K., Identification and quantification of 2',3'-cAMP release by the kidney. *J Pharmacol Exp Ther.* **2009,** *328* (3), 855-65.

8. (a) Jackson, E. K.; Gillespie, D. G., Extracellular 2',3'-cAMP and 3',5'-cAMP stimulate proliferation of preglomerular vascular endothelial cells and renal epithelial cells. *Am J Physiol Renal Physiol* **2012,** *303* (7), F954-62; (b) Jackson, E. K.; Ren, J.; Gillespie, D. G.; Dubey, R. K., Extracellular 2 ',3 '-Cyclic Adenosine 5 '-Monophosphate Is a Potent Inhibitor of Preglomerular Vascular Smooth Muscle Cell and Mesangial Cell Growth. *Hypertension* **2010,** *56* (1), 151-U246; (c) Jackson, E. K.; Ren, J.; Mi, Z., Extracellular 2',3'-cAMP is a source of adenosine. *J Biol Chem* **2009,** *284* (48), 33097-106; (d) Verrier, J. D.; Jackson, T. C.; Gillespie, D. G.; Janesko-Feldman, K.; Bansal, R.; Goebbels, S.; Nave, K. A.; Kochanek, P. M.; Jackson, E. K., Role of CNPase in the oligodendrocytic extracellular 2',3'-cAMP-adenosine pathway. *Glia* **2013,** *61* (10), 1595-606; (e) Jackson, E. K.; Gillespie, D. G.; 164

Mi, Z.; Cheng, D.; Bansal, R.; Janesko-Feldman, K.; Kochanek, P. M., Role of 2',3'-cyclic nucleotide 3'-phosphodiesterase in the renal 2',3'-cAMP-adenosine pathway. *Am J Physiol Renal Physiol* **2014,** *307* (1), F14-24; (f) Jackson, E. K.; Mi, Z., In vivo cardiovascular pharmacology of 2',3'-cAMP, 2'-AMP, and 3'-AMP in the rat. *J Pharmacol Exp Ther.* **2013,** *346* (2), 190-200; (g) Verrier, J. D.; Jackson, T. C.; Bansal, R.; Kochanek, P. M.; Puccio, A. M.; Okonkwo, D. O.; Jackson, E. K., The brain in vivo expresses the 2',3'-cAMP-adenosine pathway. *J Neurochem* **2012,** *122* (1), 115-25.

9. Van Damme, T.; Blancquaert, D.; Couturon, P.; Van Der Straeten, D.; Sandra, P.; Lynen, F., Wounding stress causes rapid increase in concentration of the naturally occurring 2',3'-isomers of cyclic guanosine- and cyclic adenosine monophosphate (cGMP and cAMP) in plant tissues. *Phytochemistry* **2014,** *103*,59-66.

10. (a) George, W. J.; Polson, J. B.; O'Toole, A. G.; Goldberg, N. D., Elevation of guanosine 3',5'-cyclic phosphate in rat heart after perfusion with acetylcholine. *Proc Natl Acad Sci U.S.A.* **1970,** *66* (2), 398-403; (b) Beste, K. Y.; Seifert, R., cCMP, cUMP, cTMP, cIMP and cXMP as possible second messengers: development of a hypothesis based on studies with soluble guanylyl cyclase alpha(1)beta(1). *Biol Chem* **2013,** *394*(2),261-70.

11. (a) Goldberg, N. D.; Larner, J.; Sasko, H.; O'Toole, A. G., Enzymic analysis of cyclic 3', 5'-AMP in mammalian tissues and urine. *Anal Biochem* **1969,** *28* (1), 523-44; (b) Hardman, J. G.; Davis, J. W.; Sutherland, E. W., Measurement of guanosine 3',5'-monophosphate and other cyclic nucleotides. Variations in urinary excretion with hormonal state of the rat. *J Biol Chem* **1966,** *241* (20), 4812-5; (c) 165

Ishikawa, E.; Ishikawa, S.; Davis, J. W.; Sutherland, E. W., Determination of guanosine 3',5'-monophosphate in tissues and of guanyl cyclase in rat intestine. *J Biol Chem* **1969,** *244* (23),6371-6.

12. (a) Steiner, A. L.; Parker, C. W.; Kipnis, D. M., Radioimmunoassay for cyclic nucleotides. I. Preparation of antibodies and iodinated cyclic nucleotides. *J Biol Chem* **1972,** *247* (4), 1106-13; (b) Steiner, A. L.; Pagliara, A. S.; Chase, L. R.; Kipnis, D. M., Radioimmunoassay for cyclic nucleotides. II. Adenosine 3',5'-monophosphate and guanosine 3',5'-monophosphate in mammalian tissues and body fluids. *J Biol Chem* **1972,** *247* (4),1114-20.

13. (a) Kingan, T. G., A competitive enzyme-linked immunosorbent assay: applications in the assay of peptides, steroids, and cyclic nucleotides. *Anal Biochem* **1989,** *183* (2), 283-9; (b) Wellard, J.; Blind, B.; Hamprech, B., An enzyme-linked immunosorbent assay for the rapid quantification of intracellular and extracellular guanosine 3',5'-cyclic monophosphate in cultured glial cells. *Neurochem Res.* **2004,** *29* (11), 2177-87; (c) Engvall, E.; Jonsson, K.; Perlmann, P., Enzyme-linked immunosorbent assay. II. Quantitative assay of protein antigen, immunoglobulin G, by means of enzyme-labelled antigen and antibody-coated tubes. *Biochim. Biophys. Acta* **1971,** *251* (3), 427-34.

14. Faupel-Badger, J. M.; Fuhrman, B. J.; Xu, X.; Falk, R. T.; Keefer, L. K.; Veenstra, T. D.; Hoover, R. N.; Ziegler, R. G., Comparison of liquid chromatography-tandem mass spectrometry, RIA, and ELISA methods for measurement of urinary estrogens. *Cancer Epidemiol Biomarkers Prev.* **2010,** *19* (1), 292-300.

15. Newton, R. P.; Groot, N.; van Geyschem, J.; Diffley, P. E.; Walton, T. J.; Bayliss, M. A.; Harris, F. M.; Games, D. E.; Brenton, A. G., Estimation of cytidylyl cyclase activity and monitoring of side-product formation by fast-atom bombardment mass spectrometry. *Rapid Commun Mass Spectrom* **1997,** *11* (2), 189-94.

16. (a) Xiao, J. F.; Zhou, B.; Ressom, H. W., Metabolite identification and quantitation in LC-MS/MS-based metabolomics. *Trends Anal Chem* **2012,** *32*, 1-14; (b) E.L. Esmans, D. B., I. Hoes, F. Lemiere, K. Vanhoutte, Liquid chromatography-mass spectrometry in nucleoside, nucleotide and modified nucleotide characterization. *J Chromatog A* **1998,** *794*, 109-127; (c) Prakash, C.; Shaffer, C. L.; Nedderman, A., Analytical strategies for identifying drug metabolites. *Mass Spectrom Rev* **2007,** *26* (3), 340-69; (d) Richards, H.; Das, S.; Smith, C. J.; Pereira, L.; Geisbrecht, A.; Devitt, N. J.; Games, D. E.; van Geyschem, J.; Gareth Brenton, A.; Newton, R. P., Cyclic nucleotide content of tobacco BY-2 cells. *Phytochemistry* **2002,** *61* (5), 531-7; (e) Witters, E.; Vanhoutte, K.; Dewitte, W.; Machackova, I.; Benkova, E.; Van Dongen, W.; Esmans, E. L.; Van Onckelen, H. A., Analysis of cyclic nucleotides and cytokinins in minute plant samples using phase-system switching capillary electrospray-liquid chromatography-tandem mass spectrometry. *Phytochem Anal* **1999,** *10* (3), 143-151.

17. (a) Becker, S.; Kortz, L.; Helmschrodt, C.; Thiery, J.; Ceglarek, U., LC-MS-based metabolomics in the clinical laboratory. *J Chromatogr B* **2012,** *883-884*, 68-75; (b) Oeckl, P.; Ferger, B., Simultaneous LC-MS/MS analysis of the biomarkers cAMP and cGMP in plasma, CSF and brain tissue. *J Neurosci. Methods* **2012,** *203* (2), 338-43.

18. (a) Martens-Lobenhoffer, J.; Dautz, C.; Bode-Boger, S. M., Improved method for the determination of cyclic guanosine monophosphate (cGMP) in human plasma by LC-MS/MS. *J Chromatogr B* **2010,** *878* (3-4), 487-91; (b) Van Damme, T.; Zhang, Y.; Lynen, F.; Sandra, P., Determination of cyclic guanosine- and cyclic adenosine monophosphate (cGMP and cAMP) in human plasma and animal tissues by solid phase extraction on silica and liquid chromatography-triple quadrupole mass spectrometry. *J Chromatogr B* **2012,** *909*, 14-21; (c) Zhang, Y.; Dufield, D.; Klover, J.; Li, W.; Szekely-Klepser, G.; Lepsy, C.; Sadagopan, N., Development and validation of an LC-MS/MS method for quantification of cyclic guanosine 3',5'-monophosphate (cGMP) in clinical applications: a comparison with a EIA method. *J Chromatogr B* **2009,** *877* (5-6), 513-20.

19. (a) Van Damme, T.; Lachova, M.; Lynen, F.; Szucs, R.; Sandra, P., Solid-phase extraction based on hydrophilic interaction liquid chromatography with acetone as eluent for eliminating matrix effects in the analysis of biological fluids by LC-MS. *Anal Bioanal Chem* **2014,** *406* (2), 401-7; (b) Van Eeckhaut, A.; Lanckmans, K.; Sarre, S.; Smolders, I.; Michotte, Y., Validation of bioanalytical LC-MS/MS assays: evaluation of matrix effects. *J Chromatogr B* **2009,** *877* (23), 2198-207; (c) Trufelli, H.; Palma, P.; Famiglini, G.; Cappiello, A., An Overview of Matrix Effects in Liquid Chromatography-Mass Spectrometry. *Mass Spectrom Rev* **2011,** *30* (3), 491-509; (d) King, R.; Bonfiglio, R.; Fernandez-Metzler, C.; Miller-Stein, C.; Olah, T., Mechanistic investigation of ionization suppression in electrospray ionization. *J Am Soci Mass Spectrom* **2000,** *11* (11), 942-50.

20. (a) Witters, E.; Van Dongen, W.; Esmans, E. L.; Van Onckelen, H. A., Ion-pair liquid chromatography-electrospray mass spectrometry for the analysis of cyclic nucleotides. *J Chromatogr B* **1997,** *694* (1), 55-63; (b) Lorenzetti, R.; Lilla, S.; Donato, J. L.; De Nucci, G., Simultaneous quantification of GMP, AMP, cyclic GMP and cyclic AMP by liquid chromatography coupled to tandem mass spectrometry. *J Chromatogr B* **2007,** *859* (1), 37-41.

21. (a) O'Kane, A. A.; Chevallier, O. P.; Graham, S. F.; Elliott, C. T.; Mooney, M. H., Metabolomic profiling of in vivo plasma responses to dioxin-associated dietary contaminant exposure in rats: implications for identification of sources of animal and human exposure. *Environ Sci Technol* **2013,** *47* (10), 5409-18; (b) Zhang, T.; Wu, X.; Ke, C.; Yin, M.; Li, Z.; Fan, L.; Zhang, W.; Zhang, H.; Zhao, F.; Zhou, X.; Lou, G.; Li, K., Identification of potential biomarkers for ovarian cancer by urinary metabolomic profiling. *J Proteome Res* **2013,** *12* (1), 505-12.

22. Buszewski, B.; Noga, S., Hydrophilic interaction liquid chromatography (HILIC)--a powerful separation technique. *Anal Bioanal Chem.* **2012,** *402* (1), 231-47.

23. Kehr, J.; Chavko, M., Separation of Nucleotides by Reversed-Phase High-Performance Liquid-Chromatography - Advantages and Limitations. *Fresen Z Anal Chem* **1986,** *325* (5), 466-469.

24. (a) Shrivastava, A. a. G., V., , Methods for the determination of limit of detection and limit of quantitation of the analytical methods. *Chron. Young Sci.* **2011,** *2* (1), 21-25; (b) ICH of Technical Requirements for Registration of Pharmaceuticals for Human Use. Validation of Analytical Procedures: Text and Methodology Q2(R1).

http://www.ich.org/fileadmin/Public_Web_Site/ICH_Products/Guidelines/Quality/Q2_R1/Step4/Q2_R1__Guideline.pdf. **Nov. 1996**.

25. Andrews, S. C.; Guest, J. R., Nucleotide sequence of the gene encoding the GMP reductase of Escherichia coli K12. *Biochem J* **1988,** *255* (1), 35-43.

26. US Department of Health and Human Services, F. D. A., Center for Drug Evaluation and Research (CDER), Guidance for industry, Bioanalytical Method Validation, BP, http://www.fda.gov/downloads/Drugs/Guidances/ucm070107.pdf. **May, 2001**.

27. Bloch, A., Cytidine 3',5'-monophosphate (cyclic CMP). I. Isolation from extracts of leukemia L-1210 Cells. *Biochem Biophys Res Commun.* **1974,** *58* (3), 652-9.

28. (a) Patton, G. C.; Stenmark, P.; Gollapalli, D. R.; Sevastik, R.; Kursula, P.; Flodin, S.; Schuler, H.; Swales, C. T.; Eklund, H.; Himo, F.; Nordlund, P.; Hedstrom, L., Cofactor mobility determines reaction outcome in the IMPDH and GMPR (beta-alpha)8 barrel enzymes. *Nat Chem Biol.* **2011,** *7* (12), 950-8; (b) Lin, T. S.; Cheng, J. C.; Ishiguro, K.; Sartorelli, A. C., Purine and 8-substituted purine arabinofuranosyl and ribofuranosyl nucleoside derivatives as potential inducers of the differentiation of the Friend erythroleukemia. *J Med Chem.* **1985,** *28* (10), 1481-5; (c) Kotra, L. P.; Manouilov, K. K.; Cretton-Scott, E.; Sommadossi, J. P.; Boudinot, F. D.; Schinazi, R. F.; Chu, C. K., Synthesis, biotransformation, and pharmacokinetic studies of 9-(beta-D-arabinofuranosyl)-6-azidopurine: a prodrug for ara-A designed to utilize the azide reduction pathway. *J Med Chem.* **1996,** *39* (26), 5202-7.

29. Banoub, J. H.; Limbach, P. A., *Mass spectrom nucleosides nucleic acids*. CRC Press: Boca Raton, 2010; p xii, 492.

30. (a) Bahre, H.; Danker, K. Y.; Stasch, J. P.; Kaever, V.; Seifert, R., Nucleotidyl cyclase activity of soluble guanylyl cyclase in intact cells. *Biochem. Biophys. Res. Commun.* **2014,** *443* (4), 1195-9; (b) Beste, K. Y.; Spangler, C. M.; Burhenne, H.; Koch, K. W.; Shen, Y.; Tang, W. J.; Kaever, V.; Seifert, R., Nucleotidyl cyclase activity of particulate guanylyl cyclase A: comparison with particulate guanylyl cyclases E and F, soluble guanylyl cyclase and bacterial adenylyl cyclases CyaA and edema factor. *PLoS One* **2013,** *8* (7), e70223.

Chapter 5: Conclusions and Perspectives

5.1 Summary

This dissertation focused on understanding of various signal transduction pathways in prokaryotic and eukaryotic systems. Although kinases are known to be involved in essential signal transduction pathways in stress adaptation in bacteria, the bacterial mechanisms used to sense stress remains unclear.[1] We studied how Gram-negative bacteria sense environmental O_2 and alter their stress-response pathways. Additionally, studying signaling pathways of additional naturally occurring potential secondary messengers provide insights into their roles in survival and tumorigenesis, and also allow for the study of interplay between secondary messenger signaling networks in eukaryotes.

5.2 A starting point for studying a novel stressosome-regulated pathway in Gram-negative bacterium *Vibrio brasiliensis*

In *Bacillus subtilis*, the stressosome complex regulates diverse signaling pathways that control transcription factor σ^B in response to various environmental challenges.[2] The stressosome-regulated pathway is modulated by reversible protein phosphorylation reactions controlled by kinase RsbT.[2a, 3] A novel stressosome from the Gram-negative marine bacterium *Vibrio brasiliensis* that contained a heme-bound GCS as the sensing protein was described in chapter 2. The *V. brasiliensis* stressosome senses environmental O_2, and alters phosphorylation activity in response to gaseous ligands. Previous studies have shown virulence genes expression require O_2-limiting conditions in human pathogen *V. cholerae*, this novel O_2-dependent stresssome pathway could play a key role to sense low O_2 concentration and induce transcription of virulence genes in the *Vibrio* genus.[4]

Characterization of the novel stressome-regulated pathway in *V. brasiliensis* will allow for future identification of ligand-dependent gene transcription and downstream effectors of the stressosome-regulated pathway *in vivo*, but also potentially offer an explanation of how a free-living environmental organism can switch upon a change in the environment to become human bacterial pathogen. Future work includes exploring protein-protein interactions between native proteins. MS-based Hydrogen-deuterium exchange (H/D exchange) will be used to study the conformations and dynamics of the proteins, in order to map the interaction surface between proteins in the stressosome complex.

5.3 Continuing to purify and investigate the functions of 3',5'-cCMP-related enzymes in mammals

Putative enzymes capable of synthesizing and hydrolyzing 3',5'-cCMP, cytidylate cyclase and phosphodiesterase respectively, as well as 3',5'-cCMP dependent protein kinase were reported in the 1970s, however, their molecular identity and functional properties still remain elusive even today.[5] In chapter 3, following previous published protein purification protocols, we have partially purified a soluble enzyme fraction contains a soluble cyclase that is capable of synthesizing 3',5'-cCMP. Future work includes developing a high-resolution fractionation technique to further purify the soluble fraction, in order to isolate and characterize the putative mammalian cytidylate cyclase. In addition, a more gentle and rapid fractionation method is needed to isolate mammalian 3',5'-cCMP specific PDE. We also have isolated a potential 3',5'-cCMP binding protein, THO complex subunit 5, from rat brains using 3',5'-cCMP affinity chromatography,

suggesting 3',5'-cCMP may be involved in mRNA export and controlling transcription level through binding and regulation of the THO complex. Identifying enzyme members on 3',5'-cCMP signal pathway will provide a starting point for establishing physiological relevance of 3',5'-cCMP in mammals.

5.4 Development of a useful tool for identification and quantification of various typical and atypical cNMPs

Progress made in identification of 3',5'-cCMP-related enzymes has been slow in recently years, mainly due to the lack of an efficient purification method and a sensitive analytical protocol. In chapter 4, we developed a sensitive and versatile method to extract and quantify cNMPs using LC-MS/MS, including both 3',5'-cNMPs and 2',3'-cNMPs, in mammalian tissues and cells.[6] The analytical method reported in this chapter allows for comparison of multiple cNMPs in the various systems, and furthermore reports the first identification and quantification of 2',3'-cIMP.[6] This LC-MS/MS based method can be adapted in the future to both hypothesis-driven and hypothesis-generating types of research. For hypothesis-driven research, this analytical method can be used to quantify analytes-of-interest on a triple quadrupole MS, whereas for hypothesis-generating research, this method can be utilized to identify and quantify unknown/novel cNMPs using a Q-TOF or an ion trap MS. This LC-MS/MS method offers a tool for quantification of cNMPs levels in cells and mammalian tissues, which will provide insight into the roles of cNMPs *in vivo*.

5.5 References

1. Marles-Wright, J.; Lewis, R. J., The stressosome: molecular architecture of a signalling hub. *Biochem Soc Trans* **2010,** *38* (4), 928-33.

2. (a) Marles-Wright, J.; Grant, T.; Delumeau, O.; van Duinen, G.; Firbank, S. J.; Lewis, P. J.; Murray, J. W.; Newman, J. A.; Quin, M. B.; Race, P. R.; Rohou, A.; Tichelaar, W.; van Heel, M.; Lewis, R. J., Molecular architecture of the "stressosome," a signal integration and transduction hub. *Science* **2008,** *322* (5898), 92-6; (b) Price, C. W.; Fawcett, P.; Ceremonie, H.; Su, N.; Murphy, C. K.; Youngman, P., Genome-wide analysis of the general stress response in Bacillus subtilis. *Mol Microbiol* **2001,** *41* (4), 757-74.

3. (a) Kim, T. J.; Gaidenko, T. A.; Price, C. W., A multicomponent protein complex mediates environmental stress signaling in Bacillus subtilis. *J Mol Biol* **2004,** *341* (1), 135-50; (b) Kim, T. J.; Gaidenko, T. A.; Price, C. W., In vivo phosphorylation of partner switching regulators correlates with stress transmission in the environmental signaling pathway of Bacillus subtilis. *J Bacteriol* **2004,** *186* (18), 6124-32; (c) Chen, C. C.; Lewis, R. J.; Harris, R.; Yudkin, M. D.; Delumeau, O., A supramolecular complex in the environmental stress signalling pathway of Bacillus subtilis. *Mol Microbiol* **2003,** *49* (6), 1657-69.

4. Fan, F.; Liu, Z.; Jabeen, N.; Birdwell, L. D.; Zhu, J.; Kan, B., Enhanced interaction of Vibrio cholerae virulence regulators TcpP and ToxR under oxygen-limiting conditions. *Infect Immun***2014,** *82* (4), 1676-82.

5. (a) Cech, S. Y.; Ignarro, L. J., Cytidine 3',5'-monophosphate (cyclic CMP) formation in mammalian tissues. *Science* **1977,** *198* (4321), 1063-5; (b) Cech, S. Y.;

Ignarro, L. J., Cytidine 3',5'-monophosphate (cyclic CMP) formation by homogenates of mouse liver. *Biochem Biophy Res Commun* **1978,** *80* (1), 119-25; (c) Cheng, Y. C.; Bloch, A., Demonstration, in leukemia L-1210 cells, of a phosphodiesterase acting on 3':5'-cyclic CMP but not on 3':5'-cyclic AMP or 3':5'-cyclic GMP. *J Biol Chem* **1978,** *253* (8), 2522-4; (d) Kuo, J. F.; Brackett, N. L.; Shoji, M.; Tse, J., Cytidine 3':5'-monophosphate phosphodiesterase in mammalian tissues. Occurrence and biological involvement. *J Biol Chem* **1978,** *253* (8), 2518-21; (e) Helfman, D. M.; Shoji, M.; Kuo, J. F., Purification to homogeneity and general properties of a novel phosphodiesterase hydrolyzing cyclic CMP and cyclic AMP. *J Biol Chem* **1981,** *256* (12), 6327-34; (f) Newton, R. P.; Salih, S. G., Cyclic CMP phosphodiesterase: isolation, specificity and kinetic properties. *Int J Biochem* **1986,** *18* (8), 743-52.

6. Jia, X.; Fontaine, B. M.; Strobel, F.; Weinert, E. E., A facile and sensitive method for quantification of cyclic nucleotide monophosphates in mammalian organs: basal levels of eight cNMPs and identification of 2',3'-cIMP. *Biomolecules* **2014,** *4* (4), 1070-